The influence of *bapx1* on amphibian head development and its role for the development of evolutionary novelties.

Dissertation

To Fulfill the

Requirements for the Degree of

„doctor rerum naturalium“ (Dr. rer. nat.)

Submitted to the Council of the Faculty

of Biological Sciences

of the Friedrich Schiller University Jena

by M.Sc. Paul Lukas

born on 02.01.1990 in Lauchhammer

Verteidigungsdatum

29.11.2018

Gutachter

Prof. Dr. Lennart Olsson, Friedrich-Schiller-Universität Jena

Prof. Dr. Martin S. Fischer, Friedrich-Schiller-Universität Jena

Prof. Dr. Alexander Haas, Universität Hamburg

Content

Introduction

What are evolutionary novelties and how can they evolve?

The presence of novel traits in organisms and the explanation of how they originate is a major problem in biology and an often-used starting point for critics to argue against Darwin´s theory of evolution. The definition of an evolutionary novelty remained unclear for several decades (Shubin et al. 2009). There were mainly two different approaches to define a novelty. The functional approach considers something as a novelty when novel functional capabilities arise. For example, the bird wing is a functional novelty because it enables the organism to fly. The other approach is structural, defining a novelty as a body part that is neither homologous to any body part in the ancestral lineage nor serially homologous to any other body part of the same organism (Wagner & Lynch 2010). From this structural approach the bird wing itself is no novelty because it is directly homologous to the forelimbs of other tetrapods. In a more general approach an evolutionary novelty is the origin of a novel body part that may serve a novel function or specialize in a function that was already performed in the ancestral lineage (Wagner 2014). These novel characters must be adaptive, heritable and must contribute to the survival of the individual. Every development of a novel body part is the consequence of changes in genetic signalling. During ontogeny cells need proper signals which "inform" them where, when and what they should do to form different body parts. Such positional information can be intracellular by inherited cytoplasmic factors, embryonic induction through emitted signals from neighbouring cells, or gene expression which patterns several domains in the developing body part (Wagner 2014). Cartilages are the precursors of the majority of the bony skeleton in osteognathostomes and a rich resource for the evolution of novelties (Rose 2014).

Svensson and Haas (2005) hypothesized three possible modes for the evolution of novel cartilages in anurans (Figure 1). One way to evolve new cartilaginous structures is so-called *de novo* evolution. A cartilage which arises through *de novo* evolution can not be homologized with any existing cartilage. *De novo* evolution of transcription factors or a shift of the expression domain of transcription factors which are able to induce cartilage formation would be a prerequisite to achieving this. Additionally, the new transcription factor expression domain must fit into the pre-existing developmental genetic context, which makes *de novo* evolution highly improbable. Furthermore, the authors point out that novel cartilages can evolve through the duplication of existing cartilages. The development of cartilages is based on a genetic network which regulates proliferation, condensation and differentiation of chondrocytes. Through the partial duplication of this genetic network, the cartilage precursor population could become divided. This division could result in the development of an additional cartilage which is the duplicate of a pre-existing cartilage. In addition, a third way of evolving novel cartilages was described. Cartilages can evolve through partitioning of existing cartilages during development. Such a partitioning could be realized by the development of an additional joint.

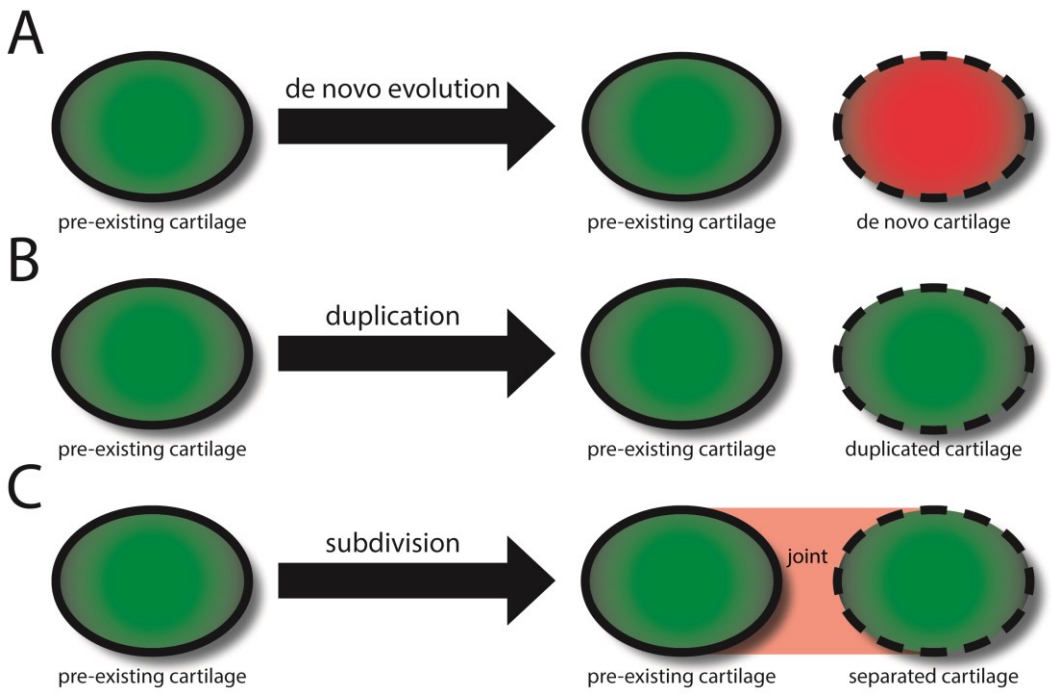

Figure 1: Hypotheses about the evolutionary origin of novel cartilages after Svensson and Haas (2005). **A** Acquisition of a novel cartilage through *de novo* evolution. As a result, an additional cartilage evolves which is not homologous to any existing cartilage. **B** Development of an additional cartilage through duplication of the existing one. **C** An additional cartilage can arise through subdivision of the existing one. In this case the joint rather than the additional cartilage is the actual novelty.

If an additional joint develops within a continuous cartilage, this joint formation will divide the cartilage. The presence of two cartilages instead of one would be the result. Therefore, the joint rather than the additional cartilage would represent the actual evolutionary novelty. An additional joint formation could be enabled through a heterotopic shift or through *de novo* expression of genes which are involved in joint formation. One aim of the present study was to reveal which of these hypothesized three modes could explain the evolution of the gnathostome jaw joint by altering the gene expression in different amphibian species.

Xenopus laevis – an amphibian model organism with lack of information

Model organisms are exemplars of a particular biological system under investigation and are assumed to be representatives of a more inclusive taxon (Cannatella & Sá 1993). Such organisms are used since the era of the ancient Greeks to study and understand several biological issues. Insights from these organisms are often generalized and extrapolated to other organisms where experiments are impossible or unethical. This extrapolation is enabled by the common descent of all living organisms through the process of evolution and the shared developmental and metabolic processes (Fox 1986). Nevertheless, it is important to consider that a model organism itself was separated from its ancient lineage a long time ago. Through this time, it may have acquired novel traits which differ from those found in even closely related organisms. These differences might interfere with the respective

experiment, which makes extrapolation of results from one organism to another difficult and sometimes even impossible. Additionally, most model organisms were not chosen with evolutionary questions in mind (Hanken & Thorogood 1993). Rather the availability or simple rearing conditions were crucial for selecting a model organism. The African clawed frog *Xenopus laevis* (Daudin) is used as a model organism, and experimental results in *Xenopus* are often thought to represent all anurans and even all amphibians (Cannatella & Sá 1993). The advantages of this species are a wholly aquatic and, in comparison to other amphibians, relatively short life cycle with relatively low demands on water quality and space. This makes it easy to rear. Mating of *Xenopus* provides numerous and robust eggs which are suitable for microsurgery and microinjections. Also advantageous is the year-round response to gonadotropin to induce breeding, while other amphibians only breed seasonally (Gurdon & Hopwood 2000; Cannatella & Sá 1993; Harland & Grainger 2011). The induction of ovulation in *Xenopus laevis* through the injection of human gonadotropin, which is an indicator of pregnancy in humans, was discovered by the British biologist Lancelot Hogben. Female frogs injected with urine from pregnant women started to deposit eggs 8-12 hours after injection. Until the early 1960´s when immunological methods were invented the so-called Hogben test was the most widely used pregnancy test (Gurdon & Hopwood 2000). This led to a rapid spread of *Xenopus laevis* breeding colonies and made it a common laboratory animal (Tinsley 2010). The injection of human gonadotropin was also used to induce ovulation independent from a seasonal rhythm and enables researchers to work continuously on their projects and consolidates its position as a model organism because of the constant replenishment of eggs and offspring (Gurdon & Hopwood 2000).

Despite its wide use in many research fields, from its introduction into science until today, some basic knowledge of the development of *Xenopus laevis* is still missing in the scientific record. Especially a comprehensive description of the development of the larval cartilaginous head skeleton, although it was often examined, is missing and particular descriptions of the larval head are inaccurate or false. The first record of a description of the larval head was published by Parker in 1876 and 1879. He described one stage of a premetamorphic larval head (Parker 1876; Parker 1879). It was followed by investigation of the development of the hyobranchial apparatus (Ridewood 1897) and detailed behavioural descriptions with an overview of the conditions for rearing of *Xenopus laevis* (Bles 1906). The specimens reared and collected by Bles were the basis for further investigations of the masticatory muscles (Edgeworth 1930) and of external features (Peter 1931). The early development of the larval head skeleton was examined by several researchers (Dreyer 1914; Kotthaus 1933; Paterson 1939; Ramaswami 1941; Weisz 1945a; Weisz 1945b). A staging table for *Xenopus laevis* development based on external features from the fertilized egg until the adult frog was published in 1956 and constantly later revised (Nieuwkoop & Faber 1994). This staging table reveals that the description of early stages of larval head development is incomplete. Furthermore, the descriptions differ greatly in precision, morphological ontology, accessibility, use of staging system and image quality. Descriptions of initial chondrocyte condensations are completely missing, while premetamorphic, metamorphic and adult stages are described very well (Trueb & Hanken 1992). In times of numerous

techniques which generate morphological phenotypes (Morpholinos, CRISP/Cas etc.) a comprehensive overview of the skeletal development is important to detect possible heterochronic changes or morphological defects at every stage of this widely used model organism. I provide this in Paper I of this Ph.D. thesis.

Studies on early skeletal development and chondrogenesis in anurans are scarce. Over a century ago the development of *Rana temporaria*, *Bufo cinereus*, and *Pelobates fuscus* were described from the onset of chondrification until the presence of the larval premetamorphic head (Gaupp 1906; Stöhr 1882). Recent investigations focus on the description of single stages and lack an end-to-end description of the entire cartilaginous development of the larval head skeleton. In other taxa the sequence of larval head skeleton chondrification was described recently. Investigations on the sequence of chondrification of the pharyngeal arches in chondrichthyes (Gillis et al. 2012; Gillis et al. 2009), in non-teleost actinopterygians (Gillis et al. 2012; Warth et al. 2017) and in teleosts (Langille & Hall 1987) all come to the same conclusion. The sequence of chondrification during ontogeny follows an anterior-posterior pattern. First the mandibular arch derived cartilages develop and are followed by hyoid arch derived cartilages. After that pharyngeal arch three-derived cartilages develop and so on. Because of this shared developmental sequence, the anterior-posterior pattern of chondrification is thought to represent the ancestral state of all jawed vertebrates. Further investigations of the sequence of chondrification during development would make it possible to identify heterochronic shifts, which may lead to novel traits, among different taxa. Additionally, such investigations would be an important foundation for homologization of the different derivatives of the pharyngeal arches in various gnathostome taxa.

Advantages of anurans for the study of skeletal evolution and development

The larval anuran jaw is unique among vertebrates and its evolution is directly connected to the extensive variety of feeding habits found in tadpoles. The acquisition of herbivorous feeding modes decouples the larval stage from the carnivorous adults. Along with an aquatic lifestyle, the tadpole stage reduces the intraspecific competition between larvae and adults and is one key for the evolutionary success of anurans within amphibians (Svensson & Haas 2005; McDiarmid & Altig 1999). The lower jaw of a typical anuran tadpole consists of two paired Meckel´s cartilages (Figure 2). They are horizontally oriented and slightly sigmoidal. Caudally Meckel´s cartilage is connected to the palatoquadrate via the jaw articulation. The infrarostral cartilage is a paired or single cartilage which is situated between the anterior tips of the two Meckel´s cartilages. Between the infrarostral and Meckel´s cartilage an additional joint is present. This intramandibular joint is also unique to anurans. Additional structures in the jaw enhance the possibilities for evolutionary adaptations and may increase variability. Such a changeable condition facilitates the evolution of numerous different feeding modes such as filter feeding, rasping, carnivory and many more.

The tadpole of *Xenopus laevis* is highly derived and shows pipoid-specific features (Figure 2). The chondrocranium is broad and flattened and the lower jaw develops precociously. The

suprarostral cartilage and its alae are fused to the cornua trabeculae and form a crescent-shaped plate called the suprarostral plate (De Sá & Swart 1999; Trueb & Hanken 1992). This plate supports the tentacular cartilage which only occurs in the upper jaw of *Xenopus laevis* tadpoles. In the lower jaw the infrarostrals are fused medially and articulate with Meckel´s cartilage (Sokol 1977). The muscular process is reduced and a lateral process of the palatoquadrate is present (De Sá & Swart 1999). Furthermore the commissura quadratocranialis is broad and the larval crista parotica is well developed (De Sá & Swart 1999; Trueb & Hanken 1992). It remains unclear whether the development of these *Xenopus*-specific features follow the ancient anterior-to-posterior pattern.

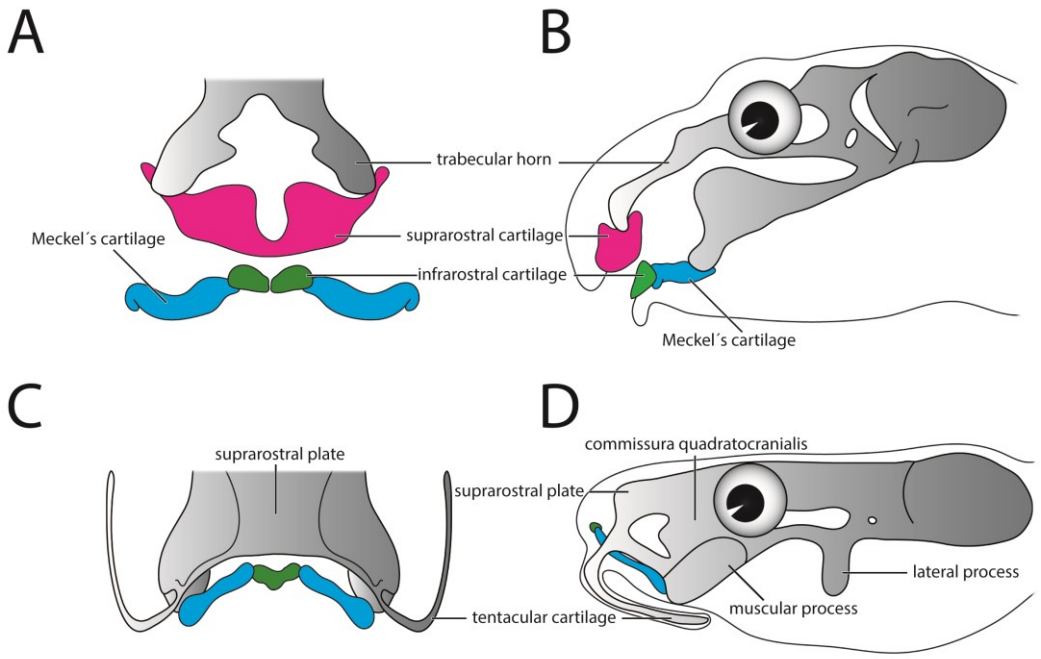

Figure 2: Overview of cartilaginous head structures of anuran tadpoles. **A** The basic stage of the jaw of an anuran tadpole in frontal view. Remarkable is the plate-like suprarostral cartilage, the paired infrarostral cartilages and the sigmoidal Meckel´s cartilages. **B** The basic stage of the cartilaginous head structures of an anuran tadpole in lateral view. **C** The derived state of the *Xenopus laevis* jaw cartilages in frontal view. The infrarostral cartilages are fused and Meckel´s cartilage is rod-like. The suprarostral cartilage is fused to the trabecular horns and forms the suprarostral plate which is no longer movable. **D** Lateral view of the larval head of *Xenopus laevis*. The tentacular cartilage, the lateral process of the palatoquadrate, a reduced muscular process and a broad commissura quadratocranialis are *Xenopus*-specific features which underline the derived state of *Xenopus laevis* larvae.

Where do the cranial cartilages come from?

The vertebrate head consists of mainly three components. Two components are endoskeletal (neurocranium and viscerocranium) and one is exoskeletal (dermatocranium). The latter ossifies without cartilaginous precursors and the endoskeletal components are often initially preformed as cartilages which are later replaced by bones through enchondral or perichondral ossification. The dermatocranium is of mixed origin (mesodermal and neural crest) and is superficial to the neurocranium. It forms the roof of the brain and the lateral walls of the skull and the bones of the upper jaw, the palate and the operculum (Gross & Hanken 2008). The neurocranium is also of mixed origin. It is the earliest encapsulation of the brain and the sensory organs during development and protects them against exterior forces. The anterior trabeculae cranii are neural crest derived and the posteriorly situated parachordals and otic capsules are derived from the cranial mesoderm (Couly et al. 1992). The viscerocranium consists of the pharyngeal arches which give rise to important structures of the vertebrate head. The rostral-most arch is involved in the evolution and development of the gnathostome jaw and therefore called the mandibular arch (Shigetani et al. 2005). It consists of the dorsal palatoquadrate and the ventral Meckel´s cartilage. The pharyngeal arches are neural crest derived (Jiang et al. 2002; Olsson & Hanken 1996; Gross & Hanken 2008). The neural crest is an embryonic tissue of pluripotent cells which is unique to vertebrates. Neural crest cells are highly movable and capable of developing into a variety of different cell types (Bronner & LeDouarin 2012). The neural crest develops during ontogeny at the border of the neural plate where the cells are specified by combinatorial gene expression. After that they pass through a nearly complete epithelial-to-mesenchymal transition and begin to delaminate. They migrate in three molecularly distinct streams, which arose in the vertebrate stem (Square et al. 2016), along determined pathways in the developing head to their final position where they differentiate dependent on local gene expression into the respective cell type (Bronner & LeDouarin 2012). The chondrogenic fate is regionalized within the cranial neural crest. The anterior regions contribute to the anterior cartilages of the head skeleton and posterior regions to posterior cartilages (Olsson & Hanken 1996). The anterior stream of neural crest cells, the mandibular stream, gives rise to the palatoquadrate, Meckel´s cartilage and the rostral cartilages in anurans. A second stream, the hyoid stream, gives rise to the ceratohyal and the basicranial plate, whereas the posterior stream, the branchial stream gives rise to the branchial basket. The posterior basicranial plate, the otic capsules, the basihyal and the basibranchial are not derived from the cranial neural crest (Olsson & Hanken 1996; Sadaghiani & Thiébaud 1987). The otic capsules are at least partially neural crest derived (Gross & Hanken 2008). The cranial neural crest and its pluripotent cells are unique to vertebrates and enable them to develop a large variety of different cell types. During vertebrate evolution various cell types which were present in non-vertebrate chordates and invertebrates were unified by the neural crest, which shows combined mesenchymal and ectodermal features. Therefore, the neural crest is often seen as the “fourth germ layer” because this novel cell population transformed the triploblastic chordate body plan into a complex quadroblastic one and led to a diversification of cell types (Bronner & LeDouarin 2012).

Early *Hox* and *dlx* expression pattern the developing gnathostome embryo

The shape of neural crest derived cartilages in the head of larval anurans depends on the existence of mainly two patterning processes in cranial neural crest progenitor cells (Figure 3). A patterning program exists which defines the anterior-posterior identity of the pharyngeal arches. Another program defines the dorsoventral identity within each of the pharyngeal arches. The expression of the so-called *Hox* genes establishes a gradual anterior-posterior pattern before the cranial neural crest progenitor cells begin to migrate. The expression of *Hox* genes provide positional information on which the morphological differentiation of the different pharyngeal arches is based (Rijli et al. 1993; Couly et al. 1998; Pasqualetti et al. 2000). *Hox* genes are expressed in a nested pattern along the anterior-posterior axis in gnathostomes. The first pharyngeal arch, which forms the jaw in all vertebrates except mammals, is defined by the absence of *Hox* transcripts ("Hox code-default") and the second pharyngeal arch is defined by the expression of *Hoxa2*. With every arch one *Hox* gene more is expressed and the combination of expressed *Hox* genes act as a combinatorial code for the specific arch (Kuratani 2012; Baltzinger et al. 2005; Minoux et al. 2010). This patterning program was present at the base of the gnathostomes, whereas in the agnathans, which lack jaws and have uniform pharyngeal arches, a more primitive *Hox* code is present. Only two *Hox* genes are expressed in the agnathan lamprey which define the *Hox*-free first pharyngeal arch, the second pharyngeal arch and the following pharyngeal arches 3-9 (Takio et al. 2004; Takio et al. 2007; Kuratani 2012; Shigetani et al. 2005). Both *Hox* codes share a common vertebrate ancestor but the differences in the *Hox*

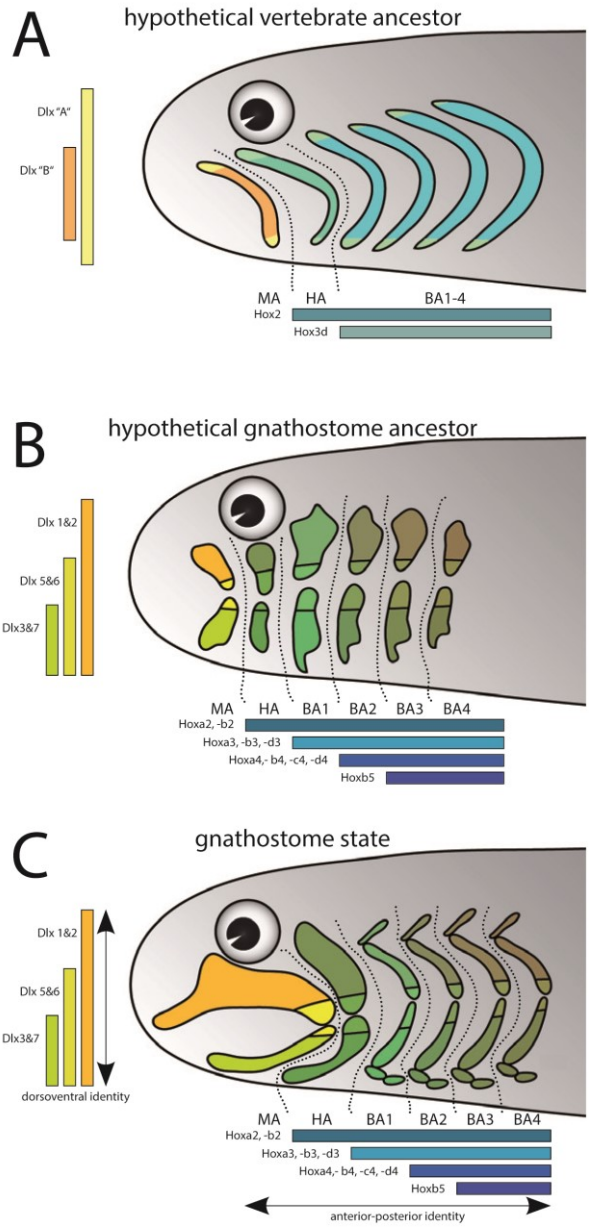

Figure 3: Comparison of dorsoventral and anterior-posterior patterning gene expression. **A** Reconstruction of the expression in a hypothetical vertebrate ancestor based on the expression patterns in lamprey and zebrafish. **B** Gene expression in a hypothetical gnathostome ancestor. **C** Gnathostome state of dorsoventral and anterior-posterior patterning. Expression based on Square et al. (2016), Shigetani (2005), Kuratani (2012) and Depew (2002).

code of agnathans and gnathostomes are one reason for the uniform morphology of the agnathan pharyngeal arches and the emergence of pharyngeal arches which are able to develop and evolve independently from each other in gnathostomes. Thus, the *Hox* code of gnathostomes is one requirement for the evolution of the gnathostome jaw, as it enables the first pharyngeal arch to develop independently from the posterior arches.

Each pharyngeal arch which is defined by the expression of *Hox* -genes is patterned in the dorsoventral direction through the nested expression of *dlx* genes (Beverdam et al. 2002; Depew et al. 2002). The evolution of this patterning program is considered to have been essential for the evolution of a distinct jaw joint because lampreys lack a gnathostome-like *dlx*-mediated dorsoventral patterning (Shigetani et al. 2005; Depew et al. 2002). A nested dlx pattern was present in the vertebrate ancestor but evolved differently in agnathans and gnathostomes (Square et al. 2016). Through the *dlx*-code three nonoverlapping domains are established within each pharyngeal arch in gnathostomes (ventral, intermediate and dorsal domain). The dorsal domain is established through the expression of *dlx*1&2, the intermediate domain through the expression of *dlx*1&2 and 5&6 and the ventral domain through the expression of *dlx*1&2, 5&6 and 3&7 (Depew et al. 2002). This patterning enables locally restricted expression of regulators downstream of the respective *dlx* gene. This could lead to the independent evolution and development of each domain within a pharyngeal arch. In gnathostomes, *hand2* is expressed most ventrally in the ventral domain of the first pharyngeal jaw. Its expression is restricted dorsally by the *barx1* expression domain. In the intermediate domain, which gives rise to the jaw joint, *bapx1* is expressed (Nichols et al. 2013). This gene is thought to play a major role in the evolution and development of the gnathostome jaw joint (Cerny et al. 2010; Square et al. 2015).

Together the two patterning processes form a grid which enables independent inter- and intra-pharyngeal arch development. Each pharyngeal arch can evolve more or less independently from the other pharyngeal arches. Even within one pharyngeal arch, morphological differences are possible through the establishment of different domains. Both patterning systems are a crucial requirement for the evolution of the jaw. A jaw per definition is the connection of a dorsal and a ventral element via a joint. To achieve this, skeletal elements must be present. This is warranted through the neural crest cells, which develop into chondrocytes and distinct pharyngeal arches during development. Furthermore, the anterior pharyngeal arch must evolve independently from the other pharyngeal arches. Therefore, the *hox*-code is needed. At least a dorsal and a ventral element have to develop independently and in between a region must be present which develops into a joint. Through the *dlx*-code, which defines three distinct domains, the latter point is also possible. Now only proper regulatory elements which can induce joint development are needed.

Bapx1 homologs are widespread within distantly related phyla

Bapx1 is part of the NK family of homeobox genes (Kim & Nirenberg 1989). Genes which belong to the NK family were present in the last common ancestor of sponges, cnidarians and bilaterians and they were the foundation for the emergence of the developmentally

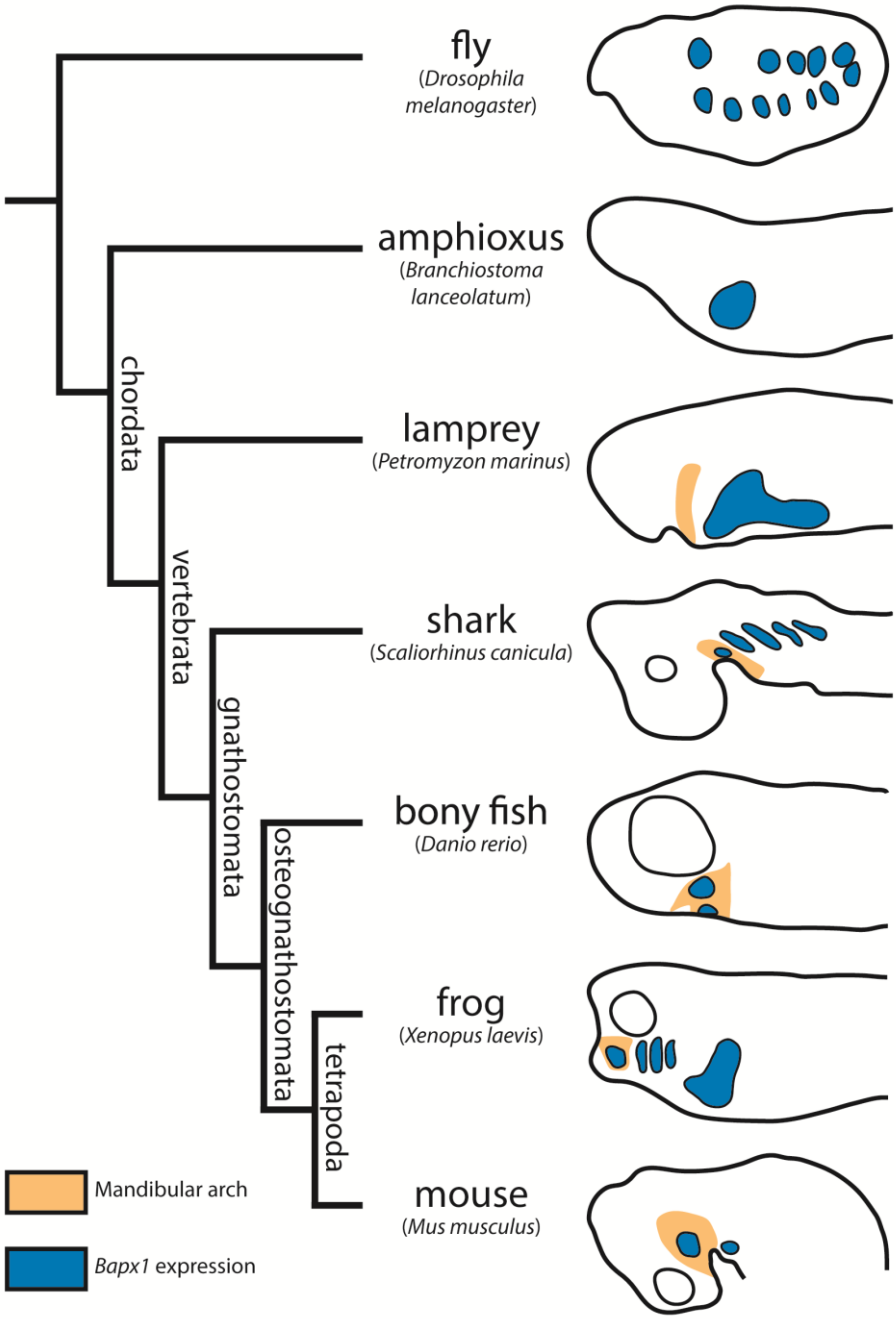

Figure 4: *Bapx1* expression in different distantly related taxa. *Bapx1* expression domains are based on in situ hybridisation data (Stathopoulos et al. 2004; Meulemans & Bronner-Fraser 2007; Cerny et al. 2010; Compagnucci et al. 2013; Miller 2003; Square et al. 2015; Tribioli et al. 1997).

important hox genes (Larroux et al. 2007). Homologs of the basal *bapx1* are present in many distantly related taxa (Figure 4). *Bapx1* was first identified in *Drosophila melanogaster* (Kim & Nirenberg 1989). It is expressed in the dorsal mesoderm during midgut formation and regulates the specification of the visceral mesoderm. It subdivides the mesoderm and is an important factor in midgut musculature formation (Azpiazu & Frasch 1993). In amphioxus a homologous *bapx1* is initially expressed in the medial somite. In the early larvae it is expressed in the pharyngeal endoderm in the area where the first gill slit arise during further development (Meulemans & Bronner-Fraser 2007). In lamprey *bapx1* is expressed in the

epidermis of the ventral pharynx but it is not expressed within the first pharyngeal arch (Cerny et al. 2010). In the shark *Scaliorhinus canicula*, the homologous *ScBapx1* is expressed in the first pharyngeal arch around the maxillary-mandibular constriction. In the caudal pharyngeal arches *ScBapx1* is expressed in the endoderm and ectoderm associated with the pharyngeal clefts (Compagnucci et al. 2013). In zebrafish *bapx1* is also expressed in an intermediate domain of the first pharyngeal arch and in the pharyngeal clefts of the pharyngeal arches 2-6 (Miller 2003). The anuran homologous gene *xbap* (*Xenopus* bagpipe) is expressed ventrolateral to the oral cavity in the first pharyngeal arch, precisely where the primary jaw joint develops later. Additionally, it is expressed in the endoderm of the pharyngeal pouches of the pharyngeal arches 3-5 and in the anterior gut mesoderm (Square et al. 2015; Newman et al. 1997). The expression domain is clearly reduced in mice. *Bapx1* is expressed in a small intermediate domain of pharyngeal arch 1 between the postero-dorsal tip of Meckel´s cartilage and the antero-ventral tip of the palatoquadrate and in a respective domain in pharyngeal arch 2 (Tribioli et al. 1997). *Bapx1* is also expressed in the early ontogeny of humans (Yoshiura & Murray 1997). Mutations, expression imbalance and epigenetic dysregulation of *bapx1* are thought to lead to serious skeletal disorders such as oculo-auriculo-vertebral spectrum and spondylo-megaepiphyseal-metaphyseal dysplasia (Hellemans et al. 2009; Fischer et al. 2006). The incorporation of *bapx1* into the first pharyngeal arch, which gives rise to the jaw joint, at the origin of the gnathostomes strongly suggests a role for *bapx1* in the evolution of that joint. Unfortunately, the results from knockdown experiments in different gnathostome taxa are contradictory.

In zebrafish the functional knockdown of *bapx1* leads to the fusion of Meckel´s cartilage and the palatoquadrate and thereby to the loss of the primary jaw joint. Furthermore, the retroarticular process of Meckel´s cartilage (the process which forms the articulation with the articular process of the palatoquadrate) and the retroarticular bone which ossifies perichondrally on the retroarticular process are lost after knockdown of *bapx1* in zebrafish (Miller 2003). Based on these results *bapx1* was hypothesized to specify the jaw joint. The gain of *bapx1* function through the knockdown of the *bapx1* antagonist *barx1* in zebrafish leads to the formation of ectopic joints (Nichols et al. 2013). This substantiates the joint inducing/forming function of *bapx1* in actinopterygians. Unfortunately, the inactivation of *bapx1* in mice did not lead to the fusion of the homologues of Meckel´s cartilage and palatoquadrate. The nonmammalian primary jaw articulation has been replaced in mammals by a secondary jaw joint which develops between the squamosal and the dentary (Fleischer 1978; Allin & Hopson 1992). The former elements which form the jaw articulation in nonmammalian vertebrates became incorporated into the mammalian middle ear such that Meckel´s cartilage is homologous to the malleus and the palatoquadrate is homologous to the incus (Reichert 1837). Based on the results in zebrafish, *bapx1* inactivation should lead to loss of the articulation between malleus and incus, but the articulation remains unperturbed after *bapx1* inactivation in mice. This contradicts the results from zebrafish and raises the question if *bapx1* is the main reason for the evolution and development of the primary jaw joint. To gain further insights into this specific question, the function of *bapx1* in further organisms needs to be tested. Amphibians have a unique phylogenetic position

because they are the most basal branch of tetrapods and the only terrestrial anamniotes. This specific position makes amphibians interesting for evolutionary and developmental issues. It is possible that downstream targets of bapx1 evolved during the evolution of mammals, which could explain the unexpected results in mice. But it can not be excluded that in early evolution either *bapx1* or its up- and downstream targets changed their function. To address this question this work presents data from an additional taxonomic group, the amphibians, which were gathered in gain-of-function and loss-of-function experiments of *bapx1* in *Xenopus laevis*, a derived anuran species, in *Bombina orientalis*, a more basal anuran species and in *Ambystoma mexicanum*, an urodele amphibian. Some aspects of *dlx* and *hox* patterning are conserved between agnathans and gnathostomes. It can be expected that precursors of these patterning programs were present in their last common ancestor. This pattern may have been dividing the cranial neural crest cells into several domains, which are specified by a combination of specific genes in all pharyngeal arches. From this ancestral pattern agnathans and gnathostomes evolved in different directions. In agnathans no jaws evolved, in contrast to in gnathostomes. The expression of *bapx1* may be one reason. *Bapx1* was exclusively co-opted to the intermediate first pharyngeal arch domain and disrupted the ancestral continuous *Barx* expression. This co-option of *bapx1*, a gene which inhibits cartilage formation, refined the prepatterned ancestral dorsoventral pattern and the following recruitment of specific joint forming genes (e.g. *gdf5*, *gdf6*, *gdf7*) may have been a key to the evolution of the gnathostome jaw (Cerny et al. 2010). Gnathostome *bapx1* first pharyngeal arch expression depends on *dlx* function which defines an intermediary domain where *bapx1* is expressed (Talbot et al. 2010). The expression domain in the first pharyngeal arch, together with the results from knockdown experiments in different taxa, strongly suggest a role for *bapx1* in the evolution and development of the jaw joint, but additional data from amphibians is needed to test this hypothesis.

Aims of this study

A general overview of the development of a frequently used model organism was the starting point for this work to interpret the following experimental results. The present work wants to provide further insight on the underlying mechanisms of evolution through the combination of classic morphological techniques and modern molecular methods. Another goal of this work is to offer new pieces of evidence to understand vertebrate evolution. The interpretation of ontogenetic malformations shall explain phylogenetic changes of several structures. Further goals are:

- ➔ To reveal a possible mechanism able to generate evolutionary novelties.
- ➔ To provide a comprehensive overview on the early skeletal development of *Xenopus laevis*.
- ➔ To investigate the function of *bapx1* in different amphibian taxa.
- ➔ To confirm the joint inducing and cartilage preventing function of *bapx1* during ontogeny.
- ➔ To define the role of *bapx1* for the evolution of the primary jaw joint and for evolutionary novelties in general.

Chapter 1

Sequence and timing of early cranial skeletal development in *Xenopus laevis*

The paper gives an overview of the early development of the cartilaginous head skeleton in *Xenopus laevis* tadpoles from the onset of chondrification until the premetamorphic stage. The timing and sequence of chondrogenesis in *Xenopus laevis* presented here offers a powerful tool for developmental biologists which alter skeletal development or which investigate the skeletal development in different taxa. The discussion highlights mistakes in the available literature about the skeletal development of *Xenopus laevis*, similarities of the pattern of chondrogenesis in anurans and other vertebrates and the late appearance of anuran- and pipoid-specific cartilaginous structures.

Paul Lukas & Lennart Olsson

Published in Journal of Morphology

PL and LO developed the concept and design of the study. PL was responsible for the experimental procedures including clearing-and- staining, immunostainings, 3D-reconstructions as well as histology. Analysis and interpretation of the data mentioned was mainly done by PL, who was also responsible for the drafting of the manuscript and its final form. LO critically revised the manuscript.

Received: 21 June 2017 | Revised: 1 September 2017 | Accepted: 5 September 2017

DOI: 10.1002/jmor.20754

RESEARCH ARTICLE

WILEY JOURNAL OF morphology

Sequence and timing of early cranial skeletal development in Xenopus laevis

Paul Lukas | Lennart Olsson

Institut für Spezielle Zoologie und Evolutionsbiologie mit Phyletischem Museum, Friedrich-Schiller-Universität, Jena, Germany

Correspondence
Paul Lukas, Institut für Spezielle Zoologie und Evolutionsbiologie mit Phyletischem Museum, Friedrich-Schiller-Universität Jena, Erbertstr. 1, 07743 Jena, Germany.
Email: paul.lukas@uni-jena.de

Funding information
Deutsche Forschungsgemeinschaft, Grant/Award Number: OL134/10-2;
Studienstiftung des Deutschen Volkes

Abstract

Xenopus laevis is widely used as a model organism in biological research. Morphological descriptions of the larval cartilaginous skeleton are more than half a century old and comprehensive studies of early cartilage differentiation and development are missing. A proper understanding of early cranial skeletal development in X. laevis requires a detailed description that can function as a baseline for experimental studies. This basis makes it possible to evaluate skeletal defects produced by experiments on gene interactions, such as gain- or loss-off unction experiments. In this study, we provide a detailed description of the pattern and timing of early cartilage differentiation and development in the larval head of X. laevis. Methods used include antibody staining, confocal laser scanning microscopy and 3D-reconstruction. Results were than compared to earlier studies based on classical histological approaches and clearing-and-staining. The first cartilage to chondrify is, in contrast to other vertebrates investigated so far, the ceratohyal. The components of the branchial basket chondrify in anterior-to-posterior direction as reported for other amphibians. Chondrification of different cartilages begins at different stages and the majority of cartilages are fully developed at Ziermann and Olsson stage 17. Our baseline data on the pattern and timing of early cartilaginous development in X. laevis is useful for evaluation of experiments which alter head skeletal development as well as for identifying heterochronic shifts in head development in other amphibians.

KEYWORDS
anura, cartilage differentiation, chondrogenesis

1 | INTRODUCTION

The comparative morphology and development of the vertebrate skull has been of great interest to generations of evolutionary biologist. Modern morphological as well as molecular studies refer mostly to only a few so-called model organisms (chicken, zebrafish, mouse, etc.). Xenopus laevis is often used as a model to represent anurans or even amphibians (Cannatella & De S á, 1993). Its development and morphology has been investigated for more than a century. Initial descriptions and depictions of the larval and adult skull of X. laevis (5 Dactylethra capensis) were published by Parker (1876, 1879). Further investigations were done on the development of the hypobranchial skeleton (Ridewood, 1897) followed by detailed behavioural descriptions at the beginning of the 20th century (Bles, 1906). Specimens collected by Bles were the basis for further analysis of the masticatory muscles (Edgeworth, 1930) and of external features (Peter, 1931). More detailed chondrocranial investigations were also published early (Dreyer, 1914; Kotthaus, 1933; Paterson, 1939; Ramaswami, 1941; Weisz, 1945a,b). Several functional analyses, which revealed the feeding and water pumping mechanisms followed (Gradwell, 1971; Satel & Wassersug, 1981; Seale & Wassersug, 1979; Wassersug & Hoff, 1979) as well as descriptions of cranial skeletal ossification (Bernasconi, 1951; Smit, 1953; Trueb & Hanken, 1992), development of single cartilages (Place, 1986, 1987; Thomson, 1986, 1987, 1989), cranial muscle homologies (Haas, 2001) and cranial muscle development (Ziermann & Olsson, 2007b) among others.

The cranial skeleton and the development of the larvae of X. laevis are unique in several aspects. The cornua trabeculae and the suprarostral cartilages are fused and form a suprarostral plate. The palatoquadrate bears a processus cornu quadratus lateralis, which unites with a lateral outgrowth of the suprarostral plate to form a tentacular cartilage. The processus muscularis palatoquadrati is reduced and the

commissura quadratocranialis anterior is broad. An urobranchial processus is absent. The crista parotica is extended and three craniobranchial commissures are present. The subocular cartilage is thin and bears a processus ventrolateralis posterior. The palatoquadrate de velops in two separate portions and Meckel 's cartilage develops precociously (De Sá & Swart, 1999; Frost et al., 2006; Haas, 2003; Sokol, 1975, 1977; Trueb & Hanken, 1992).

Cells which contribute to the larval head skeleton of X. laevis have been shown to be mainly neural-crest derived (Gross & Hanken, 2008; Olsson & Hanken, 1996; Sadaghiani & Thi ébaud, 1987). The identity and shape of these cells along the anterior-posterior body axis depends on the expression of homeobox genes in the progenitor cells before migration (Rose, 2009). Dlx genes pattern and give identities to the cranial neural-crest cells in the dorso-ventral direction (Beverdam et al., 2002; Depew, Lufkin, & Rubenstein, 2002). Both systems together form a grid that regionalises the developing larval head and therefore enables developmental and evolutionary differences as well as evolutionary novelties.

From developmental stage NF 48 (Nieuwkoop & Faber, 1994) onwards detailed descriptions of Xenopus cartilaginous head morphology are present in the literature (Candioti, 2007; Sedra & Michael, 1957; Trueb & Hanken, 1992). Earlier stages are occasionally available but the descriptions differ greatly in accuracy, anatomical ontology, and accessibility. Moreover, a description of the sequence and timing of the development of the head skeleton of X. laevis from the first condensations to the finished cartilaginous skeleton is missing. Only a few investigations on early chondrogenesis were done in anurans more than a century ago (Gaupp, 1906; St 6hr, 1882). Furthermore, comparisons ofi nvestigations on early skeletal development in X. laevis are problematic because of differences in the origin of the animals, staging of the embryos and larvae, methodological approach, and number ofl arvae investigated (Trueb & Hanken, 1992). Especially the use of different staging methods is problematic. It has been shown that X. laevis larval development is variable at different rearing conditions (Godfrey & Sanders, 2004; Hilken, Dimigen, & Iglauer, 1995; Ibler & St 6hr, 2008) which makes staging of embryos and larvae by age and/or length problematic.

Xenopus laevis is widely used in gain-of-function (Lavery & Hoppler, 2009), morpholino (Blum, De Robertis, Wallingford, & Niehrs, 2015; Eisen & Smith, 2008), and CRISPR/Cas9 (Wang et al., 2015) experiments as well as in toxicological studies (ASTM, 1991; Bantle, 1991; Bantle et al., 1999; Wagner, M 6ller, & Viertel, 2017). Depending on the gene expression altered, or the chemical substance tested, these experiments may alter the skeletal development in the larval head. Therefore, a detailed reference is needed to detect and identify changes in skeletal development caused by experimental treatments of X. laevis larvae.

Here, we provide a comprehensive description of the timing and differentiation of the cartilaginous head skeleton in X. laevis of NF 37 – 48. Our data can serve as a baseline for the identification of heterochronic shifts in the development of cartilages in studies that compromise Xenopus head skeletal development and as a foundation for further studies of head skeletal development in other anuran tadpoles.

2 | MATERIALS AND METHODS

Xenopus laevis (Daudin, 1802) adults were obtained from the Centre de Ressources Biologiques X énopes in Rennes, France. They were kept in our departmental breeding colony at 22 8C. Ovulation was induced by injection of 600 units of human chorionic gonadotropin (HCG) into the dorsal lymph sac of the females. For the induction of amplexus, 200 units of HCG were injected into the dorsal lymph sac of the male frogs. Single-pair mating and egg deposition took place at 15 8C in a darkened basin. The eggs obtained were dejellied using 2% cysteinehydrochloride and then cultured under different conditions ranging from 18 to 23 8C in 0,1x modified Barth 's saline (MBS). Developmental series from defined stages between NF 37 and NF 48 were taken from the clutch. We noticed that the skeletal development correlated well with the timing of head muscle development reported by Ziermann and Olsson (2007b) and have staged our specimens according to this alternative staging table (Ziermann & Olsson, 2007a). A table which shows the equivalent Nieuwkoop and Faber stage to each Ziermann and Olsson stage is available in the Supporting Information to the work of Ziermann and Olsson (2007b). Description of results are based on this latter staging system. Anaesthesia was performed using 1% tricaine methanesulfonate (MS-222) according to the animal welfare protocols at Friedrich-Schiller-University Jena. Depending on further investigations, larvae were fixed either in 4% phosphate-buffered formalin (PFA) or in Dent 's fixative. For examination ofi ntraspecific variation, a maximum of ten larvae per stage and method from different breeding groups were investigated. In total, 364 larvae were used in this study. Dissected larvae, whole-mount antibody stained and cleared-and-stained larvae are kept at the Institut f 6r Spezielle Zoologie und Evolutionsbiologie mit Phyletischem Museum, Friedrich-Schiller-University, Jena.

To study the cellular development of the head skeleton, PFA-fixed larvae were used for serial sectioning. Larvae were dehydrated in an ethanol series and embedded in paraffin. Sectioning was performed at 7 mm using a microtome (Microm, HM 355 S). Paraffin sections were stained with Heidenhain 's Azan technique (Heidenhain, 1915). Images were taken with an XC10 Olympus camera mounted on an Olympus BX51 microscope operated with dotSlide software. Whole-mount clearing-and-staining was done following the protocol provided by Dingerkus and Uhler (1977) with the alteration that no alizarin red was used due to the absence of bones in the stages investigated. Specimens were examined and images were taken using a Zeiss Stemi SV11 and an attached camera (ColorView) operated by AnalySIS software.

We used whole-mount antibody staining to gain a better three-dimensional understanding of the changes during cartilage development. Specimens fixed with Dent 's fixative were treated with monoclonal antibodies against collagen II (116B3-collagen II) to stain cartilages. Alexa 488 was used as a fluorescent secondary antibody. Image stacks (10 mm z-plane, 1AU) were produced using a confocal laser scanning microscope (LSM 510, Zeiss). Based on these stacks, 3D-images of the cartilaginous structures were reconstructed using Amira 6.0.1. for surface rendering and Autodesk Maya ® 2017 for smoothing and rendering of pictures.

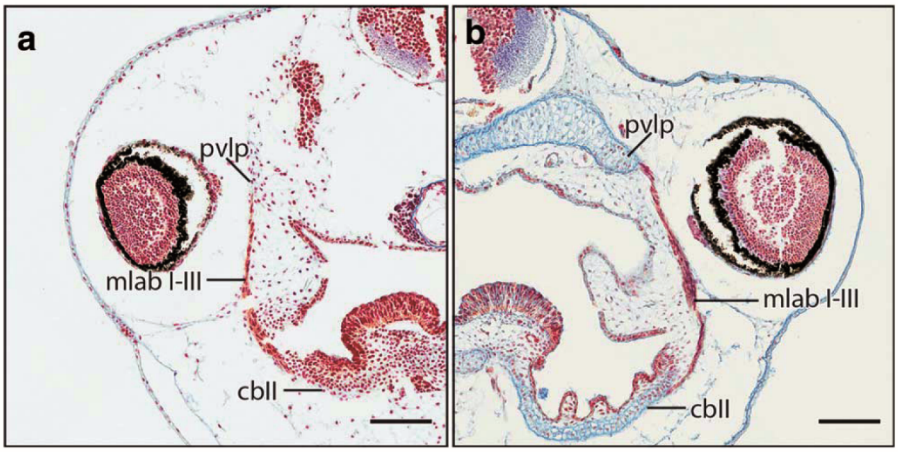

FIGURE 1 Xenopus laevis, transverse histological sections of larval stage NF 43 shows the discrepancy between NF staging and the cartilaginous developmental state of the larva. (a) mesenchymal anlage of processus ventrolateralis posterior and precartilaginous ceratobranchial II resemble the condition of a ZO 12 whereas in (b) processus ventrolateralis posterior and ceratobranchial II are chondrified as in ZO 15. Scale bar 100 mm. cbII, ceratobranchial II; mlab I –III, m. levatores arcuum branchialium I –III; pvlp, processus ventrolateralis posterior

3 | RESULTS

All tadpoles were initially staged after fixation according to the staging table of Nieuwkoop and Faber (1994). However, comparison of tadpoles at the same stage revealed that the external morphology, on which the staging table is based, does not correspond to internal skeletal development. The internal development can vary up to two stages in each direction. That means the cartilaginous skeleton of a NF 43 tadpole can be at the same state as the skeleton of a NF 41 or a NF 44 tadpole (Figure 1). Therefore, Ziermann and Olsson staging (ZO) from the detailed staging table of Ziermann and Olsson (2007a) was used instead. The sequence of skeletal development does not vary between tadpoles raised at different temperatures. Naming of cartilaginous structures and corresponding abbreviations follow the guidelines of Xenopus Anatomical Ontology (Segerdell, Bowes, Pollet, & Vize, 2008; Segerdell et al., 2013) (see als Supporting Information for terminological concordance with earlier publications).

3.1 | Infrarostral

In premetamorphic Xenopus laevis the infrarostral is an unpaired cartilage within the lower jaw. At ZO 6, where most cartilages are present as mesenchymal anlagen, no evidence of early precursors of the infrarostral can be seen. The mesenchymal anlage of the infrarostral arises as a small, spherical condensation of mesenchymal cells between the mesenchymal anlagen of Meckel 's cartilage dorsal to the anlagen of the m. geniohyoideus and ventral to the pharyngeal cavity at ZO 8 (Figure 2a). During the further stages the anlage of the infrarostral remains mesenchymal. At ZO 13, chondroblasts become visible and start to condense as a v-shaped precartilaginous band between the anterior tips of Meckel 's cartilage and the region is reached by the developing m. geniohyoideus (Figure 2b). At the transition between ZO 14 and ZO 15 the precartilaginous anlage of the infrarostral chondrifies as a small rod on which the m. geniohyoideus inserts (Figures 3c and 4a). An intramandibular joint has not yet formed. The infrarostral cartilage broadens anteriorly and fills the gap between the anterior tips of Meckel's cartilage. From ZO 16 onwards the intramandibular joint is properly formed and proceeds transversally between the infrarostral and Meckel's cartilage (Figure 4a).

3.2 | Meckel 's cartilage

Two separate, mesenchymal anlagen of Meckel 's cartilage are visible at the posterior end of the cement gland, ventral to the pharyngeal cavity at ZO 6 (Figure 2D). They unite at the level of the anterior end of the eyes with the anlage of the infrarostral cartilage and form a continuous vertical band. The two anlagen then separate and proceed laterally until the mesenchymal anlage of the palatoquadrate appears. Differentiated muscle cells of the m. levator mandibulae longus superficialis and of the m. quadrato-hyoangularis are present next to the anlagen of Meckel's cartilage. At ZO 9, the chondroblasts condense and form two spheres ventral to the pharyngeal cavity (Figure 2E). At ZO 11, Meckel's cartilage is chondrified and starts to extend posterolaterally (Figures 3c,d and 4a). A gap between Meckel 's cartilage and the palatoquadrate is visible, but no retroarticular process has yet formed. The rudiment of the m. quadratohyoangularis attaches onto the posterior edge (Figure 2f) whereas the developing m. levator mandibulae longus superficialis attaches dorsally onto the lateral edge of Meckel 's cartilage. The rudiment of the m. levator mandibulae articularis inserts more posteriorly. From ZO 13 onwards, the developing intermandibularis muscles connect the two cartilages by originating from them and inserting in a common median raphe. At the same stage the processus retroarticularis begins to form. The development of this processus is finished at ZO 14, when a proper joint is formed between it and the processus muscularis. During

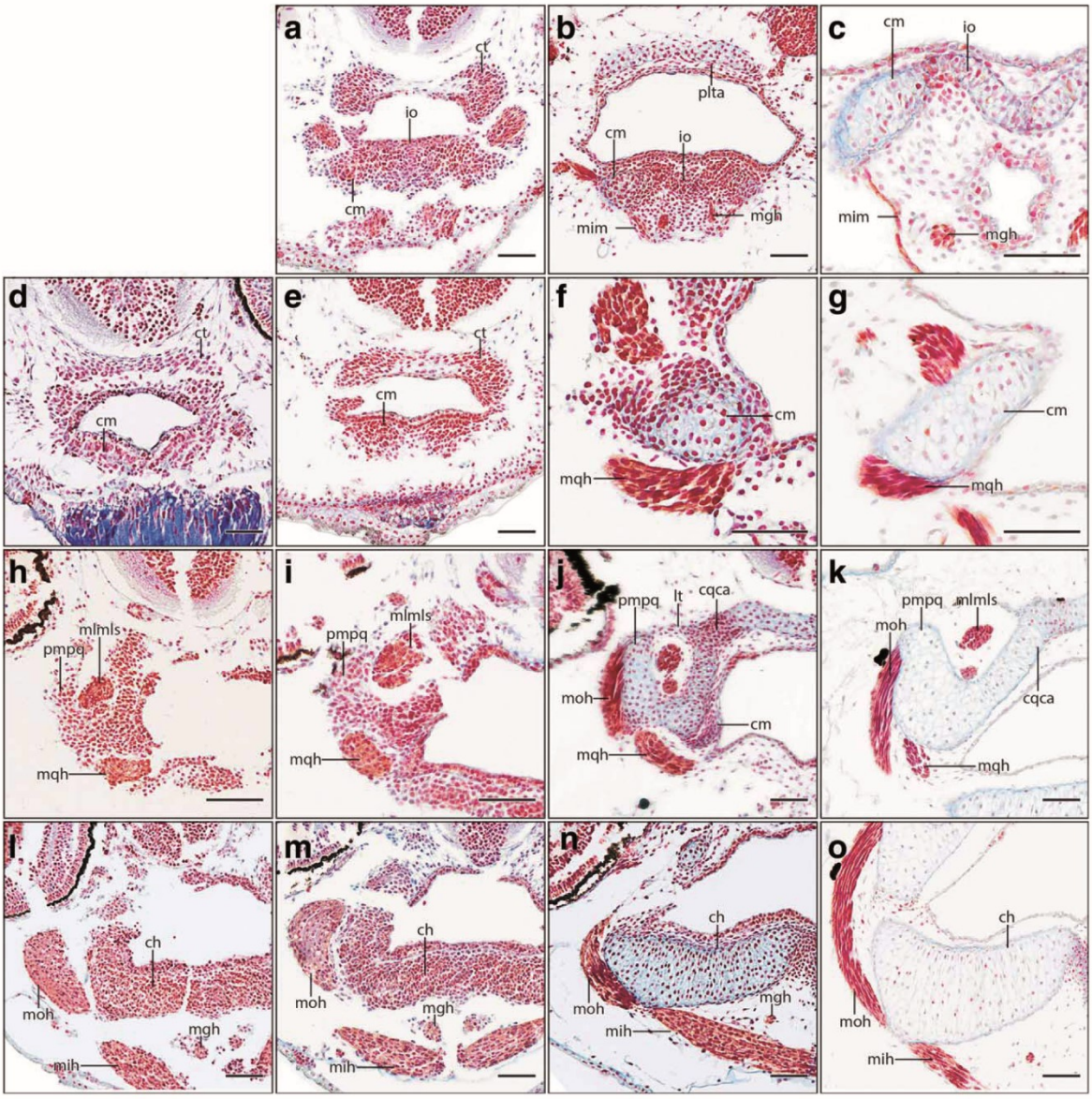

FIGURE 2 Xenopus laevis transverse histological sections of larval stages ZO 6 (first column) ZO 8 (second column), ZO 13 (third column), and ZO 17 (fourth column). (a–c) development of the infrarostral. (d–g) development of Meckel's cartilage. (h–k) development of the anterior palatoquadrate and its processes. (l–o) development of the ceratohyal. Scale bar 50 mm. ch, ceratohyal; cm, Meckel's cartilage; cqca, commissura quadratocranialis anterior; ct, cornua trabeculae; io, infrarostral; lt, ligamentum tectum; mgh, m. geniohyoideus; mih, m. interhyoideus; mim, m. intermandibularis; mlmls, m. levator mandibulae longus superficialis; moh, m. orbitohyoideus; mqh, m. quadrato-hyoangularis; plta, planum trabeculare anticum; pmpq, processus muscularis palatoquadrati

the following stages, Meckel's cartilage elongates further posterolaterally and develops a slightly sigmoid shape (Figure 4a).

3.3 | Suprarostral plate

The suprarostral plate is a common feature of pipoid larvae and develops through the fusion of the cornua trabeculae, the anterior process of the ethmoid plate and the suprarostral (De Sá & Swart, 1999). Two mesenchymal anlagen of the cornua trabeculae arise during ZO 6 ventromedial to each olfactory pit and dorsal to the pharyngeal cavity. They condense through ZO 9–12. At ZO 13, both rods are chondrified and connected to the planum trabeculare anticum (Figure 2b). The gap between the two cornua trabeculae is filled with undifferentiated cells which represent the anlage of the suprarostral. The suprarostral plate is properly formed at ZO 17 due to the chondrification of the suprarostral condensation between the two trabeculae (Figure 4b). The plate broadens anteriorly and surrounds the nasal pit (Figure 4b). A small rod develops anterolaterally, extends distally from ZO 20 onwards and forms or supports the tentacular cartilage (Figure 5a).

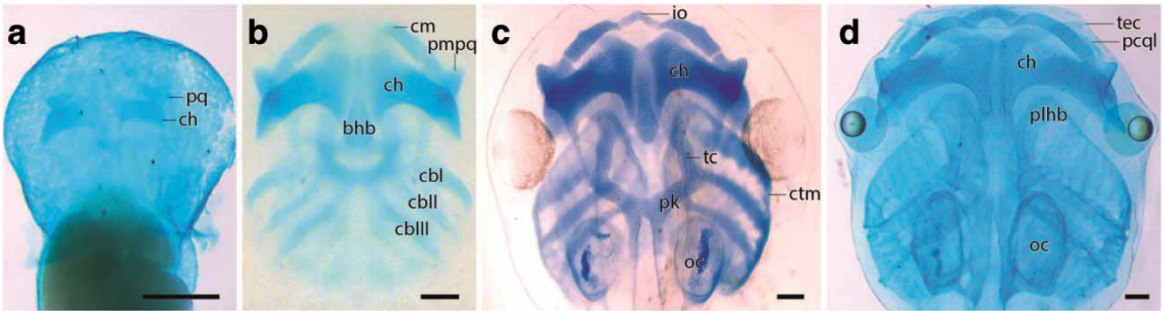

FIGURE 3 Xenopus laevis development of the cartilaginous head skeleton in larvae at different developmental stages in ventral view visualized through cleared-and-stained specimens. (a) ZO 10,5. (b) ZO 13,5. (c) ZO 17. (d) ZO 20. Scale bar 100 mm. bhb, basihyobranchial; cbI-III, ceratobranchial I –III; ch, ceratohyal; cm, Meckel´s cartilage; ctm, commissura terminalis; io, infrarostral; oc, otic capsule; pk, parachordal; pcql, processus cornu quadratus lateralis; plhb, planum hypobranchiale; pmpq, processus muscularis palatoquadrati; pq, palatoquadrate; tc, trabeculae cranii; tec, tentacular cartilage

3.4 | Palatoquadrate

The palatoquadrate develops from two mesenchymal condensations that fuse during development. The mesenchymal anlage of the anterior portion appears at ZO 6, flanking the pharyngeal cavity laterally on both sides (Figure 2h). The u-shaped anlage is bordered laterally by the developing m. orbitohyoideus, lateroventrally by the m. quadrato-hyoangularis and dorsally by the m. levator mandibulae longus superficialis. The lateral part is the mesenchymal anlage of the processus muscularis, the median part is the mesenchymal anlage of the portion which will connect the palatoquadrate to the chondrocranium via the commissura quadratocranialis anterior (Figure 2i). Ventrally, a bar of undifferentiated cells starts to elongate posteriorly. This is likely the anlage of the subocular cartilage. Precartilaginous anlagen of the processus muscularis and the palatoquadrate are present at ZO 9. The developing m. levator mandibulae articularis attaches to the precartilaginous processus muscularis at ZO 10. One stage later the palatoquadrate and its processus muscularis chondrify (Figure 4c). At the same time, the processus articularis and the subocular cartilage start to condense. The latter is extending posteriorly and its anterior part chondrifies at ZO 12. Posteriorly, its cells are still condensed and reach almost to the condensation of the parachordal. In further development, the processus muscularis extends dorsomedially. The extended processus muscularis connects with the planum trabeculare anticum at ZO 13 via the commissura quadratoorbitalis. This causes the m. levator mandibulae longus superficialis and articularis to be surrounded by cartilages (Figure 2h). The commissura quadratoorbitalis persists for one stage and is then replaced by a ligamentum tectum. At ZO 13, the anterior palatoquadrate is anchored to the chondrocranium via the recently chondrified commissura quadratocranialis anterior (Figure 2j). An earlier connection of both parts occurs infrequently. The processus articularis chondrifies and a proper jaw joint forms. The posterior portion of the palatoquadrate became visible as a condensation anterolateral to the parachordal (processus ventrolateralis posterior). The anterior portion of the m. levator arcuum branchialium I-III originates from this condensation. At ZO 15, the precartilaginous anlage of the processus ventrolateralis chondrifies and is connected to the parachordal and the subocular cartilage via the condensed processus ascendens palatoquadrati and the condensed posterior tip of the subocular cartilage, respectively (Figures 4c and 5b). The posterior tip of the subocular cartilage chondrifies at ZO 16 in most specimens and connects the anterior and the posterior portion of the palatoquadrate (Figure 4c). This connection of both parts can also occur later in development until ZO 20. The entire palatoquadrate is connected to the chondrocranium through the newly chondrified processus ascendens. Simultaneously, the fenestra subocularis is formed. Anterolaterally, the anlagen of the processus cornu quadratus lateralis become visible at ZO 17. This processus develops anteriorly and reaches the tentacular cartilage proximal to the insertion of the m. levator mandibulae longus profundus. It is fully chondrified at ZO 20 (Figures 3d and 4b,c). After ZO 17 the processus muscularis starts to bend ventrolaterally and is nearly horizontal at ZO 201 (Figure 4c).

3.5 | Ceratohyal

The anterior border of the mesenchymal anlage of the ceratohyal is visible between the two m. quadrato-hyoangularis and the two m. orbitohyoideus muscles at ZO 6 ventral to the pharyngeal cavity (Figure 2l). Laterally, the anlage is proceeding dorsally and flanks the cavity. This results in a broad u-shaped mesenchymal anlage (Figure 2m). The developing m. orbitohyoideus inserts at the dorsolateral projection which is likely the future processus lateralis hyalis. Posteriorly, the anlage of the processus posterior hyalis is divided by the anlage of the basihyobranchial. Both processes and the main body of the ceratohyal condense at ZO 9. At ZO 10, the main body of the ceratohyal is the first cartilage to form. It is present as two broad vertically proceeding bars. At ZO 11, the processus lateralis chondrifies close to the processus muscularis and surrounds its ventrolateral surface (Figure 4a,c). The m. interhyoideus originates from its ventral surface. The processus still proceeds dorsally but flattens until ZO 13 and starts to bend posterolaterally (Figure 2n). The processus posterior hyalis chondrifies at ZO 12 and flanks the developing basihyobranchial (Figure 4a). Several fibers of the m. quadrato-hyoangularis attach onto the anterodorsal part of the ceratohyal at ZO 14. With further development, the entire

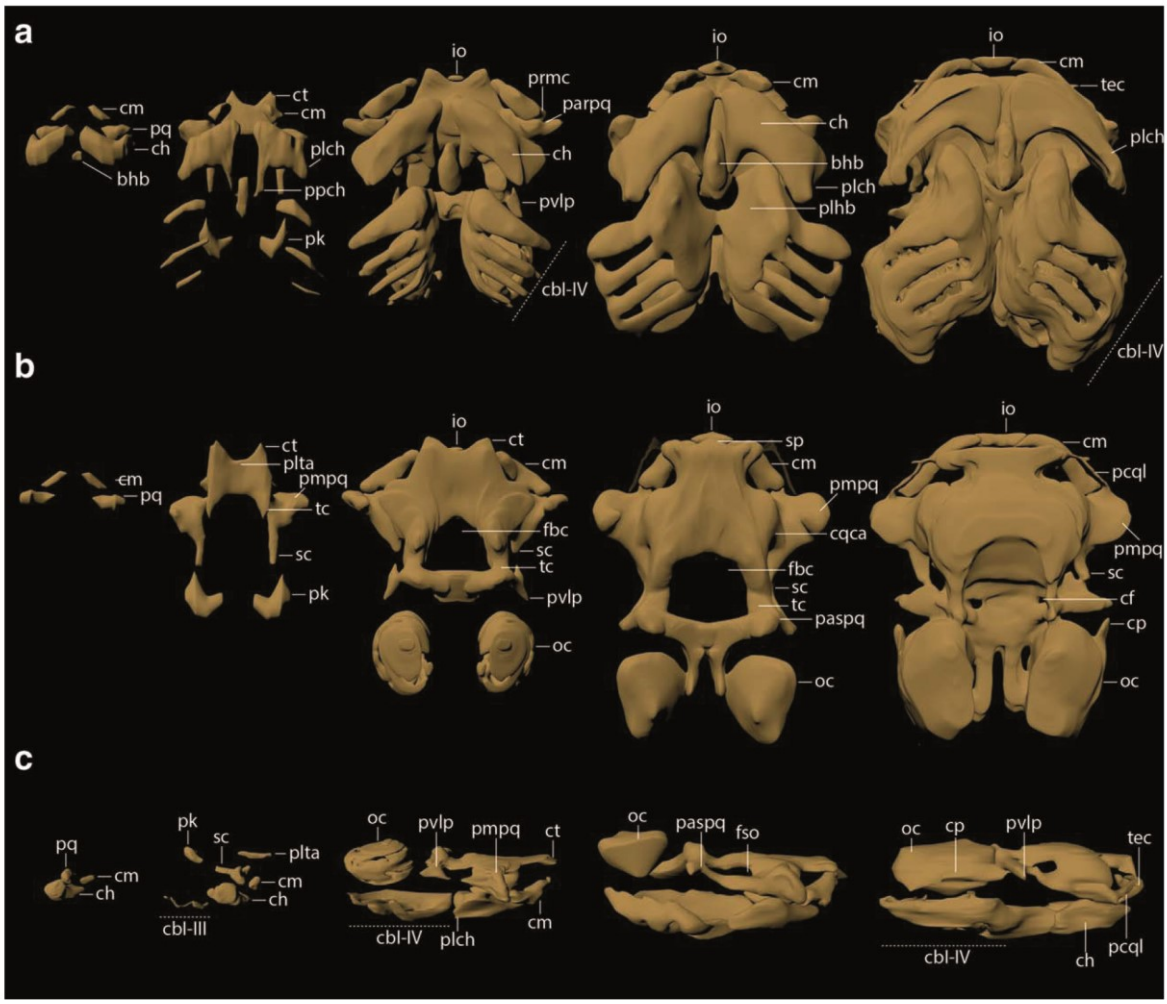

FIGURE 4 3D-reconstructions of the cartilaginous head skeleton based on collagen immunohistochemistry and confocal laser scanning microscopy of Xenopus laevis larva in ventral (a), dorsal (b) and lateral view (c) showing ZO 11, 13,5, 15, 17, and 20 1 (from left to right). In (b) the ceratohyal and elements of the branchial basket are not shown and condensations of the tentacular cartilage and its supporting processes are displayed transparent. bhb, basihyobranchial; cbl-IV, ceratobranchial I –IV; ch, ceratohyal; cm, Meckel ́s cartilage; cqca, commissura quadratocranialis anterior; cf, carotid foramen; cp, crista parotica; ct, cornua trabeculae; ctm, commissura terminalis; fbc, fenestra basi - cranialis; fso, fenestra subocularis; io, infrarostral; oc, otic capsule; parpq, processus articularis palatoquadrati; paspq, processus ascend ens palatoquadrate; pc, parachordal; pcql, processus cornu quadratus lateralis; plch, processus lateralis hyalis; plhb, planum hypobranchiale; plt a, planum trabeculare anticum; pmpq, processus muscularis palatoquadrati; ppch, processus posterior hyalis; pk, parachordal; pq, palatoqua- drate; prmc, processus retroarticularis; pvlp, processus ventrolateralis posterior; sc, subocular cartilage; sp, suprarostral plate; tc, trabe culae cranii; tec, tentacular cartilage

cartilage broadens and the processus lateralis hyalis shifts more and more posteriorly (Figure 4a). This changes the shape of the anterior margin from diagonal to a smooth curve. At ZO 17, both ceratohyals fuse anteromedially. This fusion extends caudally during the next stages, until they are both connected on the medial surface through a smooth cartilaginous band (Figure 4a).

3.6 | Basihyobranchial

The mesenchymal anlage of the basihyobranchial can already be seen at ZO 6 as a small circle of cells (data not shown). It is placed between the two anlagen of the ceratohyal dorsal to the paired m. geniohyoideus muscle cell cluster. The mesenchymal anlage of the basi- hyobranchial extends caudally to the level where the anlage of the processus posterior hyalis terminates. At ZO 9, the anlage of the basi- hyobranchial consists of densely packed chondroblasts. This precartila- ginous anlage is broader caudally than rostrally and elongates in an anterior-to-posterior direction. It proceeds from the centre of the gap between the two precartilaginous anlagen of the ceratohyal until the level of the mesenchymal ceratobranchial I anlage. It chondrifies after the ceratohyal at ZO 11 and retains its shape. Until ZO 20 it elongates caudally between the two branchial baskets ventral to the planun hypobranchiale (Figure 4a).

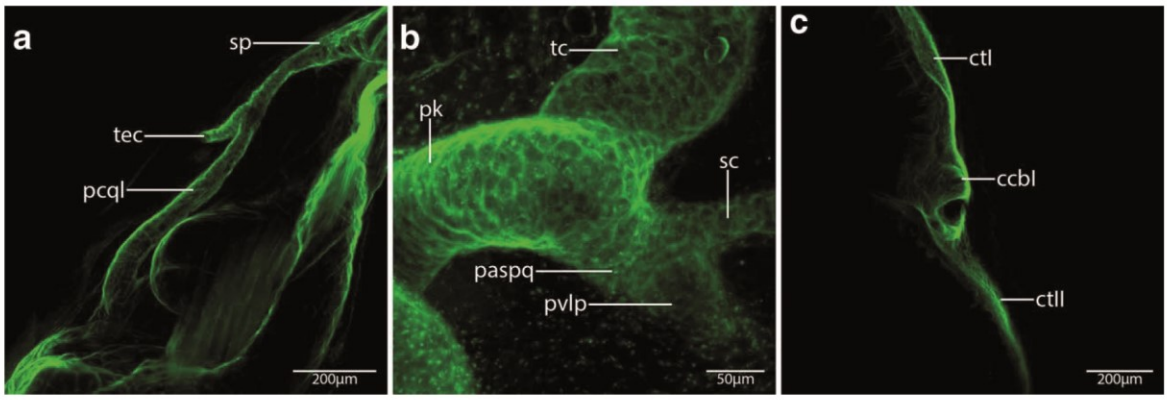

FIGURE 5 Maximum intensity projections of a ZO 20 antibody-stained Xenopus laevis larva with a detailed view of cartilaginous structures. (a) tentacular cartilage in dorsal view, (b) processus ascendens in lateral view, and (c) commissura craniobranchialis I in dorsal view. ccbII, commissura craniobranchialis I; ctI, commissura terminalis I; ctII, commissura terminalis II; paspq, processus ascendens palatoquadrate; pcql, processus cornu quadratus lateralis; pk, parachordal; pvlp, processus ventrolateralis posterior; sc, subocular cartilage; sp, suprarostral pla te; tc, trabeculae cranii; tec, tentacular cartilage

3.7 | Branchial basket

The branchial basket consists of a median planum hypobranchiale, four ceratobranchials, and a lateral commissura terminalis that connects all four ceratobranchials distally. Mesenchymal anlagen of the ceratobranchials I and II are visible at ZO 6 as bands parallel to the anlage of the ceratohyal. The anlage of ceratobranchial I lies dorsal to the anlage of the m. geniohyoideus. Both ceratobranchials proceed from median to lateral and are slightly curved in dorsoventral direction. At ZO 7, two additional parallel bands appear caudally, the ceratobranchials III and IV. The diameter of the anlagen decreases constantly from ceratobranchial I to IV. They are all connected ventrally through the anlage of the planum hypobranchiale. Distally, all anlagen of the ceratobranchials are separated from each other. At ZO 9, the mm. levatores arcuum branchialium I-IV attach onto the anlagen of all four ceratobranchials. From ZO 10 until the end of ZO 11 all four ceratobranchials have started to condense as precartilaginous anlagen in a rostrocaudal sequence (ceratobranchial I first, ceratobranchial II second, etc.). At ZO 11, the mesenchymal anlagen of the commissura terminalis become visible at the distal ends of all four ceratobranchials and connect them to each other. At ZO 12, the mesenchymal anlage of the planum hypobranchiale starts to form precartilage and the chondroblasts fill in the gap between the two ceratobranchial I condensations. At the transition between ZO 12 and ZO 13, ceratobranchial I chondrifies (Figure 6a). Chondrification continues in anterior-to-posterior direction until ZO

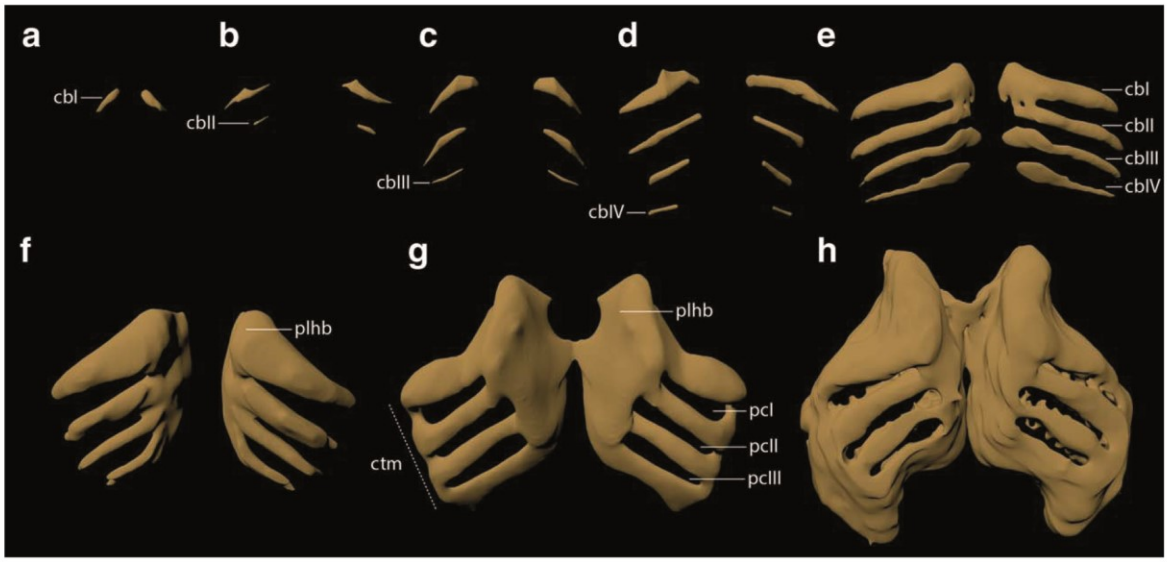

FIGURE 6 3D-reconstructions based on confocal laser scanning microscopy showing the development of the branchial basket of X. laevis in ventral view. (a –f) ZO 12,5- 15. (g) ZO 17. (h) ZO 20 1 . cbI-IV, ceratobranchial I –IV; ctm, commissura terminalis; pcI-III, pharyngeal cleft I–III; plhb, planum hypobranchiale

14, where all four ceratobranchials are chondrified (Figure 6a –d) and m. geniohyoideus attaches onto ceratobranchial I. After that, the precartilaginous anlage of the planum hypobranchiale chondrifies and starts to broaden cranially. Later, the distal tip of each ceratobranchial starts to shift caudally, which results in more and more transversely proceeding ceratobranchials (Figure 6e,f). From ZO 15 onwards, parts of the precartilaginous commissura terminalis start to condense first between ceratobranchial I and II, second, between II and III, and thirdly between III and IV. At ZO 17, all four ceratobranchials are connected laterally by a fully chondrified commissura terminalis and each pair of ceratobranchials surrounds a pharyngeal cleft (Figures 3c and 6g). At the same time the mm. constrictores branchiales II, III, and IV attach onto the commissura terminalis in an anterior-to-posterior sequence. Just like the ceratohyals the two planum hypobranchiale begin to fuse anteromedially at ZO 17 (Figure 6g). This fusion proceeds caudally until they are connected completely anteroposteriorly at ZO 20. With further development (ZO 20 1) each ceratobranchial develops rounded projections on the ventral surface where the gills attach (Figure 6h). Ventrolaterally, at the distal end of ceratobranchial II and ceratobranchial III, and distally between ceratobranchials III and IV in the centre of the commissura terminalis III a process develops that proceeds dorsally in the direction of the crista parotica. These are the commissurae craniobranchialis I–III (Figure 5c) which chondrify after ZO 20.

3.8 | Chondrocranium

At ZO 8, the mesenchymal anlage of the planum trabeculare anticum (also known as the ethmoid plate, planum ethmoidale, or trabecular plate) can be discerned posterior to the mesenchymal anlagen of the cornua trabeculae surrounding the pharyngeal cavity anteriodorsally. Posterolaterally, the mesenchymal anlagen of the trabeculae cranii extend posteriorly as two small rods. The mesenchymal anlage of the parachordal is visible ventral to the notochord. There is no connection between the mesenchymal anlagen of the trabeculae cranii and the parachordal. Planum trabeculare anticum and the parachordal form precartilage at ZO 9 and start to extend laterally and become broader. The mesenchymal anlage of the trabeculae cranii proceed posteriorly and become precartilaginous at ZO 11. In the early phase of ZO 13, planum trabeculare anticum and the parachordal chondrify and the latter proceeds anterolaterally (Figure 4b). Trabeculae cranii and parachordal are connected through a band of condensed precartilaginous cells. During this stage precartilaginous anlagen of the trabeculae cranii chondrify in an anterior-to-posterior direction. In most cases, the chondrification is finished at the beginning of ZO 14, which results in the formation of the fenestra basicranialis (Figure 4b). In a few specimens the trabeculae cranii and the parachordals are fused at ZO13. The fenestra basicranialis is bordered anteriorly by the fully chondrified planum trabeculare anticum, laterally by the trabeculae cranii, and posteriorly by the parachordals. Simultaneously, the ventral and lateral wall of the otic capsule chondrify. At ZO 15, the dorsal wall develops and chondrification becomes apparent in the median wall. At this time, the otic capsule consists of numerous holes filled with condensed chondroblasts (Figure 4b), which fully chondrify until ZO 17, with the exception of a few foramina which remain during further development. At this stage, the ventromedian wall fuses with the caudal proceeding projection of the parachordal. The crista parotica is a ventrolateral outgrowth of the capsule which chondrifies at ZO 18. The fenestra basicranialis starts to diminish in size at ZO 20 and will close completely during further development (Figure 4b). With its closing, several foramina develop. Median to the processus ascendens palatoquadrati, the carotid foramina open. The foramen opticum is situated anterior to the processus ascendens and the foramen prooticum caudal to it (Figure 4b,c).

4 | DISCUSSION

Tadpoles raised at different temperature conditions develop at different rates, but the sequence of chondrification stays the same. Although the timing of chondrification differs in different cartilages most of them are fully differentiated at ZO 17. Tadpoles begin to feed actively at around this stage and need a properly developed head skeleton.

4.1 | Previous studies of head skeletal development in Xenopus laevis

It has been reported previously that the timing of cartilaginous skeletal development in X. laevis from NF 46 onwards is variable, whereas the sequence in which cartilages develop is not (Trueb & Hanken, 1992). Our findings can confirm this pattern for earlier stages too. Only a few incidents, such as the fusion of the trabeculae cranii and the parachordal, the fusion of the commissura quadratocranialis anterior and the planum trabeculare anticum, or the fusion of the processus ascendens palatoquadrati and the subocular cartilage show variable timing, which may be a response to environmental factors. Only the timing of the fusion of the named cartilaginous parts is in some cases variable, whereas the onset of chondrification of the different cartilages follows a strict sequence. We can also confirm the weakness of the correlation between skeletal development and development of the external morphology reported before (Trueb & Hanken, 1992). This may be the result of a lack of studies ofi ntrastage variation in external morphology of the widely used NF staging table (Nieuwkoop & Faber, 1994).

Cartilaginous criteria only play a minor role in the NF staging table. In this staging system NF 42 (ZO 13) marks the beginning of chondrification, whereas in our study chondrification starts earlier in development at NF 41 (ZO 10). There are only a few small differences in the external morphology between NF 41 and NF 42 (torsion ofi ntestine, intestinal tube) but very large differences in internal morphology. In later NF stages further cartilaginous criteria are described which always appear earlier in our study (subocular cartilage, Meckel 's cartilage, ceratohyal, among others). This clearly shows the discrepancy between external and internal development. Due to this variation, stages in the NF- staging table do not sufficiently reflect changes in the cartilaginous head skeleton. A NF-stage contains no information about the specific state of the cartilaginous skeleton at a defined stage. Each NF-stage represents an amount of possible variations of the state of the cartilaginous skeleton.

Xenopus development is influenced by environmental factors (Godfrey & Sanders, 2004; Hilken et al., 1995; Trueb & Hanken, 1992). Therefore, staging tables using age and/or size may not be comparable,

TABLE 1 Overview of the sequence and timing of cartilage development in Xenopus laevis

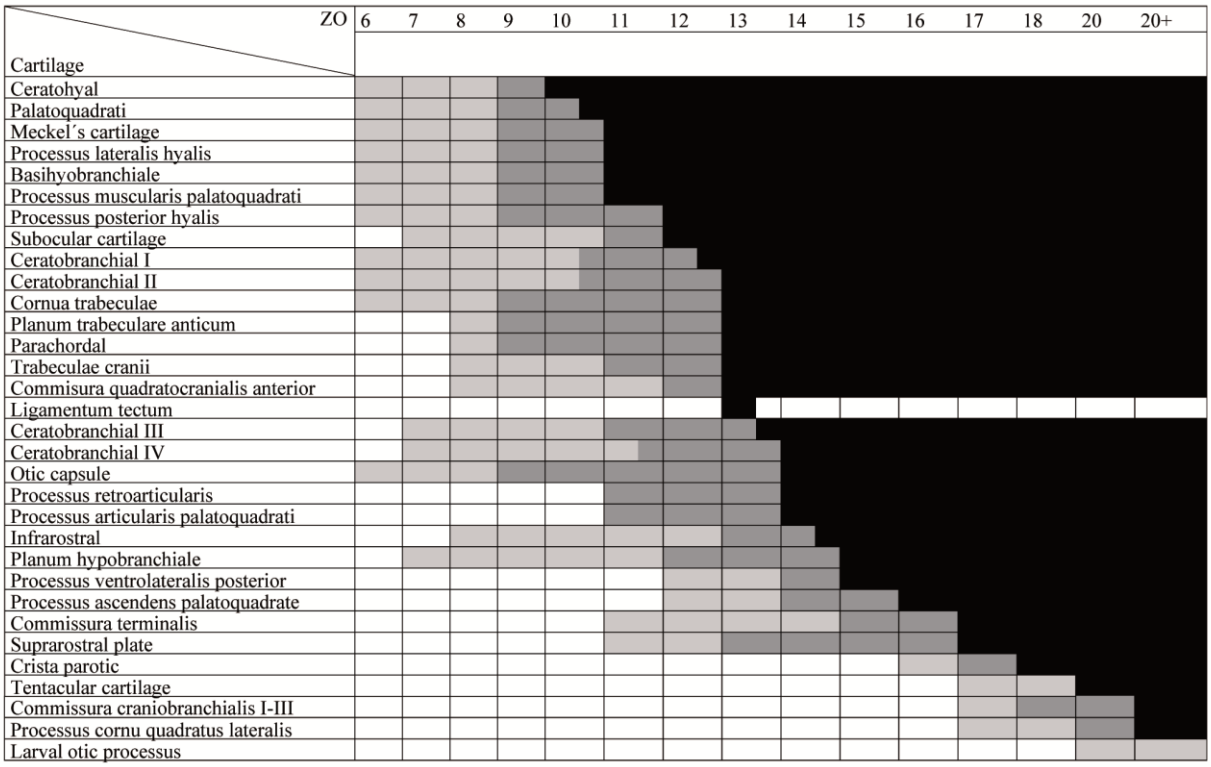

The figure is shaded according to different developmental conditions. "White" means no anlagen are visible; "Light gray" means that anlagen are visible as mesenchymal cell clusters; "Dark grey" means the chondroblasts form condensed precartilaginous cell clusters with clearly visible nuclei; "Black" indicates the presence of the cartilage itself whose chondrocytes are rich in cytoplasm and bordered by a clearly visible perichondrium.

which is why we do not indicate the size or age of the tadpoles studied. Ziermann and Olsson (2007a) staging enables identification of particular stages. This staging table is, like Nieuwkoop and Faber 's table, based on external features and links the presence of a specific set of muscles to each stage (table 1 in Ziermann & Olsson, 2007b). Each stage is represented by a specific set of muscles. We were able to add a specific set of cartilages to most of the stages mentioned (Table 1). The stages are now additionally defined through the combined state of muscles and cartilages. This should help to identify the exact developmental stage of X. laevis larvae in further investigations with focus on the musculoskeletal system. The ZO-staging cannot replace the NF-staging because it only partly covers the development of X. laevis. But for investigations who focus on the developmental stages or which alter the development of the musculoskeletal system, which initially develops at these stages, the ZO-table is useful, because results will be more comparable through use of this staging table.

The development of the suprarostral plate has already been documented (De Sá & Swart, 1999). Our findings mostly agree with this study. The stages in De S á and Swart (1999) do not necessarily match the stages in our study because of the discrepancy between skeletal development and the external morphological features used for the standard staging table (Nieuwkoop & Faber, 1994). The anterior process of the ethmoid plate described in De S á and Swart (1999) could not be found in our material. We observed that the suprarostral plate is formed by cells which fill the gap between the two cornua trabeculae as previously reported (De S á & Swart, 1999; Trueb & Hanken, 1992). Our data strongly supports the view that it is homologous to the suprarostral cartilage of non-pipoid anurans (De S á & Swart, 1999; Sokol, 1975; Trueb & Hanken, 1992).

Weisz (1945a,b) investigated the development of X. laevis using laboratory-bred animals and also developed a staging system based on external and behavioural features. He described the first-form tadpole as a stage between day two and day seven ranging from the perforation of the mouth to the onset of active feeding. His sequence of chondrification differs from our observations. The earliest stage shown consists of a complete fenestra basicranialis bordered by the planum trabeculare anticum, the trabeculae cranii, and the parachordal. The ceratohyals extends horizontally and are fused anteromedially, bearing a processus posterior hyalis on each side. The basihyobranchial is a long median rod connected to the two planum hypobranchiale. Meckel's cartilage is not present (fig. 3A in Weisz, 1945a). We never found this condition in our specimens. The basicranial fenestra is present at ZO 14. At the same stage, Meckel 's cartilage, ceratobranchial I-IV, processus muscularis, and the subocular cartilage are all present (Figure 4b). During early development, the basihyobranchial and planum hypobranchiale are not connected to each other, but the space

between them is filled with diffuse cells which could lead to misinterpretation. Weisz 's (1945a) second depiction of the first-form tadpole also differs from our findings (fig. 3B in Weisz, 1945a). Even though the trabeculae cranii are connected to the parachordal, it closely resembles our ZO 13 (Figure 4b). The ceratobranchials I –III are shown to develop as lateral outgrowths of the planum hypobranchiale. We found a similar condition during the condensation of the branchial basket, but during chondrification each ceratobranchial develops as a single rod, which later becomes connected to the planum hypobranchiale. We confirm that ceratobranchials develop in an anterior-posterior manner (Figure 5). The second-form tadpole is defined by Weisz as a phase between the beginning of active feeding and the appearance of hindlimb buds (fig. 4 in Weisz, 1945a). His description includes the presence of a developing processus cornu quadratus lateralis, which indicates a late stage of development (ZO 20 1), whereas the described unconnected subocular cartilage is a feature of ZO 15 tadpoles in our work (Figure 4c). Additionally, we observe a smaller fenestra basicranialis when the processus cornu quadratus lateralis is developed. In his second comprehensive work on X. laevis, Weisz (1945a) continues with the description of the third-from tadpole. The beginning of this stage is marked by the appearance of hindlimb buds. This stage is not described in our work but has been studied by others. Meckel 's cartilage and the infrarostral are depicted as fused but both stay divided until NF 60 (Trueb & Hanken, 1992). The total absence of the infrarostral was also stated by Edgeworth (1930) and by Dreyer (1914). However, Edgeworth (1930) only investigated two larvae and focussed on the muscles. The larval otic processus is missing in Weisz (1945a,b) work but it normally unites the otic capsule and the processus ascendens palatoquadrati (Trueb & Hanken, 1992). Parker (1876) also does not mention this process, and additionally does not mention or depict a subocular cartilage.

In their work, Trueb and Hanken (1992) described the postembryonic skeletal development of X. laevis until postmetamorphosis. They mainly focussed on the ossification sequence but also documented chondrocranial development. Their earliest stage is NF 46 which mostly reflects an early phase of our ZO 15. However, we could not observe the tentacular cartilage developing in this early phase. Additionally, the suprarostral plate is not yet chondrified in our specimens at this stage. We can confirm the observed bipartite development of the palatoquadrate. The fusion of the two parts via the subocular cartilage is complete at NF 49 (which is almost like our described ZO 20 1 with the exception that a larval otic processus is present) according to Trueb and Hanken (1992). This is an example of the variability that we observe regarding the complete chondrification of the subocular cartilage. The timing of the development of the anterior and posterior parts of the palatoquadrate differs from our findings. Trueb and Hanken (1992) state that the anterior part develops at NF 39, but it develops later in the larva we investigated (NF 40 –41, see Ziermann & Olsson, 2007a). The posterior part develops at NF 45 –46 according to Trueb and Hanken (1992). In contrast, we observed chondrification at NF 43 (Figure 4c). We can confirm the delayed development in comparison to the anterior portion.

Ziermann and Olsson (2007b) focussed on the pattern and timing of muscle development in X. laevis larvae but also partially described the development of cartilaginous elements. The description of the developmental sequence of the ceratobranchial I –IV coincides with our results as well as the pattern of Meckel 's cartilage, ceratohyal, and palatoquadrate.

Paterson (1939) as well as Sedra and Michael (1957) limit the definition of the processus ventrolateralis to the broadened ventral portion of the process and defined the proximal strap-like cartilage as part of the processus ascendens. Trueb and Hanken (1992) clarified that the processus ascendens ends at the level of the subocular cartilage and that the ventral strap-like cartilage represents the proximal part of the processus ventrolateralis and our findings support that. Furthermore, our data agree with Paterson 's (1939) observation that the infrarostral cartilage develops after Meckel 's cartilage (Figure 3b). This sequence of development might be important for revealing the evolution of this anuran-specific novelty and was confirmed in our present work. Paterson (1939) stated that the branchial basket develops through early anterior-posterior chondrification of ceratobranchials I –IV and a late median fusion of these parts to form the branchial basket, which reflects our findings (Figures 3 and 5). Her depictions of early chondrocranial development are in agreement with our findings (figs. 22A,B, and 23 in Paterson, 1939).

Most of the differences emphasized above could be caused by limitations of the methods available at the time ofi nvestigation. Our histological slices have a thickness of 7 mm whereas microtomes in the first half of the 20th century performed slices of 10 mm or even thicker. The thicker the section, the more likely it is that small gaps may be overlooked, for example, between the infrarostral and Meckel 's cartilage or between basihyobranchial and planum hypobranchiale, which leads to misinterpretations. Another point is the usage of different staining techniques. Hansens hematoxylin or a combination of basic fuchsin and picric acid was used to get an overview of a section but they do not differentiate among tissues very well. The two staining methods mentioned are not able to distinguish between chondroblasts and chondrocytes, however this distinction is necessary to decide if the cartilage is chondrified or not. This could have led to misinterpretations of the timing of chondrification [e.g., Weisz 's (1945a, 1945b)] depiction of a larvae where the processus cornu quadratus lateralis is present while the subocular bar is not yet connected to the processus ascendens). Additionally, stains can obscure the boundary between two tissues, which makes the interpretation of sections difficult. The usage of collagen antibodies in combination with fluorescent secondary antibodies and confocal laser scanning microscopy instead produces a sharp impression of the state of cells and makes their identification easier and more reliable.

4.2 | Developmental sequence of cartilage formation

The development of the visceral skeleton in X. laevis does not follow the pattern observed in other vertebrates. It has been shown that the viscerocranium of chondrichtyans, sturgeons, and teleosts, as well as anurans, develop in an antero-posterior direction (Gaupp, 1906; Gillis,

Modrell, & Baker, 2012; Langille & Hall, 1987; St 6hr, 1882; Warth, Hilton, Naumann, Olsson, & Konstantinidis, 2017). In contrast, the ceratohyal is the first cartilage to appear in X. laevis development immediately followed by the palatoquadrate (Figure 3a). The early formation of the ceratohyal might relate to its importance for filter feeding. Another possibility is that development of Meckel 's cartilage is delayed. Meckel 's cartilage in early stages of X. laevis development resembles the premetamorphic condition in other anuran species (Sokol, 1975; Trueb & Hanken, 1992). It is obvious that anuran-specific novelties such as the infrarostral and suprarostral cartilages, as well as the unique tentacular cartilage, deviate from the ancestral pattern. They are derivatives of the first visceral arch and should therefore chondrify first during development according to the anterior-posterior pattern aforementioned. The evolution of these novelties could have changed the ancestral patterning and produced the derived sequence of chondrogenesis seen in X. laevis.

Ceratobranchial I–IV develop consecutively in an anterior-to-posterior direction as described for other anurans such as Rana temporaria, Bufo cinereus, and Hyla sp. (St 6hr, 1882). Parachordals are one of the earliest appearing elements during X. laevis development. This is also the case in Oryzias latipes (Langille & Hall, 1987), sturgeons (Warth et al., 2017) and various anurans (St 6hr, 1882). Investigations of Rana fusca (now Rana temporaria) indicate similarities in the developmental pattern of anurans (Gaupp, 1906; St 6hr, 1882). (1) The elements that anchor the palatoquadrate to the neurocranium chondrify in a specific order. First, the commissura quadratocranialis chondrifies, second the processus ascendens, and third the larval otic processus. (2) The trabeculae cranii develop in an antero-posterior sequence. (3) The otic capsules chondrify after the parachordals. (4) Ceratobranchials I–IV develop separately in an antero-posterior sequence and fuse first medially and second laterally in the same order.

Here, we presented the timing and sequence of the condensation and chondrogenesis of the larval head skeleton in X. laevis from early anlagen until a fully differentiated cartilaginous head skeleton. This overview of normal head cartilage development of early stages fills a gap in the literature. The data provided in our study offer a standard sequence for developmental experiments which alter head skeletal development, such as upregulation and downregulation of genes and teratogenic tests. Despite the detailed overview provided here, a documentation of unperturbed development is still required to assess the results of such experiments. Whether the developmental sequence described displays a general pattern among anurans or if it is the result of the derived morphology of X. laevis itself cannot be answered here. To identify possible heterochronic shifts in Xenopus development and to clarify open questions on homology, comparable studies of developmental sequences in further anurans and urodeles are needed.

ACKNOWLEDGMENTS

This study was funded in part by a grant from the Deutsche Forschungsgemeinschaft (grant no. OL 134/2–4 to LO). PL is supported by the Studienstiftung des Deutschen Volkes. Detailed comments by Janine Ziermann an anonymous reviewer and the editor on earlier versions of this paper are gratefully acknowledged. We are very grateful to Katja Felbel for technical support and preparation of the histological sections. Sandra Eisenberg took care of the animals. The monoclonal antibodies against collagen II (116B3-collagen II) obtained from the Developmental Studies Hybridoma Bank were developed under the auspices of the NICHD and maintained by The University of Iowa, Department of Biological Sciences, Iowa City, IA 52242, USA. The authors declare no conflict of interest.

AUTHOR CONTRIBUTIONS

PL and LO developed the concept and design of the study. PL was responsible for the experimental procedures including clearing-and-staining, immunostainings, 3D-reconstructions as well as histology. Analysis and interpretation of the data mentioned was mainly done by PL, who was also responsible for the drafting of the manuscript and its final form. LO critically revised the manuscript.

ORCID

Paul Lukas http://orcid.org/0000-0003-2756-0465

REFERENCES

ASTM, A. (1991). Standard guide for conducting the frog embryo teratogenesis assay—Xenopus (FETAX), E1439-91. Annual Book ASTM Standards, 11, 1199–1209.

Bantle, J. A. (1991). Atlas of abnormalities: A guide for the performance of fetax. Printing Services, Stillwater, Oklahoma: Oklahoma State University.

Bantle, J. A., Finch, R. A., Fort, D. J., Stover, E. L., Hull, M., Kumsher, … Hull, A. M. (1999). Phase III interlaboratory study of FETAX part 3. FETAX validation using 12 compounds with and without an exogenous metabolic activation system. Journal of Applied Toxicology, 19, 447–472.

Bernasconi, S. M. (1951). Über den Ossifikationsmodus bei Xenopus laevis Daud. Mem Soc Helvet Sci Nat, 79, 191–252.

Beverdam, A., Merlo, G. R., Paleari, L., Mantero, S., Genova, F., Barbieri, O., … Levi, G. (2002). Jaw transformation with gain of symmetry afterDlx5/Dlx6 inactivation: Mirror of the past? Genesis, 34, 221–227.

Bles, E. J. (1906). XXXI.—The life-history of Xenopus laevis, Daud. Transactions of the Royal Society of Edinburgh, 41, 789–821.

Blum, M., De Robertis, E. M., Wallingford, J. B., & Niehrs, C. (2015). Morpholinos: Antisense and sensibility. Developmental Cell, 35, 145–149.

Candioti, M. F. V. (2007). Anatomy of anuran tadpoles from lentic water bodies: Systematic relevance and correlation with feeding habits. Zootaxa 1600, 1–175.

Cannatella, D. C., & De Sá, R. O. (1993). Xenopus laevis as a Model Organism. Systematic Biology, 42, 476–507.

De Sá, R. O., & Swart, C. C. (1999). Development of the suprarostral plate of pipoid frogs. Journal of Morphology 240, 143–153.

Depew, M. J., Lufkin, T., & Rubenstein, J. L. R. (2002). Specification of jaw subdivisions by Dlx genes. Science, 298, 381–385.

Dingerkus, G., & Uhler, L. D. (1977). Enzyme clearing of alcian blue stained whole small vertebrates for demonstration of cartilage. Stain Technology, 52, 229–232.

Dreyer, T. F. (1914). The morphology of the tadpole of Xenopus laevis. Transactions of the Royal Society of South Africa, 4, 241–258.

Edgeworth, F. H. (1930). On the masticatory and hyoid muscles of larvae of Xenopus laevis Journal of Anatomy, 64, 184–188.

Eisen, J. S., & Smith, J. C. (2008). Controlling morpholino experiments: Don't stop making antisense. Development, 135, 1735–1743.

Frost, D. R., Grant, T., Faivovich, J. N., Bain, R. H., Haas, A., Lio, C., … Wheeler, W. C. (2006). The amphibian tree of life. Bulletin of the American Museum of Natural History, 297, 1–370.

Gaupp, E. (1906). Die Entwickelung des Kopfskelettes. In Handbuch der vergleichenden und experimentellen Entwickelungslehre der Wirbeltiere (Vol. 3(2), pp. 718–756), Jena, Gustav Fischer Verlag.

Gillis, J. A., Modrell, M. S., & Baker, C. V. H. (2012). A timeline of pharyngeal endoskeletal condensation and differentiation in the shark, Scyliorhinus canicula, and the paddlefish, Polyodon spathula Journal of Applied Ichthyology 28, 341–345.

Godfrey, E. W., & Sanders, G. E. (2004). Effect of water hardness on oocyte quality and embryo development in the African Clawed Frog (Xenopus laevis). Comparative Medicine, 54, 170–175.

Gradwell, N. (1971). Xenopus tadpole: On the water pumping mechanism. Herpetologica, 27, 107–123.

Gross, J. B., & Hanken, J. (2008). Segmentation of the vertebrate skull: Neural-crest derivation of adult cartilages in the clawed frog, Xenopus laevis. Integrative and Comparative Biology 48, 681–696.

Haas, A. (2001). Mandibular arch musculature of anuran tadpoles, with comments on homologies of amphibian jaw muscles. Journal of Morphology, 247, 1–33.

Haas, A. (2003). Phylogeny of frogs as inferred from primarily larval characters (Amphibia: Anura). Cladistics, 19, 23–89.

Heidenhain, M. (1915). Über die mallorysche bindegewebsfärbung mit karmin und azokarmin als vorfarben. Zeitschrift Fur Wissenschaftliche Mikroskopie, 33, 361–372.

Hilken, G., Dimigen, J., & Iglauer, F. (1995). Growth of Xenopus laevis under different laboratory rearing conditions. Laboratory Animals, 29, 152–162.

Ibler, B., & Stöhr, W. (2008). Aufzucht und morphologische Entwicklung aus zwei Jahrzehnten Zucht des Afrikanischen Glatten Krallenfrosches (Xenopus laevis Daudin, 1803). Der Zoologische Garten, 77, 345–362.

Kotthaus, A. (1933). Die Entwicklung des Primordial-Craniums von Xenopus laevis vor der Metamorphose. Zeitschrift für Wissenschaftliche Zoologie, 144, 510–572.

Langille, R. M., & Hall, B. K. (1987). Development of the head skeleton of the Japanese medaka, Oryzias latipes (Teleostei). Journal of Morphology, 193, 135–158.

Lavery, D. L., & Hoppler, S. (2009). Gain-of-function and loss-of-function strategies in Xenopus. In E. Vincan (Ed.), Wnt Signaling Totowa (pp. 401–415). NJ: Humana Press.

Nieuwkoop, P., & Faber, J. (1994). Normal table of Xenopus laevis (Daudin). New York: Garl Publ.

Olsson, L., & Hanken, J. (1996). Cranial neural-crest migration and chondrogenic fate in the oriental fire-bellied toad Bombina orientalis: Defining the ancestral pattern of head development in anuran amphibians. Journal of Morphology 229, 105–120.

Parker, W. K. (1876). On the structure and development of the Skull in the Batrachia. Part II. Philosophical Transactions of the Royal Society of London, 166, 601–669.

Parker, W. K. (1879). On the Structure and Development of the Skull in the Batrachia. Part III. Proceedings of the Royal Society of London, 30, 1–699.

Paterson, N. F. (1939). The head of Xenopus laevis The Quarterly Journal of Microscopical Science, 81, 161–234.

Peter, K. (1931). The development of the external features of Xenopus laevis, based on material collected by the late E. J. Bles. Zoological Journal of the Linnean Society London, 37, 515–523.

Place, T. (1986). Meckel 's cartilage in Xenopus laevis during metamorphosis: A light and electron microscope study. Journal of Anatomy 149, 77–87.

Place, T. (1987). A quantitative analysis of cellular and matrix changes in Meckel 's cartilage in Xenopus laevis Journal of Anatomy 151, 249–254.

Ramaswami, L. S. (1941). Some aspects of the head of Xenopus laevis Proceedings of the Indian Science Congress, 28, 183–184.

Ridewood, W. G. (1897). On the structure and development of the hyobranchial skeleton and larynx in Xenopus and Pipa; with remarks on the affinities of the Aglossa. Zoological Journal of the Linnean Society London, 26, 53–128.

Rose, C. (2009). Generating, growing and transforming skeletal shape: Insights from amphibian pharyngeal arch cartilages. BioEssays, 31, 287–299.

Sadaghiani, B., & Thi ébaud, C. H. (1987). Neural crest development in the Xenopus laevis embryo, studied by interspecific transplantation and scanning electron microscopy. Developmental Biology 124, 91–110.

Satel, S. L., & Wassersug, R. J. (1981). On the relative sizes of buccal floor depressor and elevator musculature in tadpoles on the relative sizes of buccal floor depressor and elevator musculature in tadpoles. Copeia, 1981, 129–137.

Seale, D. B., & Wassersug, R. J. (1979). Suspension feeding dynamics of anuran larvae related to their functional morphology. Oecologia, 39, 259–272.

Sedra, S. N., & Michael, M. I. (1957). The development of the skull, visceral arches, larynx and visceral muscles of the South African clawed toad, Xenopus laeuis (Daudin) during the process of metamorphosis (from Stage 55 to Stage 66). Verhandelingen der Konlnklijke Nededandsche Akademie van Wetenschappen Afd. Natuurkunde, 51, 1–80.

Segerdell, E., Bowes, J. B., Pollet, N., & Vize, P. D. (2008). An ontology for Xenopus anatomy and development. BMC Developmental Biology, 8, 92.

Segerdell, E., Ponferrada, V. G., James-Zorn, C., Burns, K. A., Fortriede, J. D., Dahdul, W. M., … Zorn, A. M. (2013). Enhanced XAO: The ontology of Xenopus anatomy and development underpins more accurate annotation of gene expression and queries on Xenbase. Journal of Biomedical Semantics, 4, 31.

Smit, A. L. (1953). The ontogenesis of the vertebral column of Xenopus laevis (Daudin) with special reference to the segmentation of the metotic region of the skull Ann Univ Stellenbosch: Annale van die Universiteit van Stellenbosch.

Sokol, O. M. (1975). The phylogeny of anuran larvae: A new look. Copeia, 1975, 1–23.

Sokol, O. M. (1977). The free swimming Pipa larvae, with a review of pipid larvae and pipid phylogeny (Anura: Pipidae). Journal of Morphology, 154, 357–425.

Stöhr, P. (1882). Zur Entwickelungsgeschichte des Anurenschädels. Zeitschrift für Wissenschaftliche Zoologie, 36, 68–103.

Thomson, D. A. (1986). Meckel 's cartilage in Xenopus laevis during metamorphosis: A light and electron microscope study. Journal of Anatomy, 149, 77–87.

Thomson, D. A. (1987). A quantitative analysis of cellular and matrix changes in Meckel 's cartilage in Xenopus laevis Journal of Anatomy, 151, 249–254.

Thomson, D. A. (1989). A preliminary investigation into the effect of thyroid hormones on the metamorphic changes in Meckel 's cartilage in Xenopus laevis Journal of Anatomy, 162, 149–155.

Trueb, L. L., & Hanken, J. J. (1992). Skeletal development in Xenopus laevis (Anura: Pipidae). Journal of Morphology 214, 1–41.

Wagner, N., M €ller, H., & Viertel, B. (2017). Effects of a commonly used glyphosate-based herbicide formulation on early developmental stages of two anuran species. Environmental Science and Pollution Research, 24, 1495–1508.

Wang, F., Shi, Z., Cui, Y., Guo, X., Shi, Y.-B., & Chen, Y. (2015). Targeted gene disruption in Xenopus laevis using CRISPR/Cas9. Cell & Bioscience, 5, 1–5.

Warth, P., Hilton, E. J., Naumann, B., Olsson, L., & Konstantinidis, P. (2017). Development of the skull and pectoral girdle in Siberian sturgeon, Acipenser baerii, and Russian sturgeon, Acipenser gueldenstaedtii (Acipenseriformes: Acipenseridae). Journal of Morphology 278, 418–442.

Wassersug, R. J., & Hoff, K. (1979). A comparative study of the buccal pumpimg mechanism of tadpoles. Biological Journal of the Linnean Society, 12, 225–259.

Weisz, P. B. (1945a). The development and morphology of the larva of the South African clawed toad, Xenopus laevis I. The third-form tadpole. Journal of Morphology 77, 163–192.

Weisz, P. B. (1945b). The development and morphology of the larva of the south african clawed toad, Xenopus laevis Journal of Morphology 77, 193–217.

Ziermann, J. M., & Olsson, L. (2007a). A new staging table for stages relevant to cranial muscle development in the African Clawed Frog, Xenopus laevis (Anura: Pipidae). Journal of Morphology 268, (electronic supplement). 1–42.

Ziermann, J. M., & Olsson, L. (2007b). Patterns of spatial and temporal cranial muscle development in the African clawed frog, Xenopus laevis (Anura: Pipidae). Journal of Morphology 268, 791–804.

SUPPORTING INFORMATION

Additional Supporting Information may be found online in the supporting information tab for this article.

How to cite this article: Lukas P, Olsson L. Sequence and timing of early cranial skeletal development in Xenopus laevis Journal of Morphology 2017;00:000–000. https://doi.org/10.1002/jmor.20754

Chapter 2

Bapx1 is required for jaw joint development in amphibians

The paper shows that knockdown of *bapx1* causes specific primary jaw joint loss in three different species of amphibians. Initially a proper jaw joint develops after knockdown but the downregulation of *bapx1* promotes differentiation of cells in the joint cavity into chondrocytes, which leads to the fusion of Meckel´s cartilage and the palatoquadrate during further development. This calls the postulated role of *bapx1* as a major regulator of jaw joint development in question because the results show that *bapx1* is rather necessary for jaw joint maintenance than for induction of its development

Paul Lukas & Lennart Olsson

Submitted to Evolution and Development

PL and LO developed the concept and design of the study. PL was responsible for the experimental procedures including morpholino experiments, whole mount in-situ hybridisation, clearing-and-staining, immunostainings, 3D-reconstructions and histology. Analysis and interpretation of the data mentioned was mainly done by PL, who was also responsible for the drafting of the manuscript and its final form. LO critically revised the manuscript.

Abstract

The acquisition of a movable jaw and a jaw joint are key events in gnathostome evolution. Jaws are derived from the neural crest derived pharyngeal skeleton and the transition from jawless to jawed vertebrates consists of major morphological changes, which must have a genetic foundation. Recent studies on the effects of *bapx1* knockdown in fish and chicken indicate that *bapx1* has acquired such a role in primary jaw joint development during vertebrate evolution, but evidence from amphibians is missing so far. In the present study, we use *Ambystoma mexicanum*, *Bombina orientalis* and *Xenopus laevis* to investigate the effects of *bapx1* knockdown on the development of these three different amphibians. Using morpholinos we downregulated the expression of *bapx1* and obtain morphants with altered mandibular arch morphology. In the absence of *bapx1* Meckel´s cartilage and the palatoquadrate jaw joint initially develop separately but during further development the joint cavity between both fills with chondrocytes. This results in the fusion of both cartilages and the loss of the jaw joint. Despite this the jaw itself remains usable for feeding and breathing. We show that *bapx1* plays a role in jaw joint maintenance during development and that the morphants morphology possibly mirrors the morphology of the jawless ancestors of the gnathostomes

Keywords: *nkx 3.2*, *xbap*, mandibular arch

Introduction

The evolution of joints and the acquisition of a movable jaw are key events in the evolution of gnathostomes. Jaws are derived from the pharyngeal skeleton and the transition from jawless to jawed vertebrates consists of major morphological changes which must have a genetic foundation. A movable jaw enables predation on large and motile prey and the jaw consists of several ventral and dorsal elements connected by a joint (Cerny et al., 2010). These craniofacial elements are largely derived from pluripotent neural crest cells. The shape of the skeletal derivatives of the neural crest depends on partitioning of the precursor cell populations along the anterior-posterior and dorsoventral axes. The expression of homeobox genes in the cranial neural crest progenitor cells establishes a gradual anterior-posterior pattern before migration, which defines specific regions and therefore the shape of the cartilages that develop later along the anterior-posterior axis (Baltzinger, Ori, Pasqualetti, Nardi, & Rijli, 2005; Kuratani, 2012; Minoux et al., 2010; Pasqualetti, Ori, Nardi, & Rijli, 2000). The first pharyngeal arch, the mandibular arch, which forms the jaw in all gnathostomes except mammals, is defined by the absence of hox transcripts (Couly, Grapin-Botton, Coltey, Ruhin, & Le Douarin, 1998; Rijli et al., 1993). Nested expression of dlx genes patterns the pharyngeal arches in dorsoventral direction (Beverdam et al., 2002; Depew, Lufkin, & Rubenstein, 2002). The evolution of such a dorsoventral patterning program may have been a keystone in jaw evolution (Depew et al., 2002; Kuratani, 2005). It enables locally restricted expression of different regulators. Along the dorsoventral axis, the mandibular region is subdivided into three nonoverlapping domains during jaw development (Nichols, Pan, Moens, & Kimmel, 2013). *Hand2* is expressed ventrally and its domain is dorsally restricted by barx1 expression in the subintermediate domain. Dorsally *bapx1* is expressed in the intermediate domain which marks the future jaw joint (Nichols et al., 2013).

Bapx1, also known as *nkx3.2*, was first identified in *Drosophila* and is part of the NK family of homeobox genes (Kim & Nirenberg, 1989). In *Drosophila* it specifies the visceral mesoderm during midgut musculature formation (Azpiazu & Frasch, 1993). A homologous gene is expressed in the pharyngeal endoderm of the first forming gill slit in amphioxus (Meulemans & Bronner-Fraser, 2007). *Bapx1* is also expressed in the pharyngeal endoderm of lampreys (Cerny et al., 2010). During gnathostome evolution, *bapx1* has acquired novel functions and craniofacial expression patterns (Lettice, Hecksher-Sørensen, & Hill, 2001). Vertebrate homologs of *Bapx1* expressed in the first pharyngeal arch have been found in numerous vertebrates including *Scyliorhinus* (Compagnucci et al., 2013),Zebrafish (Miller, 2003), *Xenopus* (Newman, Grow, Cleaver, Chia, & Krieg, 1997), *Pleurodeles* (Nicolas, Caubit, Massacrier, Cau, & Le Parco, 1999), chicken (Schneider et al., 1999), Mouse (Tribioli, Frasch, & Lufkin, 1997) and human (Yoshiura & Murray, 1997).

Lampreys and gnathosthomes share a common jawless ancestor. Expression analysis in lampreys revealed, that *bapx1* is not expressed in the first arch (Cerny et al., 2010). The incorporation of *bapx1* into a pre-existing dorsoventral patterning program may have driven the evolution of the jaw by altering the ancestral intermediate first arch expression pattern

(Cerny et al., 2010; Medeiros & Crump, 2012). In zebrafish, *bapx1* is regulated by *edn1*. It is expressed in an intermediate domain in the first pharyngeal arch, which later marks the jaw joint (Miller, 2003). Functional knockdown of *bapx1* in zebrafish revealed that the development of the jaw joint, the retroarticular process of Meckel´s cartilage and the retroarticular bone all require proper *bapx1* function. Absence of *bapx1* led to fusion of Meckel´s cartilage and the palatoquadrate and therefore to loss of the primary jaw joint (Miller, 2003). In mice, *bapx1* is expressed during embryogenesis in a region which marks the future malleus and incus (Tribioli et al., 1997). In all vertebrates except mammals the homologous structures to these middle ear ossicles form the jaw and are connected through the primary jaw joint. Unlike in fishes, after inactivation of *bapx1* in mice, a proper joint formed between malleus and incus. Only the width of the malleus is affected (Tucker, 2004). Mutation and the resulting inactivation of *bapx1* is proposed to also play an important role in humans as it may cause spondylo-megaepiphyseal dysplasia (Hellemans et al., 2009).

Results from lamprey and zebrafish strongly suggest a role for *bapx1* in jaw joint evolution, whereas the outcomes of *bapx1* knockdown in fishes and *bapx1* inactivation in mice show large differences. Larval fishes lack a joint after *bapx1* knockdown between Meckel´s cartilage and the palatoquadrate whereas mice have a functioning joint between Malleus and Incus after knockout. The mammalian Malleus is homologous to the retroarticular processus of Meckel´s cartilage and the Incus is homologous to the quadrate region of the palatoquadrate and both are part of the mammalian middle ear whereas a secondary jaw joint is formed between the dentary and the squamosal (Hanken & Hall, 1993). Therefore, the *bapx1*-containing gene regulatory network must have evolved during the evolution of tetrapods. Studies in amphibians can increase our knowledge of the function of *bapx1* in evolution and development because amphibians are basal tetrapods and the only recent land-living anamniotes. Life on land requires the adaptation of many morphological traits and the gene regulatory networks that give rise to them during development. In *Xenopus laevis* *bapx1*, also known as *xbap*, is expressed in the intermediate region of the first branchial arch surrounding the developing jaw joint (Newman et al., 1997; Square et al., 2015) and shares this first pharyngeal arch expression pattern with those observed in zebrafish (Miller, 2003). In *Xenopus laevis* two duplicates of *bapx1,* nkx3.2-S and nkx3.2-L, are present (Square et al., 2015).

Here we present further investigations on the function of *bapx1* in amphibians. To investigate its role in jaw joint development we performed functional knockdown of *bapx1* using morpholino antisense oligonucleotides in three amphibian species (*Ambystoma mexicanum*, *Bombina orientalis*, *Xenopus laevis*). Our results indicate that *bapx1* is involved in the correct formation of the primary jaw joint in amphibians. Understanding the underlying developmental programs which are involved in generating morphological novelties such as the primary jaw joint is interesting from both evolutionary and developmental perspectives and could shed light on how an evolutionary novelty can arise during evolution.

Material and Methods

Amphibian maintenance

Xenopus laevis (Daudin), *Bombina orientalis* (Boulenger) and *Ambystoma mexicanum* (Shaw) were kept in our departmental breeding colony. Males and females were kept separately. *X. laevis* adults were kept at 22°C. To obtain eggs pairs of *X. laevis* were put together over night at 16°C in a darkened basin with lowered water level to induce mating. The eggs were dejellied using 2% cysteine hydrochloride. After a cool down period of two months at 8°C *B. orientalis* adults were kept at 22°C and fed *ad libitum*. After two weeks, single pairs were put together under humid conditions over night to induce mating. The eggs obtained were dejellied manually. *A. mexicanum* were kept at 18°C. Single pairs were transferred into a basin with fresh water. Ice was added to lower the temperature and induce mating. The eggs were dejellied manually. Developmental stages were determined according to Nieuwkoop and Faber (Nieuwkoop & Faber, 1994) Ziermann and Olsson (Ziermann & Olsson, 2007) for *X. laevis*, Gosner (Gosner, 1960) for *B. orientalis* and Schreckenberg and Jacobson (Schreckenberg & Jacobson, 1975) for *A. mexicanum*.

Morpholino oligo injections

For each experimental approach described below 30 eggs were used and each experiment was performed three times with eggs from different mating pairs (N=90 for each experiment). *Bapx1* morpholino oligos were derived from the NK 3 homeobox 2 mRNA from *Xenopus tropicalis* provided by NCBI (XM_002940741.4). The sequence from *Xenopus tropicalis* was used because the available sequence from *Xenopus laevis* contained no information about the untranslated region upstream from the start codon, which is necessary for proper morpholino design. Two morpholinos which inactivate the two *bapx1* duplicates bapx-MO1 5′-CCTCTGAACATAAAGGGACCCGGGT-3′ (ATG start complementary sequence underlined) and bapx-MO2 5′-GTGCAAAGACCAGTGTCTCTTGGCA-3′ were purchased from Gene Tools, Inc. and diluted in autoclaved water to a stock concentration of 1mM (Fig. 1). Subsequent dilutions were made to concentrations of 10, 20 and30 µM (bapx-MO1) and 90 and100 µM (bapx-MO2). Initially both morpholinos were injected separately. To further confirm the specificity of the phenotypes obtained both morpholinos were injected together at relatively lower concentrations. Injections were performed in 4% Ficoll/ 0,1x MBS. After 4 hours, *Xenopus laevis* and *Bombina orientalis* embryos were transferred to 0,1x MBS, *Ambystoma mexicanum* embryos were transferred to 1x Steinbergs solution with Gentamycin. For unilateral injections, approximately 10 nl was injected into one blastomere at the 2-cell stage. For bilateral injections 10 nl morpholino was injected at the 1-cell stage or 5nl morpholino was injected into both blastomeres at the 2-cell stage. Fluorescein was co-injected to check for proper injection. Only fluorescent specimen were used for further investigations. Injected animals were observed daily for phenotypes, dead and unperturbed embryos. The injection of 30µM of bapx-MO 1 gave clear phenotypes in *X. laevis* and was therefore used for further phenotypic analyses in *A. mexicanum* and *B. orientalis*. For control, a control Morpholino oligonucleotide (Co-MO) against human β-globin 5′-

CCTCCTACCTCAGTTACAATTTATA-3′ (Gene Tools) was injected under the same conditions in *X. laevis*, *B. orientalis* and *A. mexicanum*. Anaesthesia was performed 6-10 days after egg deposition using 1% tricaine methanesulfonate (MS-222) according to the animal welfare protocols at Friedrich-Schiller-Universität Jena. Larvae were fixed either in 4% phosphate-buffered formalin (PFA) or in Dent´s fixative depending on following investigations.

Tissue staining

After dehydration and embedding in paraffin, PFA-fixed larvae were serially sectioned at 7µm using a microtome (Microm, HM 355 S). Sections were stained with Heidenhain´s Azan technique (Heidenhain, 1915) or nuclear fast red staining (Anken & Kappel, 1992). Images were taken with an XC10 Olympus camera mounted on an Olympus BX51 microscope operated with dotSlide software. Whole-mount clearing and staining was done according to Dingerkus and Uhler (1977) without the use of alizarin red due to the absence of bones in the investigated stages. Images of cleared and stained larvae (and of unstained larvae) were taken using a Zeiss Stemi SV11 and an attached camera (ColorView) operated by AnalySIS software. Whole-mount antibody staining was used to specifically stain for cartilage and muscle cells. A monoclonal antibody against newt skeletal muscle (12/101) and a monoclonal antibody against collagen II (11683-collagen II) were used. Secondary antibodies were conjugated with Alexa 488 and Alexa 568 (Molecular Probes). Specimens were scanned using a confocal laser scanning microscope (Zeiss LSM 510). The image stacks obtained were processed with Amira 6.0.1. and Autodesk Maya® 2017.

In situ hybridisation

Whole-mount in situ hybridisations were carried out according to the protocol in Harland (Harland, 1991) with few modifications described by Square et al.(Square et al., 2015). NF 30-40 larvae were treated for 15 min and NF 40-45 larvae were treated for 20 min with Proteinase K. BM-Purple (Roche) was used for signal development. Probes of *bapx1* and *sox9* were kindly provided by Jennifer Schmidt.

Results

Bapx1 is expressed in PA1 during chondrocyte differentiation in *Xenopus laevis*

Spatial expression of *bapx1* is visualized for Ziermann and Olsson stage (ZO) 5 (Fig. 2A) and ZO 14 (Fig. 2B). At ZO 5 *bapx1* is expressed in the ventral region of the first pharyngeal arch (PA1) flanking the cement gland dorsolaterally and marking the precursors of the palatoquadrate and the proximal part of Meckel´s cartilage (Fig. 2D). Three stripes of expression domains are visible posterior to it. They correspond to the endoderm of the pharyngeal pouches of PA 3-5 (Fig. 2E). At ZO 14 a domain of *bapx1* surrounds a broad region at the level of the palatoquadrate and the proximal Meckel´s cartilage (Fig. 2B). This region includes the developing primary jaw joint. *bapx1* is also widely expressed on both sides of the anterior gut mesoderm at ZO 5 (Fig. 2F) and ZO 14. After knockdown of *bapx1* the expression domains are clearly reduced (Fig. 2C). At the level of PA1 the domain is diminished ventrally and dorsally. The expression marking PA 3-5 is completely lost and expression in the anterior gut mesoderm is restricted to a small ventral area. The expression of *sox9* was investigated as a control to identify possible non-specific suppression of transcription. N=80 unperturbed and N= 72 tadpoles injected with 30µM bapx-MO1 were screened for sox9 disruptions. Sox9 is essential for the specification and differentiation of mesenchymal cells toward the chondrogenic lineage (Lee & Saint-Jeannet, 2011). Normally developed tadpoles at ZO 5 show typical expression in mesenchyme of the mandibular, hyoid, anterior and posterior branchial arches (Fig. 2G). The same expression can be observed after knockdown of *bapx1* (Fig. 2H). This indicates that the altered temporal and spatial expression pattern of *bapx1* is a direct result of the knockdown using *bapx1* morpholinos and not a consequence of non-specific transcription suppression.

Bapx1 knockdown leads to mild head deformation

Initially bapx-MO1 was injected at different concentrations (10µM, 20µM, 30µM) into *X. laevis* fertilized eggs. No difference in external morphology and a slight increase in mortality was observed in Co-MO and larvae treated with 10mM and 20µM bapx-MO1. Larvae treated with 30µM bapx-MO1 showed an increased number of phenotypes and increased mortality (Table 1). The head of unperturbed *X. laevis* larvae normally starts to flatten dorsoventrally around ZO 14 (Fig. 3D). In 30µM bapx-MO1-treated larvae the head remained more roundish and the region around the mouth opening was swollen (Fig. 3A). Injections of 30µM bapx-MO1 also caused more severe phenotypes, including bent axes and dislocated mouth openings (Fig. 3E, F), but at low frequency (N=4). The latter did not survive until head cartilages started to chondrify. A second morpholino was then tested as a control. Larvae treated with 90µM bapx-MO2 displayed no signs of external deformation. Phenotype occurence and mortality was not significantly increased, similar to injections of 10µM and 20µM of bapx-MO1. Instead, injections of 100µM bapx-MO2 led to roundish heads (Fig. 3B) and a slightly increased mortality, similar to the results of 30µM bapx-MO2 injections (Table 1). The number of phenotypes was also increased compared to 90µM bapx-MO2 treatment. To further confirm the specificity of the phenotypes, both morpholinos were injected at lower concentrations. Injecting 10µM bapx-MO1 alone lead to 10% mortality and

4% phenotype occurrence. In combination with 30µM bapx-MO2, mortality was almost constant but phenotype occurrence increased to 43%. Coinjection of 20µM bapx-MO1 and 60µM bapx-MO2 further enhances the occurrence of phenotypes to 65% which showed roundish heads (Fig. 3C), similar to the results of MO1 and MO2.

Jaw joint development depends on *bapx1* in amphibians

X. laevis larvae (phenotypes and normal larvae) that survived until day 6 (NF 44-46), were screened for skeletal alterations via clearing and staining (N=703). This technique revealed, that the phenotypes that were recognized by external morphology also show changes in the mandibular arch. Meckel´s cartilage and the palatoquadrate are fused at the point, where the primary jaw joint is located in normal larvae (compare Figs. 4A and B). Uninjected and Co-MO injected larvae never show this fusion (Table 1). In bapx-MO injected larvae fusion of both parts rarely happened at lower doses but joint loss occurred frequently at higher doses of both bapx-MO1 and bapx-MO2 (Table 1). Combined injections of both morpholinos at lower doses lead to more larvae with loss of the primary jaw joint. Additional unilateral injections of 30µM bapx-MO1, 100µM bapx-MO2 and 20µM and 60µM bapx-MO1 and MO2 were performed to further confirm the specificity of the jaw joint loss phenotype. Unilateral injection of 30µM bapx-MO1 causes a mild deformation of the cranial skeleton on the injected side (Fig. 5 A, right side). The processus muscularis is flattened and extends more laterally. On the control side, it extends dorsally and is narrower. The lateral projection of the suprarostral plate is shorter on the injected side and does not cover Meckel´s cartilage in dorsal view as it does on the control side (Fig. 5A). Furthermore, Meckel´s cartilage and the palatoquadrate are fused on the injected side (compare Figs. 5B and C). The two parts of the lower jaw are connected by a u-shaped cartilaginous band. The processus retroarticularis of Meckel´s cartilage and the processus articularis palatoquadrati are not visible. Unilateral injection of 100µM bapx-MO2 lead to similar malformations (Fig. 5D). Processus muscularis is flattened and the projection of the suprarostral is shortened on the injected side (Fig. 5D, right side). The fusion between Meckel´s cartilage and the palatoquadrate is more complete and only a small depression is visible dorsally. The processus cornu quadratus lateralis of the palatoquadrate is well developed on the control side (Fig. 5E), but fails to develop on the injected side (Fig. 5F). Combinatorial injection of 20µM and 60µM bapx-MO1 and MO2 also lead to a flattened processus muscularis and shortened suprarostral plate projection on the injected side (Fig. 5G, right side). Meckel´s cartilage and the palatoquadrate are fused and the point of fusion is characterized by a small dorsal depression (Fig. 5I). No malformations of the posterior cartilaginous structures were observed.

Because of the loss of the jaw joint, we expected that the muscles which insert on Meckel´s cartilage and enable a proper opening and closing of the jaw might also be malformed. To test this, we performed additional unilateral injections. Knockdowns with 30µM bapx-MO1 showed both low mortality and a high frequency of joint loss. Therefore, we used this concentration in *X. laevis* to detect additional musculoskeletal abnormalities. On the control side, the m. levator mandibulae articularis is a short muscle which originates on the anterior dorsal surface of the palatoquadrate and inserts on the posterior dorsal surface of Meckel´s

cartilage. The m. levator mandibulae longus superficialis originates from the subocular bar and inserts on the dorsolateral surface of Meckel´s cartilage anterior to the insertion of the m. levator mandibulae articularis. The m. quadrato-hyoangularis originates from the anterodorsal surface of the ceratohyal and the lateral surface of the palatoquadrate. Its insertion covers the dorsolateral surface of the posterior end of Meckel´s cartilage (Fig. 5J). The muscles described have the same origination on the injected side and they all insert on Meckel´s cartilage. The insertion of the m. levator mandibulae articularis was shifted anteriorly and laterally. It is not bordered by the m. levator mandibulae longus superficialis at the point of insertion as it is in unperturbed larvae. The origination of the latter muscle was shifted anteriorly. The insertion of the m. quadrato-hyoangularis remains the same as on the control side (Fig. 5K). Observation of living tadpoles revealed that malformed larvae were able to open and close their mouth in the same typical manner as unperturbed larvae. Even with fused lower jaw elements, ingestion and respiration was no problem and malformed larvae could survive.

We wanted to investigate whether the observed jaw joint phenotypes and the *bapx1* dependent jaw joint development in *X. laevis* represent a common amphibian feature, or whether they are a consequence of the highly specialized morphology of *X. laevis* larvae. To test this, we extended our investigations by adding *Bombina orientalis* and *Ambystoma mexicanum* as two further amphibian representatives. We used 30µM bapx-MO1 to knock *bapx1* down in both species. Larvae of *B. orientalis* treated with 30µM bapx-MO1 (N=90) show a swollen mouth region similar to *X. laevis* larvae. Additionally, the mouth opening is located more anteriorly than in control larvae (compare Figs. 6A and B). There is no difference in the external morphology of a *A. mexicanum* larvae treated with 30µM (N=90) and Co-MO treated larvae (compare Figs. 6C and D). Unilaterally injected *B. orientalis* (N=90) and *A. mexicanum* (N=90) larvae also fail to develop a joint on the injected side. In *B. orientalis* Meckel´s cartilage is broadly fused to the palatoquadrate and the distal portion is partly lost. The ala of the suprarostral is reduced and malformed (compare Figs. 7A and B) whereas the infrarostral is not malformed. In *A. mexicanum* the joint loss is the only observed malformation (Figs. 7C and D).

Jaw joint morphogenesis is altered after *bapx1* knockdown

Having established that Meckel´s cartilage and the palatoquadrate are fused in bapx-MO treated amphibians, a logical next step was to investigate how this fusion is established during embryonic and larval development. To this end, *X. laevis* embryos were unilaterally injected with 30µM bapx-MO1 at the 2-cell stage. Meckel´s cartilage and the palatoquadrate mesenchymal condensation develop and chondrify separately on both the control and the injected side (Figs. 8A, B). A gap which is supposed to be the joint cavity is clearly visible on both sides between the recently chondrified Meckel´s cartilage and the palatoquadrate at ZO 12. Until ZO 14 the joint cavity remains fully opened. On the injected side a small band of connective tissue cells becomes visible between the freshly chondrified retroarticular processus of Meckel´s cartilage and the processus articularis of the palatoquadrate (compared Figs. 8C and D). During further stages this band of dense cells thickens and

chondrifies. At ZO 17 Meckel´s cartilage and the palatoquadrate are connected ventrally through this band of cartilaginous cells on the injected side (black arrowhead in Fig. 8F). On the control side both parts of the lower jaw are separated by the joint cavity. Indeed, a ventrally proceeding small band of connective tissue is present between Meckel´s cartilage and the palatoquadrate on the control side (Fig. 8E), but shows no signs of chondrification.

Discussion

The efficiency of the two morpholinos used in this investigation was tested in multiple ways. Two non-overlapping morpholinos were used to confirm phenotype specificity. Bapx-MO1 is antisense to the ATG-containing region of the *bapx1* gene, whereas bapx-MO2 was designed to bind upstream of the start codon. Therefore, a higher concentration of bapx-MO2 was needed according to manufacturer's recommendation. Unilateral and bilateral injections of the two morpholinos have shown the same joint loss phenotype in a dose-dependent manner. For further confirmation of the specificity both morpholinos were injected together at relatively lower doses. Combinatorial injection lead to an increase of joint loss frequency at lower doses, which further supports the specificity of these non-overlapping morpholinos. Whole mount in-situ hybridisations of treated specimens both show a clear reduction of *bapx1* expression after *bapx1* knockdown. *Sox9* negative control in-situ hybridisations show that the morphological changes of the morphants are not caused by general retardation. This further supports the specific efficiency of the morpholino used. All in all, we have shown, that the morpholino used is able to specifically downregulate *bapx1* expression and that the obtained morphants, which display loss of the primary jaw joint, are a result of *bapx1* knockdown.

Bapx1 expression in the first pharyngeal arch is conserved among gnathostomes

The spatial expression pattern of *bapx1* during development of *X. laevis* has been investigated before (Newman et al., 1997; Square et al., 2015). Our findings confirm the presence of *bapx1* in the intermediate domain of PA1 in this species. This ventromedial part of PA1 marks the area from which the primary jaw joint develops. Expression of homologous *bapx1* around this area can also be seen in shark, zebrafish, chicken and mouse (Compagnucci et al., 2013; Miller, 2003; Schneider et al., 1999; Tribioli et al., 1997). *Bapx1* is not expressed in the intermediate domain of PA1 in lamprey and no expression in the head region of the non-vertebrate amphioxus can be seen (Cerny et al., 2010; Meulemans & Bronner-Fraser, 2007). The presence of an intermediate domain expressing *bapx1* in gnathostomes and the loss of the jaw articulation after *bapx1* knockdown experiments in zebrafish (Miller, 2003), *A. mexicanum*, *B. orientalis* and *X. laevis* (present study) strongly suggests a role for *bapx1* in the evolution of the primary jaw joint.

Bapx1 represses cartilage development in the jaw joint

Loss of the primary jaw joint is the predominant morphant after *bapx1* knockdown. Through additional testing of bapx-MO in *Ambystoma mexicanum* and *Bombina orientalis,* we can

confirm that joint loss is not a result of the derived state of *Xenopus laevis*, nor a feature specific to anurans. Instead, the function of *bapx1* in intermediate first arch patterning is conserved among the amphibians studied. The joint loss phenotype after *bapx1* knockdown in amphibians is congruent with phenotypes resulting from the knockdown of other genes known to be involved in first pharyngeal arch patterning. *Barx1* is a gene which is excluded from the intermediate domain of the PA1 of *X. laevis*, zebrafish and mouse (Sperber & Dawid, 2008; Square et al., 2015; Tissier-Seta et al., 1995) whereas it is consistently expressed in the lamprey PA1, while *bapx1* is absent from this arch (Cattell, Lai, Cerny, & Medeiros, 2011; Cerny et al., 2010). Overexpression of *barx1* in zebrafish revealed, that *barx1* is able to repress jaw joint formation by promoting cartilage development (Nichols et al., 2013). Obtained phenotypes show variable joint loss after overexpression, including presence of ectopic chondrocytes in the jaw joint and jaw joint fusion. These phenotypes resemble the morphants we obtained after *bapx1* knockdown in amphibians. The knockdown of *bapx1* may have caused a dorsal expansion of the cartilage promoting *barx1* domain in our experiments because the cartilage preventing *bapx1* was downregulated, which caused the observed joint loss.

Bapx1 expression has been shown to be positively regulated by *edn1* in zebrafish and knockdown of this gene in zebrafish also causes joint loss and further defects in cranial muscle and endodermal patterning (Miller, 2003; Miller, Schilling, Lee, Parker, & Kimmel, 2000). The less fatal phenotype obtained in our *bapx1* knockdown experiments and the similar joint loss in amphibians suggests that *bapx1* may act downstream of *edn1* in amphibians, too.

5-HTB2 is a receptor of the well-known neurotransmitter serotonin, which is involved in the development and evolution of the vertebrate mandibular arch (Berger, Gray, & Roth, 2009). Downregulation of 5-HTB2 in *Xenopus laevis* caused simultaneous downregulation of *bapx1* (Reisoli, De Lucchini, Nardi, & Ori, 2010). The lowered expression of *bapx1* in PA1 of *X. laevis* after 5-HTB2 knockdown resembles the pattern after *bapx1* knockdown. The same loss of the primary jaw joint and the retroarticular process can be observed after 5-HTB2 and *bapx1* knockdown in *X. laevis*. The muscular connectivity is also altered. The m. hyoangularis and the m. quadratoangularis, mostly regarded as one muscle named m. quadrato-hyoangularis, fail to attach to Meckel´s cartilage (Reisoli et al., 2010). In the present study, the m. quadrato-hyoangularis reaches Meckel´s cartilage almost normally and enables jaw opening in the morphants. According to these results we suggest that *bapx1* acts downstream of 5-HTB2, because of the milder phenotype, and that *bapx1* has no influence on the development of PA1-derived muscles.

Developmental evidence from our knockdown experiments support considerations that *bapx1* may not be a master regulator of joint formation (Medeiros & Crump, 2012). Although zebrafish and chicken lost the primary jaw joint after *bapx1* knockdown such a loss can not be seen in mice, where a proper joint forms despite *bapx1* knockdown (Miller, 2003; Tucker, 2004; Wilson & Tucker, 2004). Results in mice indicate that an upstream target of *bapx1* must exist, which directly regulates primary jaw joint development (Tucker,

2004). Unlike in chicken, where Meckel´s cartilage and the palatoquadrate develop from one condensation (Wilson & Tucker, 2004), in *X. laevis* they develop from two distinct condensations (Lukas & Olsson, 2017). If *bapx1* is a master regulator of joint formation, *bapx1* knockdown should disturb joint development right from the beginning of chondrogenesis. The result would be, that the two developing condensations fuse in *X. laevis* early in development. But this is not the case. After knockdown of *bapx1* the condensations of Meckel´s cartilage and the palatoquadrate arise and chondrify separately. They fuse later during development because of the invasion of ectopic chondrocytes (Fig. 8). The fusion arises at ZO14 when processus retroarticularis of Meckel´s cartilage and processus articularis of the palatoquadrate have recently chondrified (Fig. 8D). A band of cells migrates into the gap between the two processes and chondrifies during further development, whereas normally they are connected through a thin band of connective tissue. We hypothesize that *bapx1* acts as a cartilage preventing gene in unperturbed larval development and ensures that the joint region does not chondrify. In perturbed larvae, *bapx1* expression might be replaced by dorsally expanded *barx1* expression as reported in *barx1* overexpression experiments (Nichols et al., 2013). *Barx1* promotes cartilage development and could lead to chondrification of the cells present in the joint region when *bapx1* is absent. The anuran-specific intramandibular joint separates the infrarostral cartilage from Meckel´s cartilage. Neither is *bapx1* expressed in a domain predicting this joint nor is the formation of the joint perturbed by the knock down of *bapx1*. Therefore, the present work provides no support that the evolution of this cartilage was caused by *bapx1*. It is rather considered that the gene *zax* which is a paralogue of *bapx1* is involved in the development and evolution of the intramandibular joint (Svensson & Haas, 2005).

Bapx1 morphants resemble the ancestral unjointed first pharyngeal arch

Indirect loss of *bapx1* function through the addition of *fgf8* or *bmp4* beads lead to the loss of the jaw joint and the retroarticular process in chicken embryos (Wilson & Tucker, 2004). Knockdown of *bapx1* in zebrafish lead to loss of the jaw joint and the retroarticular process of Meckel´s cartilage (Miller, 2003). In the present study the jaw joint and the retroarticular process are also lost after *bapx1* knockdown. The reduction of *bapx1* function in fishes and birds, as well as in amphibians, possibly mirrors the unjointed mandibular arch of agnathan ancestors as hypothesized before (Medeiros & Crump, 2012). The insertion of the musculature responsible for opening and closing the jaw was slightly affected by the knockdown (Fig. 5K) but its function retained. Morphants were able to move the jaw up and down almost normally even without a jaw joint and were also able to breathe and filter feed. The nearly unperturbed musculature in combination with the resilient and smooth elastic traits of the cartilaginous tissue seem to ensure the proper function of the jaw. The larval m. quadratohyoangularis develops into the adult inner part of the depressor mandibulae, the larval m. levator mandibulae articularis develops into the adult adductor mandibulae A2 PVM (postero-ventro-mesial) and the larval m. levator mandibulae longus surperficialis develops into the adult adductor mandibulae A2 longus during metamorphosis (Ziermann & Diogo, 2014). These postmetamorphic muscles are a crucial part of the adult masticatory apparatus. A hypothetical stem line representative of gnathostomes could have had a feeding

apparatus which consists of a continuous and cartilaginous PA1. In this hypothetical gnathostome ancestor a set of muscles homologous to the adductor mandibulae complex and the depressor mandibulae may insert in the same way as in the *bapx1* morphants and facilitate jaw movement before evolution of a jaw joint itself. The absence of *bapx1* in agnathans (Cerny et al., 2010) and its role in various gnathostomes suggest that a ventral pharyngeal patterning system was present before the rise of gnathostomes. Later during evolution *bapx1* might have refined this system by altering the ancestral *barx1* expression domain. This alteration led to a spatial prevention of chondrification within PA1. This alteration in combination with the evolution of upstream regulators and downstream targets could have contributed to the evolution of the jaw joint in gnathostomes.

Conclusion

In the present study, the expression of *bapx1* was downregulated. It was shown that the reduction of *bapx1* expression causes a specific loss of the primary jaw joint in three different amphibian species. Normal *bapx1* expression prevents existing cells in the joint cavity from differentiating into chondrocytes. Reduced expression of *bapx1* instead promotes chondrification of these cells, which leads to the fusion of Meckel´s cartilage and the palatoquadrate. This unjointed mandibular arch mirrors features of a possible jawless gnathostome ancestor and thus gives insight into how the integration of a new gene in a pre-existing gene regulatory network can lead to major morphological changes. *Bapx1* can not be seen as a key regulator of joint formation in amphibians, but it is responsible for keeping the joint cavity free of chondrocytes and thus for maintaining the primary jaw joint.

Acknowledgements

This study was supported in part by a grant from the Deutsche Forschungsgemeinschaft (grant no. OL 134/2-4 to LO) and the Studienstiftung des Deutschen Volkes (to PL). We are very grateful to Katja Felbel for technical support and preparation of the histological sections. Sandra Eisenberg took care of the animals. Bernhard Bock helped with the clearing and staining procedure. The monoclonal antibodies against collagen II (116B3-collagen II) and newt skeletal muscle (12/101) obtained from the Developmental Studies Hybridoma Bank were developed under the auspices of the NICHD and maintained by The University of Iowa, Department of Biological Sciences, Iowa City, IA 52242, USA. The authors declare no conflict of interest.

Author contributions

PL and LO developed the concept and design of the study. PL was responsible for the experimental procedures including morpholino experiments, whole mount in-situ hybridisation, clearing-and-staining, immunostainings, 3D-reconstructions and histology. Analysis and interpretation of the data mentioned was mainly done by PL, who was also responsible for the drafting of the manuscript and its final form. LO critically revised the manuscript.

Literature cited

Anken, R. H., & Kappel, T. (1992). Die Kernechtrot-Kombinationsfärbung in der Neuroanatomie. *Winke Fürs Labor*, *81*(2), 62–63.

Azpiazu, N., & Frasch, M. (1993). tinman and bagpipe: two homeo box genes that determine cell fates in the dorsal mesoderm of Drosophila. *Genes & Development*, *7*(7B), 1325–40.

Baltzinger, M., Ori, M., Pasqualetti, M., Nardi, I., & Rijli, F. M. (2005). Hoxa2 knockdown in Xenopus results in hyoid to mandibular homeosis. *Developmental Dynamics*, *234*(4), 858–867.

Berger, M., Gray, J. A., & Roth, B. L. (2009). The Expanded Biology of Serotonin. *Annual Review of Medicine*, *60*(1), 355–366.

Beverdam, A., Merlo, G. R., Paleari, L., Mantero, S., Genova, F., Barbieri, O., … Levi, G. (2002). Jaw transformation with gain of symmetry after Dlx5/Dlx6 inactivation: Mirror of the past? *Genesis*, *34*(4), 221–227.

Cattell, M., Lai, S., Cerny, R., & Medeiros, D. M. (2011). A New Mechanistic Scenario for the Origin and Evolution of Vertebrate Cartilage. *PLoS ONE*, *6*(7), e22474.

Cerny, R., Cattell, M., Sauka-Spengler, T., Bronner-Fraser, M., Yu, F., & Medeiros, D. M. (2010). Evidence for the prepattern/cooption model of vertebrate jaw evolution. *Proc Natl Acad Sci U S A*, *107*(40), 17262–17267.

Compagnucci, C., Debiais-Thibaud, M., Coolen, M., Fish, J., Griffin, J. N., Bertocchini, F., … Depew, M. J. (2013). Pattern and polarity in the development and evolution of the gnathostome jaw: Both conservation and heterotopy in the branchial arches of the shark, Scyliorhinus canicula. *Developmental Biology*, *377*(2), 428–448.

Couly, G., Grapin-Botton, A., Coltey, P., Ruhin, B., & Le Douarin, N. M. (1998). Determination of the identity of the derivatives of the cephalic neural crest: incompatibility between Hox gene expression and lower jaw development. *Development (Cambridge, England)*, *125*(17), 3445–59.

Depew, M. J., Lufkin, T., & Rubenstein, J. L. R. (2002). Specification of jaw subdivisions by Dlx genes. *Science (New York, N.Y.)*, *298*(5592), 381–5.

Dingerkus, G., & Uhler, L. D. (1977). Enzyme clearing of alcian blue stained whole small vertebrates for demonstration of cartilage. *Stain Technology*, *52*(4), 229–32.

Gosner, K. L. (1960). A Simplified Table for Staging Anuran Embryos Larvae with Notes on Identification. *Herpetologists' League*, *16*(3), 183–190.

Hanken, J., & Hall, B. K. (Brian K. (1993). *The Skull*. University of Chicago Press.

Harland, R. M. (1991). In situ hybridization: an improved whole-mount method for Xenopus embryos. *Methods in Cell Biology*, *36*, 685–695.

Heidenhain, M. (1915). Über die mallorysche bindegewebsfärbung mit karmin und azokarmin als vorfarben. *Z Wiss Mikrosk*, *33*, 361–372.

Hellemans, J., Simon, M., Dheedene, A., Alanay, Y., Mihci, E., Rifai, L., … Mortier, G. (2009). Homozygous Inactivating Mutations in the NKX3-2 Gene Result in Spondylo-Megaepiphyseal-Metaphyseal Dysplasia. *American Journal of Human Genetics*, *85*(6), 916–922. https://doi.org/10.1016/j.ajhg.2009.11.005

Kim, Y., & Nirenberg, M. (1989). Drosophila NK-homeobox genes. *Proceedings of the National Academy of Sciences of the United States of America*, *86*(20), 7716–7720.

Kuratani, S. (2005). Developmental studies of the lamprey and hierarchical evolutionary steps towards the acquisition of the jaw. *Journal of Anatomy*, *207*(5), 489–99.

Kuratani, S. (2012). Evolution of the vertebrate jaw from developmental perspectives. *Evolution and Development*, *14*(1), 76–92.

Lee, Y.-H., & Saint-Jeannet, J.-P. (2011). Sox9 function in craniofacial development and disease. *Genesis*, *49*(4), 200–208.

Lettice, L., Hecksher-Sørensen, J., & Hill, R. (2001). The role of Bapx1 (Nkx3.2) in the development and evolution of the axial skeleton. *Journal of Anatomy*.

Lukas, P., & Olsson, L. (2017). Sequence and timing of early cranial skeletal development in Xenopus laevis. *Journal of Morphology*.

Medeiros, D. M., & Crump, J. G. (2012). New perspectives on pharyngeal dorsoventral patterning in development and evolution of the vertebrate jaw. *Developmental Biology*, *371*(2), 121–135.

Meulemans, D., & Bronner-Fraser, M. (2007). Insights from Amphioxus into the Evolution of Vertebrate Cartilage. *PLoS ONE*, *2*(8), e787.

Miller, C. T. (2003). Two endothelin 1 effectors, hand2 and bapx1, pattern ventral pharyngeal cartilage and the jaw joint. *Development*, *130*(7), 1353–1365.

Miller, C. T., Schilling, T. F., Lee, K., Parker, J., & Kimmel, C. B. (2000). sucker encodes a zebrafish Endothelin-1 required for ventral pharyngeal arch development. *Development (Cambridge, England)*, *127*(17), 3815–28.

Minoux, M., Rijli, F. M., Paleari, L., Zerega, B., Postiglione, M. P., Mantero, S., … Levi, G. (2010). Molecular mechanisms of cranial neural crest cell migration and patterning in craniofacial development. *Development (Cambridge, England)*, *137*(16), 2605–21.

Newman, C. S., Grow, M. W., Cleaver, O., Chia, F., & Krieg, P. (1997). Xbap, a vertebrate gene related to bagpipe, is expressed in developing craniofacial structures and in anterior gut muscle. *Developmental Biology*, *181*(2), 223–33.

Nichols, J. T., Pan, L., Moens, C. B., & Kimmel, C. B. (2013). Barx1 Represses Joints and Promotes Cartilage in the Craniofacial Skeleton. *Development*, *140*(13), 2765–2775. https://doi.org/10.1242/dev.090639

Nicolas, S., Caubit, X., Massacrier, A., Cau, P., & Le Parco, Y. (1999). Two Nkx-3-related genes are expressed in the adult and regenerating central nervous system of the urodele Pleurodeles waltl. *Developmental Genetics*, *24*(3–4), 319–28.

Nieuwkoop, P., & Faber, J. (1994). Normal Table of Xenopus laevis (Daudin). *New York: Garland Publishing*.

Pasqualetti, M., Ori, M., Nardi, I., & Rijli, F. M. (2000). Ectopic Hoxa2 induction after neural crest migration results in homeosis of jaw elements in Xenopus. *Development*, *127*, 5367–5378.

Reisoli, E., De Lucchini, S., Nardi, I., & Ori, M. (2010). Serotonin 2B receptor signaling is required for craniofacial morphogenesis and jaw joint formation in Xenopus.

Development, *137*(17), 2927 LP-2937.

Rijli, F. M., Mark, M., Lakkaraju, S., Dierich, A., Dollé, P., & Chambon, P. (1993). A homeotic transformation is generated in the rostral branchial region of the head by disruption of Hoxa-2, which acts as a selector gene. *Cell*, *75*(7), 1333–1349.

Schneider, A., Mijalski, T., Schlange, T., Dai, W., Overbeek, P., Arnold, H. H., & Brand, T. (1999). The homeobox gene NKX3.2 is a target of left-right signalling and is expressed on opposite sides in chick and mouse embryos. *Current Biology*, *9*(16), 911–914.

Schreckenberg, G. M., & Jacobson, A. G. (1975). Normal stages of development of the axolotl, Ambystoma mexicanum. *Developmental Biology*, *42*(2), 391–399.

Sperber, S. M., & Dawid, I. B. (2008). barx1 is necessary for ectomesenchyme proliferation and osteochondroprogenitor condensation in the zebrafish pharyngeal arches. *Developmental Biology*, *321*(1), 101–110.

Square, T., Jandzik, D., Cattell, M., Coe, A., Doherty, J., & Medeiros, D. M. (2015). A gene expression map of the larval Xenopus laevis head reveals developmental changes underlying the evolution of new skeletal elements. *Developmental Biology*, *397*(2), 293–304.

Svensson, M. E., & Haas, A. (2005). Evolutionary innovation in the vertebrate jaw: A derived morphology in anuran tadpoles and its possible developmental origin. *BioEssays*, *27*(5), 526–532.

Tissier-Seta, J. P., Mucchielli, M. L., Mark, M., Mattei, M. G., Goridis, C., & Brunet, J. F. (1995). Barx1, a new mouse homeodomain transcription factor expressed in cranio-facial ectomesenchyme and the stomach. *Mechanisms of Development*, *51*(1), 3–15.

Tribioli, C., Frasch, M., & Lufkin, T. (1997). Bapx1: an evolutionary conserved homologue of the Drosophila bagpipe homeobox gene is expressed in splanchnic mesoderm and the embryonic skeleton. *Mechanisms of Development*, *65*(1–2), 145–62.

Tucker, A. S. (2004). Bapx1 regulates patterning in the middle ear: altered regulatory role in the transition from the proximal jaw during vertebrate evolution. *Development*, *131*(6), 1235–1245. https://doi.org/10.1242/dev.01017

Wilson, J., & Tucker, A. S. (2004). Fgf and Bmp signals repress the expression of Bapx1 in the mandibular mesenchyme and control the position of the developing jaw joint. *Developmental Biology*, *266*(1), 138–150.

Yoshiura, K. I., & Murray, J. C. (1997). Sequence and chromosomal assignment of human BAPX1, a bagpipe-related gene, to 4p16.1: a candidate gene for skeletal dysplasia. *Genomics*, *45*(2), 425–8.

Ziermann, J. M., & Diogo, R. (2014). Cranial muscle development in frogs with different developmental modes: Direct development versus biphasic development. *Journal of Morphology*, *275*(4), 398–413.

Ziermann, J. M., & Olsson, L. (2007). A new staging table for stages relevant to cranial muscle development in the African Clawed Frog, Xenopus laevis (Anura: Pipidae). *Journal of Morphology*, *268*.

Tables and Figure

	concentration	mortality	phenotype	joint loss
uninjected	-	8%	4%	0%
control-MO	10µM	12%	3%	0%
MO1	10µM	10%	4%	0%
	20µM	11%	5%	1%
	30µM	20%	55%	47%
MO2	90µM	12%	9%	4%
	100µM	16%	39%	33%
MO1+2	10µM+30µM	12%	43%	33%
	20µM+60µM	18%	65%	59%

Table 1: Frequency of mortality, phenotype and joint loss occurrence in *Xenopus laevis* after treatment with different concentrations of bapx-MO. Phenotypes were determined six days after injection based on external features. Joint loss was scored after clearing and staining with alcian blue. n=90 for controls and each concentration of Co-MO and bapx-MO.

Figure 1: (**A**) Sequence alignment showing the position of morpholinos used in the present study (coding region highlighted). Alignment of the *Xenopus tropicalis* nkx3-2 derived sequence in comparison to Bapx-MO1 and the *Xenopus laevis* derived sequence of the L (**B**) and S (**C**) nkx3-2 duplicate.

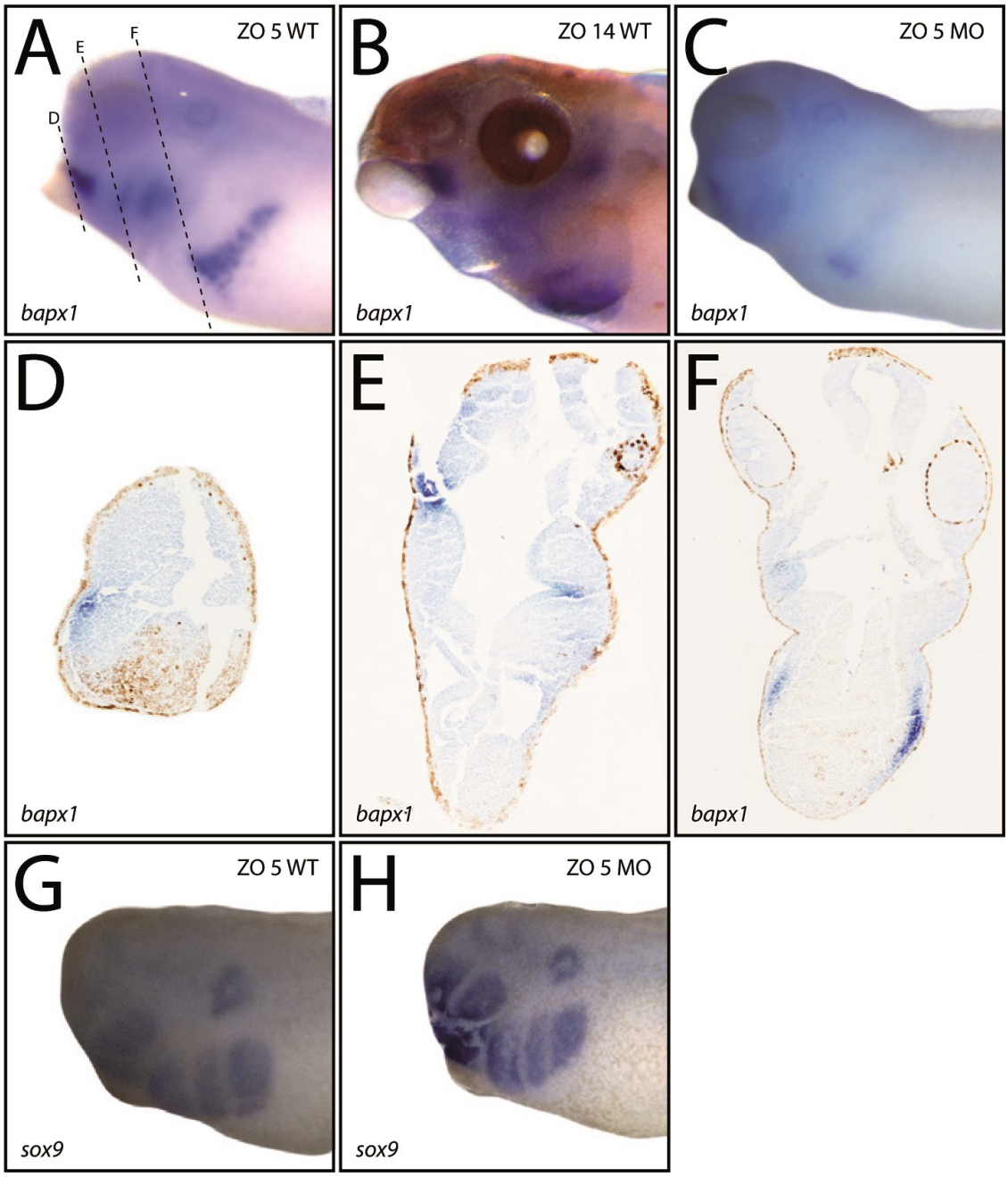

Figure 2: *Bapx1* and *sox9* expression in the developing head of *Xenopus laevis*. Lateral views of *bapx*1 in-situ hybridisations with anterior to the left (A-C) and histological cross sections (D-F) of larvae stained by in situ hybridisation and lateral views of *sox9* in-situ hybridisations as control. (**A**) *Bapx1* expression is visible in the precursors of PA 1, 3, 4, and 5 and in the endoderm of the foregut at ZO 5. Dashed lines indicate the plane of sectioning in D-F. (**B**) At ZO 14 *bapx1* expression surrounds the jaw joint and marks the foregut. (**C**) *Bapx1* expression after treatment with 30µM bapx-MO1 is clearly reduced. *Bapx1* transcripts are found in the ventral region of PA1 (**D**), in the endoderm of pharyngeal pouches (**E**) and the foregut (**F**). *Sox9* expression in unperturbed (**G**) and in *bapx1* knockdown (**H**) tadpoles at ZO 5. *Bapx1* knockdown has no effect on *sox9* expression.

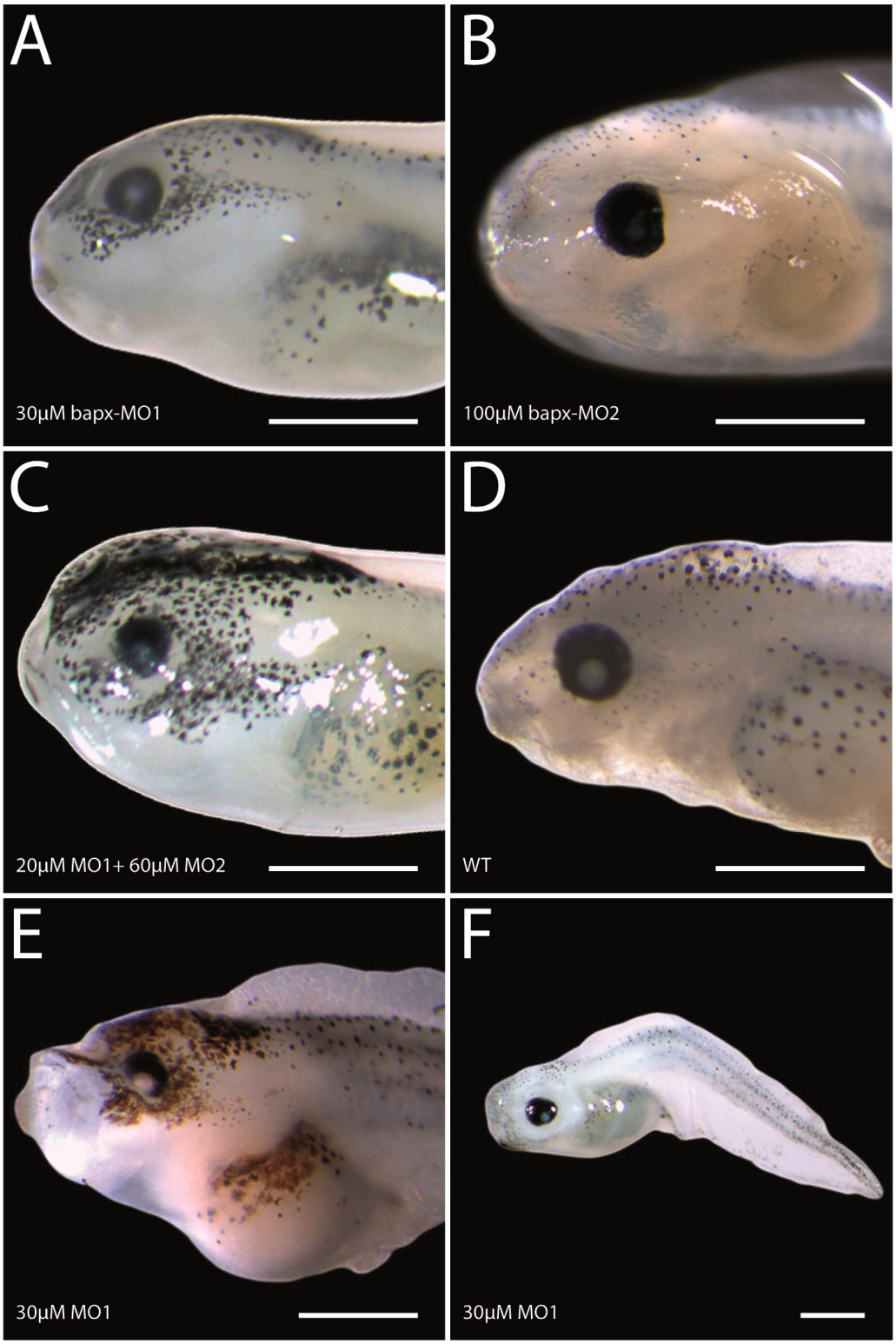

Figure 3: Effects of *bapx1* knockdown on the external head morphology of *Xenopus laevis* larvae. Frequent phenotypes caused by injection of (**A**) 30µM bapx-MO1, (**B**) 100µM bapx-MO2, (**C**) combined 20µM bapx-MO1 and 60µM bapx-MO2 and (**D**) unperturbed larva after 144h. Infrequently, phenotypes with (**E**) dorsally shifted mouth opening (n=3) and (**F**) bent axis (n=7) occurred after injection of 30µM bapx-MO1. Scale bar 500µm

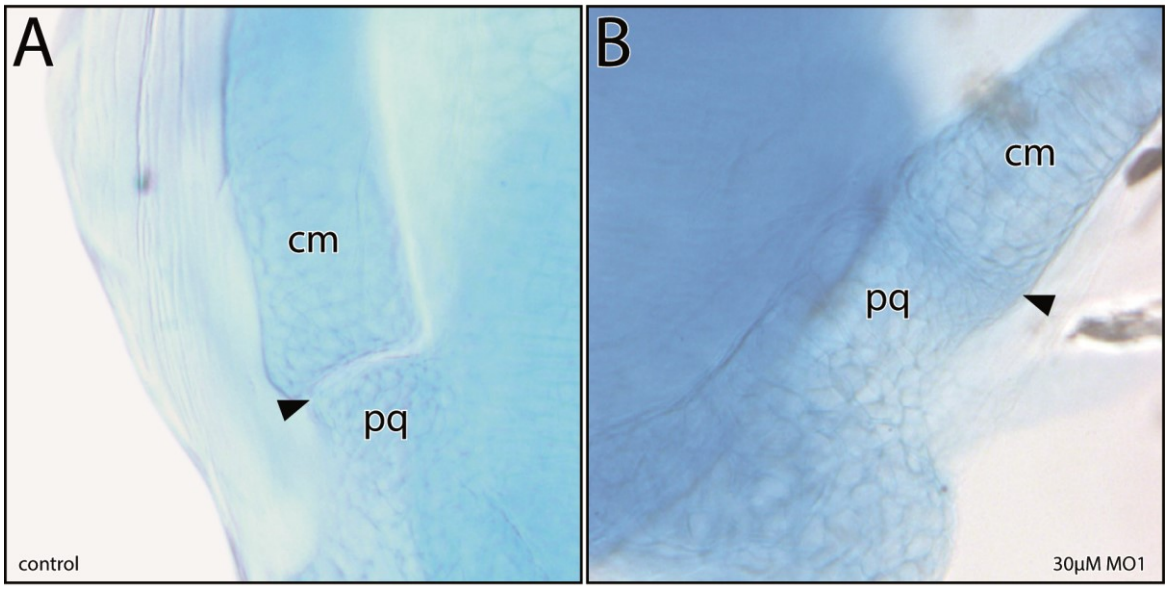

Figure 4: Cleared and stained *Xenopus laevis* tadpole (ZO 17) after unilateral injection of 30µM bapx-MO1. (**A**) Uninjected control side with clearly visible primary jaw joint (black arrowhead). (**B**) Bapx-MO1 treated side showing a broad fusion of Meckel´s cartilage and the palatoquadrate at the point, where the primary jaw joint is normally situated (black arrowhead). cm, Meckel´s cartilage; pq, palatoquadrate

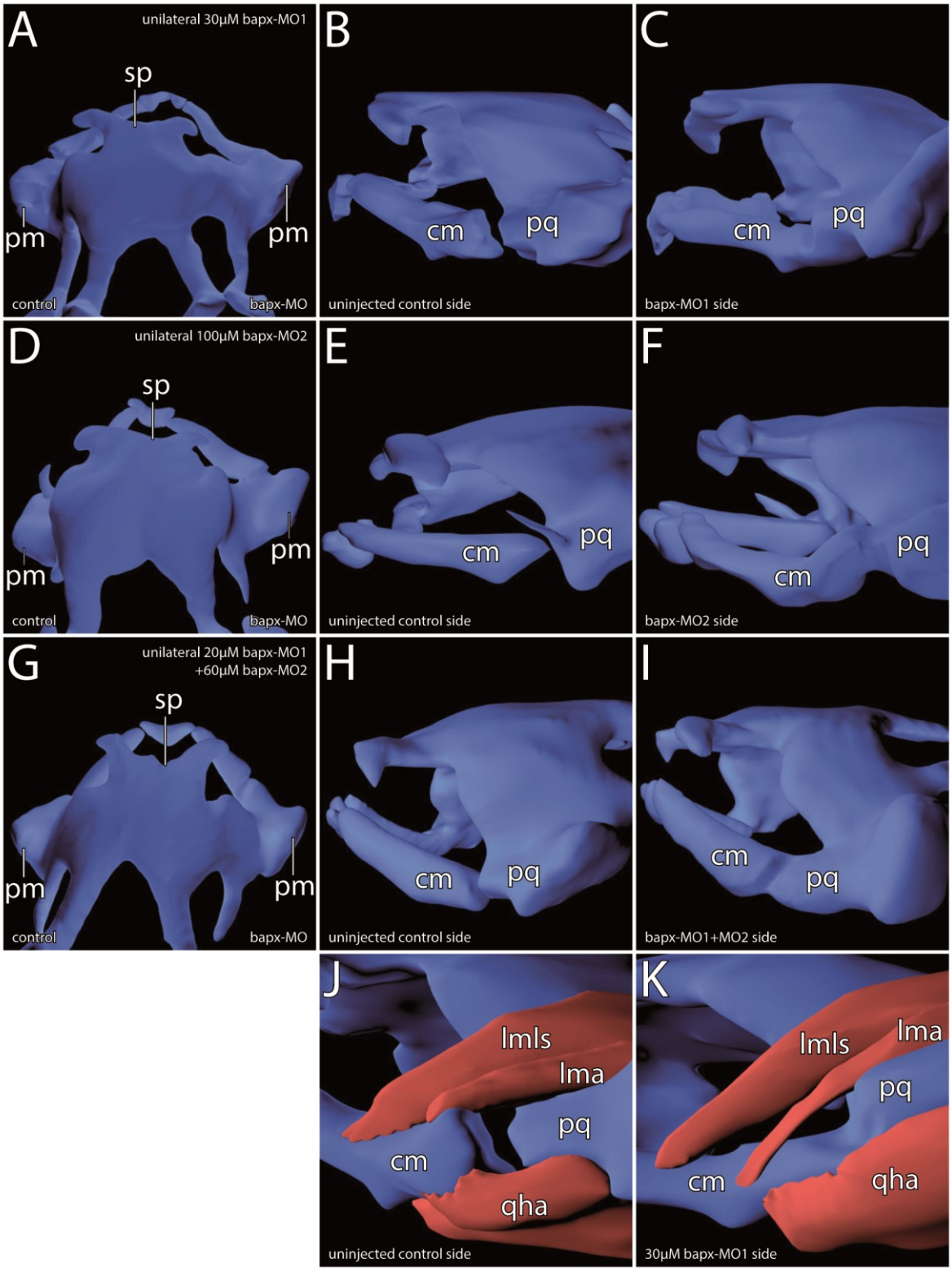
A
unilateral 30µM bapx-MO1
sp
pm
pm
control
bapx-MO
B
cm
pq
uninjected control side
C
cm
pq
bapx-MO1 side
D
unilateral 100µM bapx-MO2
sp
pm
pm
control
bapx-MO
E
cm
pq
uninjected control side
F
cm
pq
bapx-MO2 side
G
unilateral 20µM bapx-MO1
+60µM bapx-MO2
sp
pm
pm
control
bapx-MO
H
cm
pq
uninjected control side
I
cm
pq
bapx-MO1+MO2 side
J
lmls
lma
pq
cm
qha
uninjected control side
K
lmls
lma
pq
cm
qha
30µM bapx-MO1 side

Figure 5: 3D-reconstructions based on confocal laser scanning microscopy showing the effects of *bapx1* knockdown on the internal head morphology of *Xenopus laevis* larvae. Cartilaginous head skeleton after unilateral 30µM bapx-MO1 injection in dorsal view (**A**, control side on the left) and lateral view of the control (**B**) and the perturbed (**C**) side. (**D**) Dorsal view of the head skeleton after unilateral injection of 100µM bapx-MO2 (control side on the left). Lateral view of the control (**E**) and perturbed (**F**) side on the specimen shown in D. (**G**) Head skeleton of a specimen treated with 20µM bapx-MO1 and 60µM bapx-MO2 in dorsal view (control side on the left). Lateral view of the same specimen on the (**H**) control and (**I**) perturbed side. All morphants show loss of the primary jaw joint on the injected side, whereas the control side developed a proper joint. Effects of unilateral 30µM bapx-MO1 treatment on the musculature of the jaw joint are shown on the (**J**) control and (**K**) perturbed side in lateral view. All muscles insert properly on Meckel´s cartilage after *bapx1* knockdown. cm, Meckel´s cartilage; lma, m. levator mandibulae articularis; lmls, m. levator mandibulae superficialis; pm, processus muscularis palatoquadrate; pq, palatoquadrate; qha, m. quadrato-hyoangularis; sp, suprarostral plate

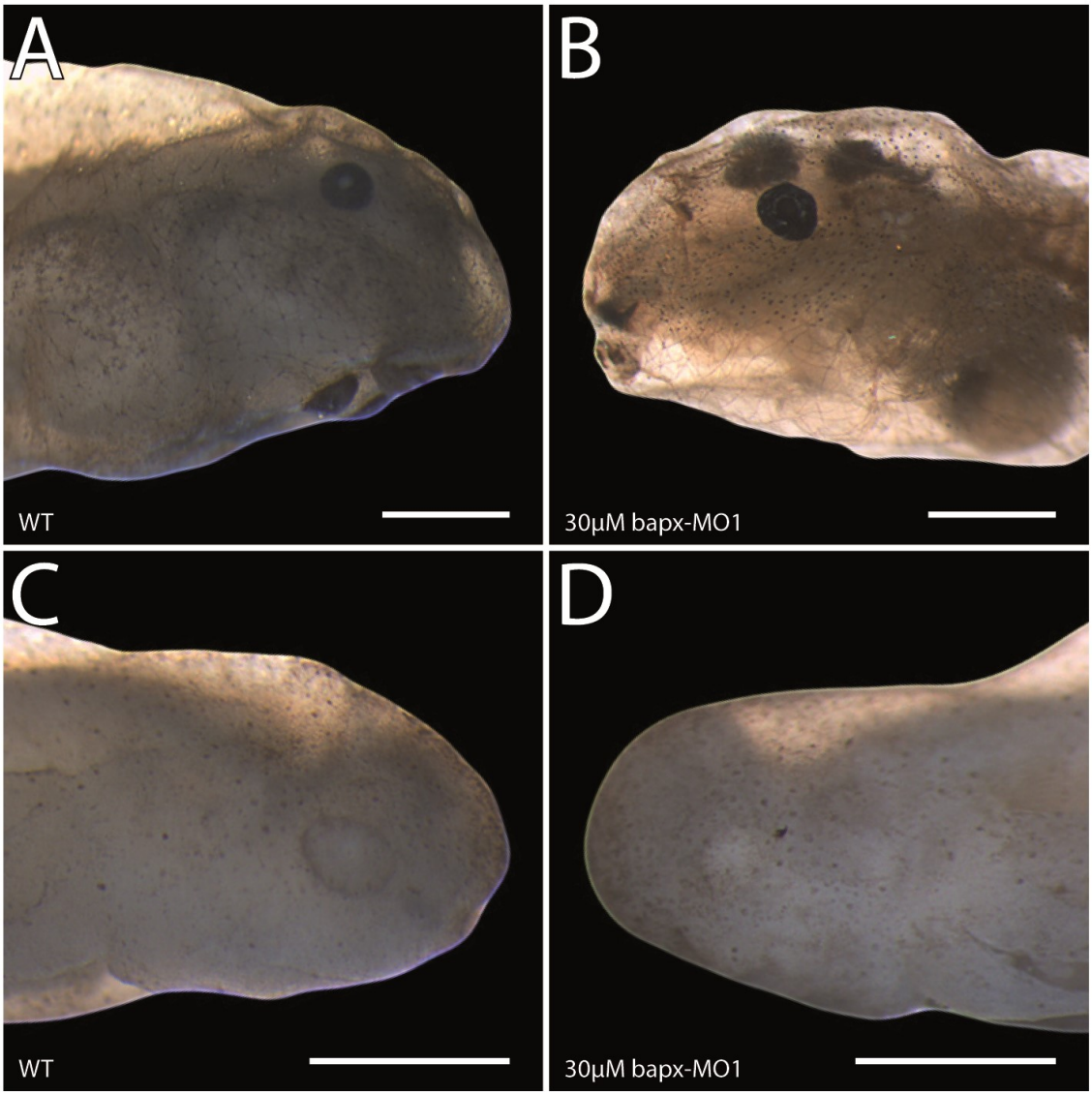

Figure 6: Effects of *bapx1* knockdown 196h after injection of 30µM bapx-MO1 on the external morphology of further amphibians. (**A**) Control and (**B**) perturbed larvae of *Bombina orientalis* in lateral view. The mouth opening is dislocated in perturbed larvae. (**C**) Control and (**D**) perturbed larvae of *Ambystoma mexicanum* in lateral view. No difference can be seen between the normally developed and the treated larva. Scale bar 500µm

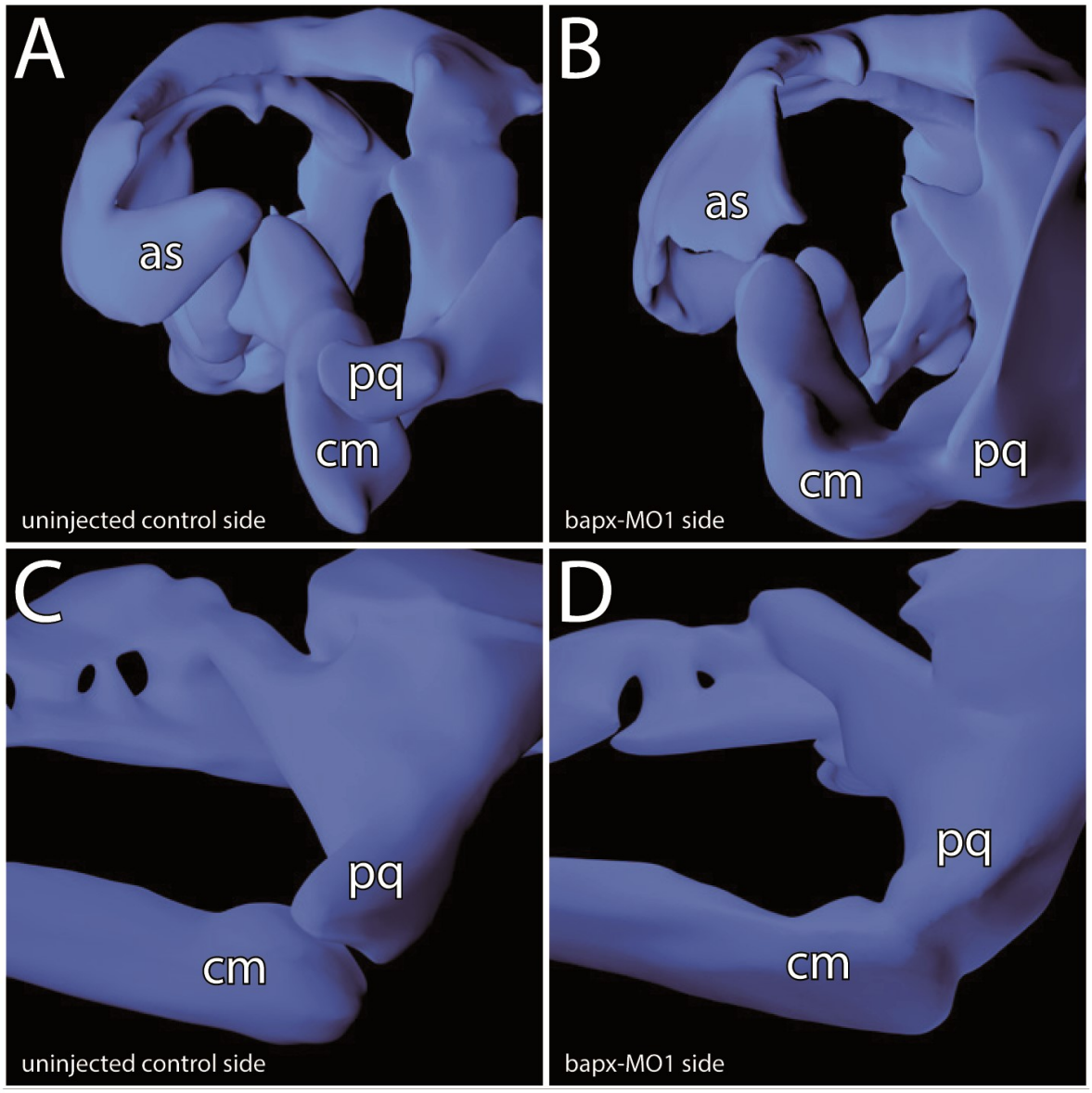

Figure 7: 3D-reconstructions based on confocal laser scanning microscopy showing the effects of *bapx1* knockdown after unilateral 30µM bapx-MO1 injection on the internal head morphology of *Bombina orientalis* and *Ambystoma mexicanum* larvae. (**A**) Control and (**B**) perturbed side of a *B. orientalis* tadpole in lateral view 196h after injection. (**C**) Control and (**D**) perturbed side of A. mexicanum tadpole in lateral view 240h after injection. Meckel´s cartilage and the palatoquadrate are fused, whereby the primary jaw joint is lost in both species. as, ala of the suprarostral; cm, Meckel´s cartilage; pq, palatoquadrate

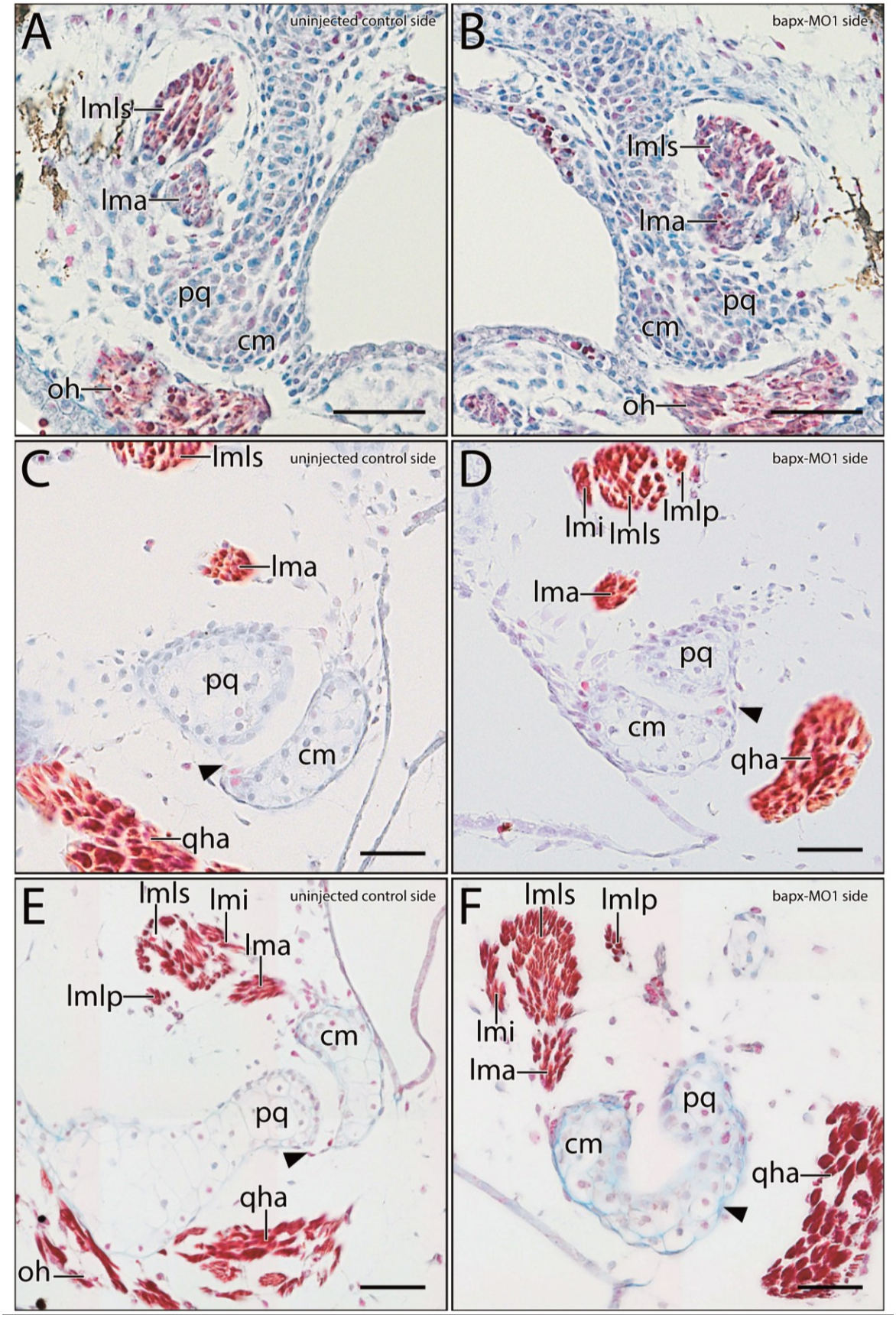
A
uninjected control side
lmls
lma
pq
cm
oh
B
bapx-MO1 side
lmls
lma
pq
cm
oh
C
lmls
uninjected control side
lma
pq
cm
qha
D
bapx-MO1 side
lmi
lmls
lmlp
lma
pq
cm
qha
E
lmls
lmi
uninjected control side
lma
lmlp
cm
pq
qha
oh
F
lmls
lmlp
bapx-MO1 side
lmi
lma
pq
cm
qha

Figure 8: Transverse histological sections of *Xenopus laevis* showing development of the jaw joint after unilateral treatment with 30µM bapx-MO1. Larval stages ZO 12 (**A**, **B**), ZO 14 (**C**, **D**) and ZO 17 (**E**, **F**) are depicted. Left column shows development on the uninjected and right column on the injected side. Black arrowhead in C and E marks the connection of Meckel´s cartilage and the palatoquadrate through a thin band of connective tissue. The same band (black arrowhead in D and F) chondrifies on the injected side, which causes the fusion of the jaw joint. Scale bar 50µm (A-B), 100µm (C-F). cm, Meckel´s cartilage; lma, m. levator mandibulae articularis; lmi, m. levator mandibulae internus; lmlp, m. levator mandibulae longus profundus; lmls, m. levator mandibulae superficialis; oh, m. orbitohyoideus; pq, palatoquadrate; qha, m. quadrato-hyoangularis

Chapter 3

Bapx1 upregulation is associated with ectopic mandibular cartilage development in amphibians

The paper shows that treatment with Ly-294,002 leads to the formation of mandibular arch-derived ectopic cartilages in two different amphibian species. The ectopic cartilage develops lateral to the palatoquadrate and Meckel´s cartilage and comprises of cells which were separated from the two cartilages during development. This further enhances the postulated cartilage preventing function of *bapx1* and suggests that an increase in *bapx1* expression within anurans may have cause the appearance of additional mandibular cartilages such as adrostralia and sub-meckelian cartilages.

Paul Lukas & Lennart Olsson

Submitted to Zoological Letters

PL and LO developed the concept and design of the study. PL was responsible for the experimental procedures including Ly-294,002 experiments, whole mount in-situ hybridisation, immunostainings, qPCR, 3D-reconstructions and histology. Analysis and interpretation of the data mentioned was mainly done by PL, who was also responsible for the drafting of the manuscript and its final form. LO critically revised the manuscript.

Abstract

Background

In emergence of novel structures during evolution is crucial for creating the variation among organisms, but the underlying processes which lead to the emergence of evolutionary novelties are poorly understood. The gnathostome jaw joint is such a novelty and the incorporation of *bapx1* expression into the intermediate first pharyngeal arch might have played a major role in the evolution of this joint. Knockdown experiments revealed that loss of *bapx1* function lead to the loss of the jaw joint because Meckel´s cartilage and the palatoquadrate fuse during development. We used *Xenopus laevis* and *Ambystoma mexicanum* to further investigate the function of *bapx1* in amphibians. *Bapx1* expression levels were upregulated through the use of Ly-294,002 and we investigated the consequences of the enhanced *bapx1* expression in amphibians to test the hypothesized joint inducing function of *bapx1*.

Results

We show that Ly-294,002 is able to upregulate bapx1 expression in vivo. Additionally, ectopic mandibular arch derived cartilages develop after Ly-294,002 treatment. These ectopic cartilages are dorsoventrally orientated rods situated lateral to the palatoquadrate. The development of these additional cartilages did not change the muscular arrangement of mandibular arch derived muscles.

Conclusions

Development of additional mandibular cartilages is not unusual in larval anurans. Therefore, changes in the *bapx1* expression during evolution may have been the reason for the development of several additional cartilages in the larval anuran jaw. Furthermore, our observations imply a joint promoting function of *bapx1*, which further substantiates its hypothetical role in the evolution of the gnathostome jaw joint.

Keywords: *Xenopus laevis*, *Ambystoma mexicanum*, evolutionary novelties, Ly-294,002, *nkx 3.2*, *xbap*

Background

The acquisition and incorporation of novel skeletal structures into an existing skeletal environment is a process that can cause morphological diversification. How such evolutionary novelties arose during evolution and under which circumstances they arose is an important question in evo-devo research. An important example is the evolution of the gnathostome jaw and its skeletal diversification in different phyla. The jaw itself consists basically of a dorsal and a ventral element, which are connected by a distinct joint [1]. Its evolution enables predation on large and motile prey and can therefore be seen as one of the central innovations in gnathostomes.

The larval anuran jaw is unique compared to other vertebrates. At the base of anurans two additional jaw structures, the rostralia, evolved. The suprarostral cartilage forms the anterior part of the upper jaw, whereas the infrarostral cartilage is part of the lower jaw and movable against Meckel´s cartilage via the intramandibular joint [2]. These two additional structures made possible the evolution of numerous different feeding modes in anuran tadpoles, which enabled the decoupling of larval and adult stages. The diverse feeding modes, which are based on the derived morphology, could be the reason why anurans are the dominant recent amphibian group [3]. During further evolution several anuran taxa evolved one or more additional cartilages within the larval jaw. Such adrostral cartilages are described in *Heleophryne natalensis*, *Pelobates fuscus*, *Alytes obstetricans* and *Pelodytes punctatus*, to just name a few species [4, 5]. Three different mechanisms for the evolution of such additional cartilaginous structures have been proposed by Svensson and Haas (2005): (1) through duplication of existing cartilages; (2) through partitioning of existing cartilages through the development of new joints; (3) through *de novo* evolution of cartilages not homologous to existing elements. In all three cases, one or more genetic regulators must be responsible for the evolution of the novel cartilage.

Bapx1 (also known as *nkx3.2*and *xbap*) homologues are present in different, distantly related phyla. It was first identified in *Drosophila* where it spatially subdivides the mesoderm and thus is essential for midgut musculature formation [6]. In amphioxus and lamprey *bapx1* is expressed in the pharyngeal endoderm [1, 7]. During pre-gnathostome evolution *bapx1* is suggested to have been incorporated into an existing pharyngeal arch patterning system [1]. In such a system, a gradual expression of homeobox genes defines an anterior-posterior axis. Overlapping expression of these genes defines different regions along this axis [8–10]. For instance, the first pharyngeal arch is defined by the absence of *hox* expression, whereas the second pharyngeal arch is defined by *hoxa2* expression [11, 12]. Gnathostome pharyngeal arches are patterned dorsoventrally by a nested expression of *dlx* genes [13, 14]. These two patterning programs together form a developmental grid that enables locally restricted gene expression dependent on the specific spatial configuration. The incorporation of *bapx1* into this pre-gnathostome head patterning program has been suggested to have played a major role in the evolution of the gnathostome jaw [1, 15]. In lamprey, which lacks a dorsoventral patterning mediated by *dlx* genes, *bapx1* is not expressed in the first pharyngeal arch, whereas in *Scyliorhinus* and zebrafish *bapx1* expression dependent on *dlx* function within the first pharyngeal arch was reported [16–18]. In zebrafish *bapx1* expression can be found

in an intermediate domain of the first pharyngeal arch and is ventrally restricted by a *barx1* expressing domain [17, 19]. *Barx1* expression is ventrally restricted by *hand2* expression which inhibits *bapx1* expression during development [19]. In zebrafish *bapx1* is expressed in the intermediate domain of the first pharyngeal arch, exactly where the primary jaw joint will form. Homologous genes with similar first pharyngeal arch expression can be found in *Xenopus* [20], *Pleurodeles* [21], chicken [22], mouse [23] and human [24]. *Bapx1* knockdown in zebrafish led to fusion of Meckel´s cartilage and the palatoquadrate, which caused loss of the primary jaw joint [17]. The same result is seen after downregulation of *bapx1* in amphibians (Lukas and Olsson, submitted) indicating a role for *bapx1* in both development and evolution of the primary jaw joint. Loss of *barx1* function in zebrafish led to dorsal expansion of *hand2* expression and the formation of an ectopic joint within Meckel´s cartilage where *hand2* and *bapx1* expression domains met [19]. This ectopic joint development after *barx1* inactivation and the following expansion of the *bapx1* expression domain further indicates that *bapx1* expression can induce joint development in the first pharyngeal jaw.

The role of the phosphatidylinositol 3-kinase (PI3K) in cell metabolism, regulation of gene expression, cell survival and cell growth is well-documented [25, 26]. It has been shown that PI3Ksignalingcan down-regulate *bapx1* specifically by using the catalytic subunit p85β in mice [27]. *Pik3ca*, the PI3K subunit responsible for the *bapx1* suppression pathway, is expressed in *X. laevis* in the pharyngeal region from NF 26 to NF 32 [28]. Ly-294,002 (2-(4-Morpholinyl)-8-phenyl-4H-1-benzopyran-4-one hydrochloride) is a specific inhibitor of PI3K [29]. PI3K suppression mediated by Ly-294,002 causes raised *bapx1* expression levels [27]. To test the effects of overexpression of *bapx1* in the development of the first pharyngeal arch in amphibians, Ly-294,002 was used in this study to inhibit *pik3ca* function and enhance *bapx1* expression in vivo.

Methods

Amphibian husbandry

Males and females of *Xenopus laevis* (Daudin) and *Ambystoma mexicanum* (Shaw) were kept in separate groups in our breeding colony in Jena. Adults and larvae of *Xenopus laevis* were kept at 22°C. To induce mating and obtain fertilized eggs *Xenopus laevis* adults were put pairwise into darkened basins with lowered water level. They were kept there over night at 16°C. After successful egg deposition the eggs were collected and then dejellied using a solution of 2% cysteine hydrochloride. The eggs were washed several times and cultured in 0,1x modified Barth´s saline (MBS) with 50µg/ml gentamycin at 22°C. *Ambystoma mexicanum* adults were kept at 18°C. Single pairs were transferred into basins with fresh water and ice was added to lower the temperature and induce mating overnight. After successful egg deposition and fertilisation, the eggs were collected and manually dejellied using dissecting forceps. The eggs were cultured in 20% Steinberg´s solution with 50µg/ml gentamycin at 22°C. Developmental stages were determined according to Nieuwkoop and Faber (1994), Ziermann and Olsson (2007) for *X. laevis* and Schreckenberg and Jacobson (1975) for *A. mexicanum*. Nieuwkoop and Faber (NF) staging was used for the identification

of early developmental stages. For the description and comparison of the inner morphology of treated embryos Ziermann and Olsson staging (ZO) was used because this staging table provides more comparable stages during chondrification and initial skeletal development than Nieuwkoop and Faber.

In vivo experiments

Embryos of *X. laevis* were incubated with different concentrations of LY-294,002 hydrochloride (Merck) at different developmental stages. LY-294,002 was initially dissolved in dimethyl sulfoxide (DMSO). A stock solution containing 10µM DMSO and 1mM LY-294,002 was prepared and diluted with MBS to concentrations of 10µM, 20µM, 30µM, 40µM and 50µM LY-294,002. *X. laevis* embryos (N=90 for each stage and concentration) were then incubated at NF 10 (onset of gastrulation), at NF 13 (onset of neurulation), at NF 22 (early tailbud stage), at NF 29 (late tailbud stage) and NF 39 (onset of cartilage development) in the different LY-294,002 dilutions. *X. laevis* embryos were also kept in 1x MBS and 0,1µM DMSO in 0,1xMBS as a control. To specifically test the influence of LY-294,002 on mandibular arch development, 10nl of 20µM LY-294,002 was injected in the area of the mandibular neural crest segment [33] antero-ventral to the eye at NF 29. Injection was performed in 4% Ficoll/ 0,1x MBS and after 4 hours the embryos were transferred into 0,1x MBS. *A. mexicanum* embryos were incubated with 20µM Lys-294,002 at Schreckenberg and Jacobson stage (SJ) 36. *X. laevis* embryos were cultured until they reached NF 45 and *A. mexicanum* embryos were cultured for five days. The 0,1µM DMSO and the 0,1xMBS solution as well as the different Lys-294,002 solutions were changed daily. Living, dead and malformed larvae were counted and images were taken using a Zeiss Stemi SV11 and an attached camera (ColorView) operated by AnalySIS software. Anaesthesia was performed using 1% tricaine methanesulfonate (MS-222) according to the animal welfare protocols at the Friedrich-Schiller-Universität Jena. Depending on further investigations larvae were fixed in 4% phosphate-buffered formalin (PFA), Dent´s fixative or RNA stabilisation reagent.

Tissue staining

PFA-fixed larvae were dehydrated and embedded in paraffin. Serial sectioning was performed using a rotary microtome (Microm, HM 355 S). Sections of 7µm thickness were obtained and subsequently stained with Heidenhain´s Azan technique [34] or nuclear fast red staining [35]. Images were taken with an XC10 Olympus camera mounted on an Olympus BX51 microscope operated with dotSlide software. *X. laevis* and *A. mexicanum* larvae fixed with Dent´s fixative were used for whole mount antibody staining. Cartilage cells were specifically stained with a monoclonal antibody against collagen II (II6B3-collagen II). A polyclonal antibody against newt skeletal muscle (12/101) was used to specifically stain muscle cells. For the colour reaction secondary antibodies conjugated with Alexa 488 and Alexa 568 (Molecular Probes) were used. The specimens were scanned with a confocal laser scanning microscope (Zeiss LSM 510) operated with Zen software. The image stacks obtained were further processed with Amira 6.0.1 (surface render) and Autodesk Maya® 2017 (rendering).

In situ hybridisation and quantitative PCR

Whole-mount in situ hybridisations were carried out according to the protocol in Harland (1991) with a few modifications described by Square et al. (2015). NF 30-40 larvae were treated for 15 min and NF 40-45 larvae were treated for 20 min with Proteinase K. BM-Purple (Roche) was used for signal development. Probe of *bapx1* was kindly provided by Jennifer Schmidt. RNA from whole embryos kept in 0,1x MBS, in 0,1µM DMSO and different Ly-294,002 solutions was isolated using QIAzol Lysis Reagent (Qiagen) and purified using RNeasy Mini Kit (Qiagen) according to manufacturer's instructions. RevertAid Transcriptase (Thermo Scientific) was used to synthesize complementary DNA from 2µg RNA extracted from embryo. Quantitative PCR was performed using a Stratagene Mx3005P (Agilent Technologies) and one- step qPCR SYBR green kit (Roche). Sequences of primers used for amplification of *bapx1* were taken from Square et al. (2015). Target gene expression was normalized [37] to the expression level of histone H4 (5´-GACGCTGTCAACCGAG-3´and 5´- CGCCGAAGCCAGAGTG-3´).

Results

The effect of Ly-294,002 treatment on tadpole survival

Initially embryos of *X. laevis* were treated with different concentrations of Ly-294,002 at different developmental stages. No embryos incubated at NF 10 survived the treatment with the different amounts of Lys-294,002 (Fig. 1). Embryos treated with 10µM and 20µM at the onset of neurulation (NF 13) survived the treatment at moderate rates (27% and 20% respectively) whereas only a minority of embryos treated with 30µM (2%) and 40µM (4%) survived. No embryo survived the treatment with 50µM Ly-294,002. Survival rates slightly increased when embryos were reared in different Ly-294,002 solutions at NF 22. As before, no embryo survived treatment with 50µM Ly-294,002. Larvae incubated at the late tailbud stage (NF 29) showed a much higher survival rate at lower Ly-294,002 concentrations. 70% of the larvae survived the treatment with 10µM and 76% survived the treatment with 20µM Ly-294,002, whereas no larvae survived the treatment with 50µM. Larvae reared in the different concentrations of Ly-294,002 at the onset of chondrification (NF 39) show almost normal survival rates. No significant difference in the survival rate at the different developmental stages was observed between embryos reared in 0,1µM DMSO and embryos reared normally in 0,1x MBS. Additionally, no abnormalities developed after DMSO treatment (Fig. 1). These circumstances indicate that changes in survival rate and morphology are not the result of the necessary presence DMSO in Ly-294,002 in vivo experiments and indicate a specific effect of Ly-294,002.

Ly-294,002 treatment induces development of an ectopic mandibular cartilage

The external morphology of all surviving *X. laevis* larvae from these incubation experiments was checked for potential morphological changes. We did not observe any external morphological or behavioural abnormalities in either control larvae, larvae raised in 0,1µM DMSO or in Ly-294,002 treated larvae (Fig. 2 A-C). We also checked for internal

musculoskeletal changes. No such changes were observed in larvae treated with the different concentrations of Ly-294,002 at NF 10, NF 13, NF 22 or NF 39. Interestingly, larvae treated at NF 29 that survived this procedure developed changes in the mandibular skeleton. The highest rate of larvae with disturbed mandibular arch morphology was seen after treatment with 20µM Ly-294,002 at NF 29 (Table 1). 57% of the larvae which survived the treatment had developed an additional mandibular cartilage, whereas in larvae treated with other concentrations of Ly-294,002, lower rates of this mandibular arch phenotype were observed (Table 1). For further analyses, we used 20µM Ly-294,002 and treated larvae from NF 29 onwards. At ZO 10 (NF 40-41) the palatoquadrate, Meckel´s cartilage and the ceratohyal were present in unperturbed larvae (Fig. 3A). In treated larvae an ectopic cartilage with a rounded shape was visible lateral to the palatoquadrate and Meckel´s cartilage. This ectopic cartilage was bordered postero-dorsally by the palatoquadrate and antero-dorsally by Meckel´s cartilage. The ectopic cartilage was separated from the two cartilages by a cavity-like gap (Fig. 3B). During further development the rounded shape and the location of the ectopic cartilage remained the same (Fig. 3D). At ZO 17 (NF 44) Meckel´s cartilage is normally sigmoidally elongated (Fig. 3C) but in treated larvae Meckel´s cartilage was shortened and thicker than in controls (Fig. 3D). The suprarostral plate bent more dorsally than normal and the muscular process had partly lost its dorsal projection in treated larvae. The area where the ectopic cartilage arose during development was nearly the same in all treated larvae. The changed morphology seemed to have no large effect on the behaviour because treated larvae showed normal feeding and respiration. Next, we investigated whether mandibular muscles display any abnormalities and if muscles insert onto or originate from the ectopic cartilage. We observed only two muscles which are affected by the Ly-294,002 treatment. The M. levator mandibulae articularis normally originates from the posterior-ventral surface of the muscular process of the palatoquadrate and inserts onto the dorsal surface of the posterior end of Meckel´s cartilage (Fig. 4A). In perturbed larvae the muscle originated more anteriorly from the muscular process of the palatoquadrate and inserted more laterally and anteriorly onto Meckel´s cartilage than in controls (Fig. 4B). The M. quadratohyoangularis normally originates from the ventral surface of the palatoquadrate and from the dorsal surface of the ceratohyal and inserts onto the ventro-lateral edge of Meckel´s cartilage (Fig. 4A). In perturbed larvae origination and insertion were similar, but the insertion onto Meckel´s cartilage was smaller than in controls. The dorsal portion of this muscle surrounded the ectopic cartilage, but not even a single fibre inserted onto or originated from this cartilage (Fig. 4B).

Ly-294,002 treatment upregulates *bapx1* expression levels

To test if the development of mandibular ectopic cartilages is correlated to changes in *bapx1* expression, we used quantitative PCR to investigate the relative expression of *bapx1*. We checked the expression levels for larvae reared in 0,1µM DMSO, to investigate the effect of DMSO on *bapx1* expression, and for larvae reared in 20µM Ly-294,002 from 29NF onwards. Rearing larvae in 0,1µM DMSO had no effect on *bapx1* expression levels (Fig. 5 white bar). The unaltered *bapx1* expression in tadpoles raised in 0,1µM DMSO further confirmed that DMSO did not interfere with our experiments. The inhibition of PI3K

mediated by Ly-294,002 treatment raised the expression levels of *bapx1* more than fivefold (Fig. 5 dark grey bar). To further check for differences in the spatial expression we used whole mount in situ hybridisation of *bapx1* transcripts. Normally, *bapx1* was expressed in the ventral region of the mandibular arch at NF 37. The expression domain surrounded the cement gland dorsolaterally and marked the precursors of the palatoquadrate and the proximal part of Meckel´s cartilage (Fig. 2D). Posteriorly, *bapx1* expression was visible in the endoderm of the pharyngeal pouches of pharyngeal arches 3-5. More posteriorly *bapx1* was expressed in the foregut (Fig. 2D). In larvae treated with 20µM Ly-294,002 from NF 29 onwards *bapx1* expression was visible in the same regions as described for the control larva (Fig. 2E). No duplicated expression domain was visible. The expression domain in the mandibular arch was broader than in the control larvae and extended more posteriorly. Treatment with Ly-294,002 led to increased *bapx1* expression levels and to an extension of the *bapx1* expression domain in the mandibular arch.

Ectopic cartilage development after mandibular arch *bapx1* upregulation

To investigate if the observed cartilaginous changes in *X. laevis* are correlated to raised *bapx1* expression in the mandibular arch, we injected 20µM Ly-294,002 into the area of the mandibular crest identified by Sadaghiani and Thiébau (1987) at NF 29. In the Ly-294,002-treated specimen an ectopic cartilage occurred more posterior than in larvae reared in Ly-294,002 solution. Posterior to the primary jaw joint articulation, a dorsoventral elongated cartilaginous rod was visible at ZO 17. It seemed to comprise cells from the muscular process of the palatoquadrate, because the process was reduced in size and lacks the dorsal projection seen in controls (comp. Figs. 6A and B). The ectopic cartilage was embedded in connective tissue and no muscle inserted onto or originated from its surface. Furthermore, the ectopic cartilage was distantly located in relation to Meckel´s cartilage and the palatoquadrate and did not articulate with any of these cartilages (Fig. 6 D). During further development, the muscular process of the palatoquadrate slightly extended its surface dorsally and formed a miniaturized process compared to unperturbed larvae at ZO 20 (NF 45-46; comp. Figs. 6C and D). The ectopic cartilages remained as dorsoventral elongated rod-like structures lateral to the muscular process of the palatoquadrate.

Ly-294,002 treatment in Axolotl

We have observed that Ly-294,002 treatment upregulates *bapx1* expression in *X. laevis* and that the treatment simultaneously led to the development of mandibular ectopic cartilage. Next, we wanted to repeat the experiments with another amphibian to test if the obtained results are a consequence of the derived state of *X. laevis* or if they display a common feature among amphibians. Therefore, we investigated the effects of Ly-294,002 treatment on the development of *A. mexicanum*. We treated *A. mexicanum* larvae at SJ 36, which approximately corresponds to *X. laevis* NF 29, with 20µM Ly-294,002 and reared them for five days. As in *X. laevis*, no significant changes in external morphology were observed (comp. Figs. 7A and B). However, the cartilaginous structures of the mandibular arch were malformed in similar ways compared to *X. laevis*. Postero-dorsal to Meckel´s cartilage and latero-ventral to the palatoquadrate an ectopic cartilage occurred in treated larvae (Fig. 7D).

This cartilage seems to be separated from Meckel´s cartilage and the palatoquadrate and was rounded in shape. Ventrally, the palatoquadrate was broader and narrower than in control larvae (comp. Figs. 7C and D). Laterally it had lost contact to Meckel´s cartilage and only articulated medially with it. Meckel´s cartilage also forfeited lateral contact to the palatoquadrate and only articulated medially. The lateral side of the posterior end seemed to articulate with the ectopic cartilage. The insertion and origination of the different muscles required for proper jaw movement were not affected by the Ly-294,002 mediated *bapx1* upregulation (comp. Figs. 7E and F). No such muscle inserted on the ectopic cartilage (Fig. 7F).

Discussion

High doses of the PI3K-inhibitor Ly-294,002 and incubation at early stages (beginning of gastrulation, beginning and end of neurulation) lead to dramatically decreased survival rates in treated specimens (Fig. 1). These decreased survival rates might be a consequence of the major role of PI3K in various developmental processes such as cell growth, cell differentiation and cell survival [25, 26]. High doses of Ly-294,002 at early developmental stages may restrict the function of PI3K in cell growth and survival which leads to premature death. When incubated at relatively low concentrations of Ly-294,002 the PI3K regulated key processes probably proceed normally, whereas the inhibition of *bapx1* regulation remains disturbed. Between NF 29 and NF 39 the sensory organs develop, first muscle anlagen develop and differentiate into muscle fibres, the nervous system develops and excretory as well as digestive systems forms [30]. Ly-294,002 treatment during this period and earlier has a very large influence on mandibular arch development. We have shown that treatment with 20µM Ly-294,002 from NF 29 onwards significantly elevates the expression of *bapx1* in *X. laevis* larvae using quantitative PCR. This upregulation additionally leads to a posterior expansion of the *bapx1* expression in the mandibular arch primordia as visualized through in-situ hybridisation. Furthermore, we have shown that DMSO, which was used to dissolve Ly-294,002, has no effect on tadpole survival and does not influence *bapx1* expression.

Raised *bapx1* expression is correlated to subdivision of existing cartilage

The treatment with Ly-294,002 in *X. laevis* and *A. mexicanum* has an effect on the development of mandibular arch derived cartilaginous elements. Neither in incubation nor in injection experiments were morphological changes of the non-mandibular arch derived cartilaginous skeletal elements observed. In both species tested, an ectopic cartilage develops after Ly-294,002 treatment. This cartilage appears lateral to the palatoquadrate and postero-lateral to Meckel´s cartilage (Fig. 6B). In *X. laevis* it is clearly visible that the lateral projection of the palatoquadrate, the muscular process, is reduced after Ly-294,002 treatment (Fig. 6D). The location of the ectopic cartilage suggests that the chondrocytes which form the ectopic cartilage became separated from the palatoquadrate during early development. These separated chondrocytes together might have formed a new lateral condensation which developed into the ectopic cartilage. Normally the m. orbitohyoideus and the m. quadratohyangularis originate from the lateral edge of the muscular process, but their origin

is not the ectopic cartilage which is assumed to be made of chondrocytes from the muscular process. Instead, they originate from the small remains of the muscular process. The chondrocytes which form the ectopic cartilage might have lost the ability to attract muscle progenitor cells. Additionally, no muscle inserts onto this ectopic cartilage, which indicates that no identity shift has taken place that would cause a muscle to shift its insertion. In *A. mexicanum* chondrocytes which normally form the lateral part of the palatoquadrate and the postero-dorsal part of Meckel´s cartilage become separated during development and seem to form the ectopic cartilage after *bapx1* upregulation. An indentation is visible where chondrocytes are missing at both Meckel´s cartilage and the palatoquadrate. Just like in *X. laevis* no muscle originates from or inserts onto the ectopic cartilage. In both species the ectopic cartilage seems to consist of chondrocytes which originate from existing cartilaginous structures. The mandibular arch derived cartilaginous structures which are situated next to the ectopic cartilage are reduced in size where they adjoin to the ectopic cartilage. We suggest, that the ectopic cartilage can not be characterized as a *de novo* developed cartilage, because Meckel´s cartilage and the palatoquadrate are reduced in size and developed altered shape after Ly-294,002 treatment, which indicates that the ectopic cartilage comprises of chondrocytes separated from these cartilages. The development of the ectopic cartilage as a consequence of the Ly-294,002 treatment is correlated to the raised *bapx1* expression levels which are also caused by the Ly-294,002 treatment. *Bapx1* expression is thought to be joint promoting in the mandibular arch [19]. Normally, *bapx1* function keeps the region between Meckel´s cartilage and palatoquadrate chondrocyte-free and enables the formation of the jaw joint. In perturbed specimens with elevated and expanded expression of *bapx1*, cartilage development was prevented within the muscular process of the palatoquadrate. The prevention of cartilage development led to the establishment of additional chondrocyte-free regions. Such a region separates numerous chondrocytes from their primordial cartilage. These chondrocytes can then condense and develop into a new cartilage.

Thus, our results show that Ly-294,002 treatment led to simultaneous upregulation of *bapx1* and development of an ectopic cartilage. *Bapx1* might be able to prevent cartilage formation in a restricted area and this prevention might subdivide existing cartilages. We suggest that *bapx1* promotes the formation of cartilage free regions within existing cartilages, which could lead to the formation of cartilage-free region within an existing cartilage and/or the formation of an ectopic cartilage. This function could be the foundation for the emergence of novel cartilages during anuran evolution and it suggests that new cartilages can arise during development and therefore during evolution by subdivision of existing cartilages.

The evolution of adrostral cartilages might be caused by changed *bapx1* expression

It has been suggested that *bapx1* was involved in the evolution of the gnathostome jaw joint. *Bapx1* was co-opted into the first arch in gnathostomes and replaced *barx1* in the ventral-intermediary region of the mandibular arch [1]. *Barx1* has been shown to repress joint formation and promote cartilage formation, whereas *bapx1* promotes joint formation and represses cartilage formation [19]. Thereby, *barx1* function in the agnathan mandibular arch ensures that no joint develops within this arch. The replacement of *barx1* by *bapx1* and thus

the expression of *bapx1* in the ventral intermediary region of the mandibular arch might have caused the development of a joint within this arch in gnathostomes. This potential of *bapx1* to prevent cartilage formation and subdivide existing cartilages might be the explanation for the evolution of additional cartilages in larval anurans. The larval anuran jaw consists of Meckel´s cartilage and the infrarostral in the lower jaw. The upper jaw is formed by the paired cornua trabeculae and a plate-like suprarostral. Both rostralia are unique in anurans but no *bapx1* expression can be seen during development in the region of the rostralia or their respective precursors. Additionally, *bapx1* knockdown has no effect on the formation of the rostralia in *X. laevis* (unpublished).

Several anurans such as *Alytes obstetricans* [4], *Heliophryne purcelli* [38] and *Pelobates fuscus* [39] have been described in which one or more paired additional cartilages develop during the tadpole stage. Their shape and location within the jaw is different in the different species. They can appear as dorsoventral proceeding rods lateral to the suprarostral cartilages, as in *Pelobates fuscus* (Fig. 8B), or as cuneiform cartilages ventral to Meckel´s cartilage and lateral to the suprarostral cartilage, as in *Heliophryne orientalis* (Fig. 8C). In both cases they are located laterally within the lower jaw. The ectopic cartilages in Ly-294,002 treated *X. laevis* specimen are also located laterally, but more posteriorly (Fig. 8D). Our observations on *Heliophryne orientalis* tadpoles have shown that both additional cartilages, the sub-meckelian cartilage and the adrostral cartilage, lack muscle insertion or origination. The muscle-free sub-meckelian and adrostral cartilage are similar to the muscle-free condition of the ectopic cartilages in *A. mexicanum* and *X. laevis* treated with Ly-294,002. Both the absence of musculature and the lateral position of the additional cartilages are shared similarities between the naturally occurring adrostral cartilages and the ectopic cartilages which develop after Ly-294,002 treatment. These similarities and the ability of *bapx1*, whose upregulation is correlated to the development of the ectopic cartilages after Ly-294,002 treatment, to subdivide existing cartilages indicate that changes in *bapx1* expression (upregulation or a heterotopic shift) may have been the reason for the evolution of novel cartilages in the mandibular arch within anurans. Expression analysis of *bapx1* in the appropriate species can be used to test this hypothesis.

Conclusion

In the present work we have successfully treated two different amphibian species with Ly-294,002. As a result of Ly-294,002 treatment, *bapx1* expression increased and mandibular arch derived ectopic cartilages developed lateral to the palatoquadrate in the larvae. The appearance of additional cartilages, which develop through separation from pre-existing cartilages, simultaneously to *bapx1* upregulation supports the notion that *bapx1* has a joint-promoting function. The assumed function further substantiates the possible role of *bapx1* in the evolution of the gnathostome jaw joint. Additionally, *bapx1* function might explain the development of additional cartilages in the anuran jaw which could be caused by overexpression of *bapx1* or by a heterotopic shift of its expression domain. The development of the ectopic cartilages implies that subdivision of pre-existing structures through changes in the expression of a developmental regulator is one possibility for the evolution of morphological novelties.

Declarations

Ethics approval and consent to participate

All animal experiments were carried out according to the animal welfare protocols at Friedrich-Schiller-University, Jena.

Consent for publication

Not applicable

Availability of data and material

The datasets generated and/or analysed during the current study are available from the corresponding author on reasonable request.

Competing interests

The authors declare that they have no competing interests.

Funding

This study was supported in part by a grant from the Deutsche Forschungsgemeinschaft (grant no. OL 134/2-4 to LO) and the Studienstiftung des Deutschen Volkes (to PL).

Authors' contributions

PL and LO developed the concept and design of the study. PL was responsible for the experimental procedures including Ly-294,002 experiments, whole mount in-situ hybridisation, immunostainings, qPCR, 3D-reconstructions and histology. Analysis and interpretation of the data mentioned was mainly done by PL, who was also responsible for the drafting of the manuscript and its final form. LO critically revised the manuscript.

Acknowledgements

We are very grateful to Katja Felbel for technical support and preparation of the histological sections. Sandra Eisenberg took care of the animals. The monoclonal antibodies against collagen II (116B3-collagen II) and newt skeletal muscle (12/101) obtained from the Developmental Studies Hybridoma Bank were developed under the auspices of the NICHD and maintained by The University of Iowa, Department of Biological Sciences, Iowa City, IA 52242, USA.

Literature cited

1. Cerny R, Cattell M, Sauka-Spengler T, Bronner-Fraser M, Yu F, Medeiros DM. Evidence for the prepattern/cooption model of vertebrate jaw evolution. Proc Natl Acad Sci U S A. 2010;107:17262–7.

2. McDiarmid RW, Altig R. Tadpoles : the biology of anuran larvae. University of Chicago Press; 1999.

3. Svensson ME, Haas A. Evolutionary innovation in the vertebrate jaw: A derived morphology in anuran tadpoles and its possible developmental origin. BioEssays. 2005;27:526–32.

4. Haas A. Phylogeny of frogs as inferred from primarily larval characters (Amphibia: Anura). Cladistics. 2003;19:23–89.

5. Sokol OM. The larval chondrocranium ofPelodytes punctatus, with a review of tadpole chondrocrania. J Morphol. 1981;169:161–83.

6. Azpiazu N, Frasch M. tinman and bagpipe: two homeo box genes that determine cell fates in the dorsal mesoderm of Drosophila. Genes Dev. 1993;7:1325–40.

7. Meulemans D, Bronner-Fraser M. Insights from Amphioxus into the Evolution of Vertebrate Cartilage. PLoS One. 2007;2:e787.

8. Baltzinger M, Ori M, Pasqualetti M, Nardi I, Rijli FM. Hoxa2 knockdown in Xenopus results in hyoid to mandibular homeosis. Dev Dyn. 2005;234:858–67.

9. Pasqualetti M, Ori M, Nardi I, Rijli FM. Ectopic Hoxa2 induction after neural crest migration results in homeosis of jaw elements in Xenopus. Development. 2000;127:5367–78.

10. Minoux M, Rijli FM, Paleari L, Zerega B, Postiglione MP, Mantero S, et al. Molecular mechanisms of cranial neural crest cell migration and patterning in craniofacial development. Development. 2010;137:2605–21.

11. Kuratani S. Evolution of the vertebrate jaw from developmental perspectives. Evol Dev. 2012;14:76–92.

12. Couly G, Grapin-Botton A, Coltey P, Ruhin B, Le Douarin NM. Determination of the identity of the derivatives of the cephalic neural crest: incompatibility between Hox gene expression and lower jaw development. Development. 1998;125:3445–59.

13. Depew MJ. Specification of Jaw Subdivisions by Dlx Genes. Science (80). 2002;298:381–5.

14. Beverdam A, Merlo GR, Paleari L, Mantero S, Genova F, Barbieri O, et al. Jaw transformation with gain of symmetry after Dlx5/Dlx6 inactivation: Mirror of the past? Genesis. 2002;34:221–7.

15. Medeiros DM, Crump JG. New perspectives on pharyngeal dorsoventral patterning in development and evolution of the vertebrate jaw. Dev Biol. 2012;371:121–35.

16. Compagnucci C, Debiais-Thibaud M, Coolen M, Fish J, Griffin JN, Bertocchini F, et al. Pattern and polarity in the development and evolution of the gnathostome jaw: Both conservation and heterotopy in the branchial arches of the shark, Scyliorhinus canicula. Dev Biol. 2013;377:428–48.

17. Miller CT. Two endothelin 1 effectors, hand2 and bapx1, pattern ventral pharyngeal cartilage and the jaw joint. Development. 2003;130:1353–65.

18. Talbot JC, Johnson SL, Kimmel CB. hand2 and Dlx genes specify dorsal, intermediate and ventral domains within zebrafish pharyngeal arches. Development. 2010;137:2507–17.

19. Nichols JT, Pan L, Moens CB, Kimmel CB. Barx1 Represses Joints and Promotes Cartilage in the Craniofacial Skeleton. Development. 2013;140:2765–75.

20. Newman CS, Grow MW, Cleaver O, Chia F, Krieg P. Xbap, a vertebrate gene related to bagpipe, is expressed in developing craniofacial structures and in anterior gut muscle. Dev Biol. 1997;181:223–33.

21. Nicolas S, Caubit X, Massacrier A, Cau P, Le Parco Y. Two Nkx-3-related genes are expressed in the adult and regenerating central nervous system of the urodele Pleurodeles waltl. Dev Genet. 1999;24:319–28.

22. Schneider A, Mijalski T, Schlange T, Dai W, Overbeek P, Arnold HH, et al. The homeobox gene NKX3.2 is a target of left-right signalling and is expressed on opposite sides in chick and mouse embryos. Curr Biol. 1999;9:911–4.

23. Tribioli C, Frasch M, Lufkin T. Bapx1: an evolutionary conserved homologue of the Drosophila bagpipe homeobox gene is expressed in splanchnic mesoderm and the embryonic skeleton. Mech Dev. 1997;65:145–62.

24. Yoshiura KI, Murray JC. Sequence and chromosomal assignment of human BAPX1, a bagpipe-related gene, to 4p16.1: a candidate gene for skeletal dysplasia. Genomics. 1997;45:425–8.

25. Cantley LC. The phosphoinositide 3-kinase pathway. Science. 2002;296:1655–7. doi:10.1126/science.296.5573.1655.

26. Engelman JA, Luo J, Cantley LC. The evolution of phosphatidylinositol 3-kinases as regulators of growth and metabolism. Nature Reviews Genetics. 2006;7:606–19.

27. Kim JA, Im S, Cantley LC, Kim DW. Suppression of Nkx3.2 by phosphatidylinositol-3-kinase signaling regulates cartilage development by modulating chondrocyte hypertrophy. Cell Signal. 2015;27:2389–400.

28. Zhang Z, Lei A, Xu L, Chen L, Chen Y, Zhang X, et al. Similarity in gene-regulatory networks suggests that cancer cells share characteristics of embryonic neural cells. J Biol

Chem. 2017;292:12842–59.

29. Vlahos CJ, Matter WF, Hui KY, Brown RF. A specific inhibitor of phosphatidylinositol 3-kinase, 2-(4-morpholinyl)-8-phenyl-4H-1-benzopyran-4-one (LY294002). J Biol Chem. 1994;269:5241–8.

30. Nieuwkoop P, Faber J. Normal Table of Xenopus laevis (Daudin). New York Garl Publ. 1994.

31. Ziermann J, Olsson L. A new staging table for stages relevant to cranial muscle development in the African Clawed Frog, Xenopus laevis (Anura: Pipidae). J Morphol. 2007;268.

32. Schreckenberg GM, Jacobson AG. Normal stages of development of the axolotl, Ambystoma mexicanum. Dev Biol. 1975;42:391–9.

33. Sadaghiani B, Thiébaud CH. Neural crest development in the Xenopus laevis embryo, studied by interspecific transplantation and scanning electron microscopy. Dev Biol. 1987;124:91–110.

34. Heidenhain M. Über die mallorysche bindegewebsfärbung mit karmin und azokarmin als vorfarben. Z wiss Mikrosk. 1915;33:361–72.

35. Anken RH, Kappel T. Die Kernechtrot-Kombinationsfärbung in der Neuroanatomie. Winke fürs Labor. 1992;81:62–3.

36. Square T, Jandzik D, Cattell M, Coe A, Doherty J, Medeiros DM. A gene expression map of the larval Xenopus laevis head reveals developmental changes underlying the evolution of new skeletal elements. Dev Biol. 2015;397:293–304.

37. Livak KJ, Schmittgen TD. Analysis of Relative Gene Expression Data Using Real-Time Quantitative PCR and the 2−ΔΔCT Method. Methods. 2001;25:402–8.

38. van der Westhuizen CM. The development of the chondrocranium of Heleophryne purcelli Sclater with special reference to the palatoquadrate and the sound-conducting apparatus. Acta Zool. 1961;42:1–72.

39. Heatwole H. Amphibian biology. Surrey Beatty & Sons; 2003.

Tables and Figures

	concentration	mortality	phenotype
control	-	9%	0%
DMSO	0,1µM	14%	0%
Ly294 (29NF)	10µM	30%	43%
	20µM	24%	57%
	30µM	78%	35%
	40µM	81%	18%
	50µM	100%	0%

Table 1: Frequency of mortality and phenotype occurrence in *Xenopus laevis* after treatment with different concentrations of Ly-294,002 from 29 NF onwards. Phenotypes were determined six days after incubation based on mandibular arch abnormalities including the appearance of ectopic cartilages. n=90 for controls and each concentration of Ly-294,002.

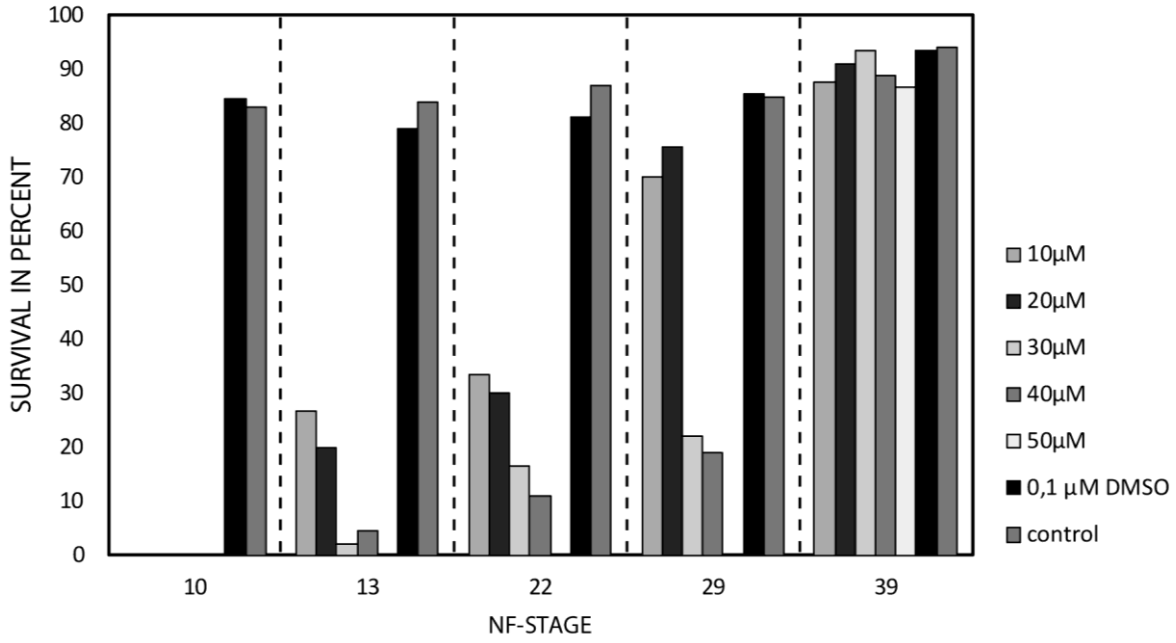

Fig. 1: Quantitative analysis of *X. laevis* tadpole survival after Ly-294,002 treatment. *X. laevis* larvae were treated with different amounts of Ly-294,002 at different developmental stages until NF 45. As controls, *X. laevis* larvae were raised either in 0,1µM DMSO or in 0,1x MBS. Larvae treated with DMSO and with 0,1x MBS show no significant differences in survival rates. The survival rate in Ly-294,002 treated larvae declines with increasing Ly-294,002 concentration and early start of the incubation.

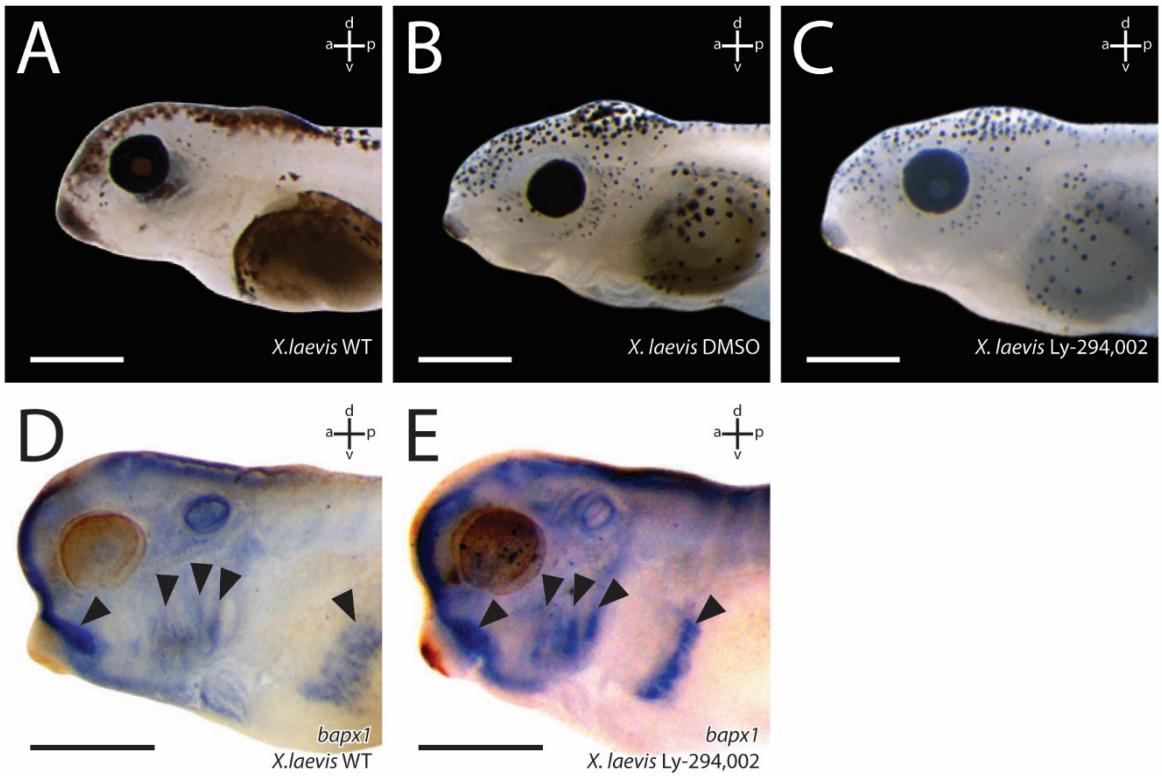

Fig. 2: Effects of Ly-294,002 treatment on external head morphology and *bapx1* expression in *X. laevis*. Lateral view of larvae at NF 44 after rearing in (A) 0,1x MBS as control, (B) 0,1µM DMSO and (C) 20µM Ly-294,002 from NF 29 onwards. No significant differences in the external morphology can be observed. In situ hybridisation of NF 37 *X. laevis* larvae raised in (D) 0,1xMBS as control and (E) 20µM Ly-294,002 from NF 29 onwards in lateral view reveal differences in the expression of *bapx1* in the mandibular arch. After *bapx1* upregulation the mandibular arch expression domain is broader and extends postero-dorsally. scale bar 500µm

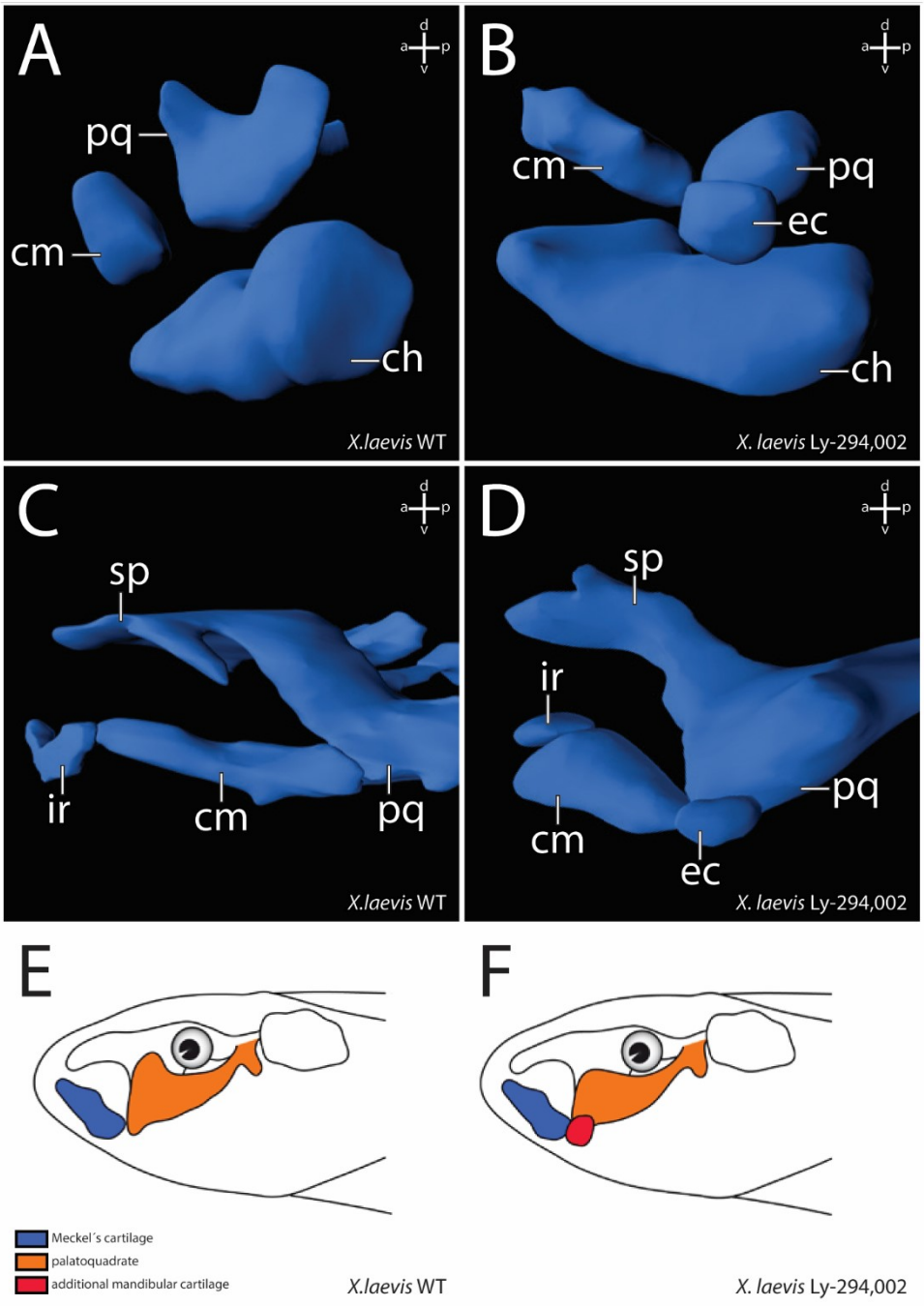

Fig. 3: 3D-reconstructions based on confocal laser scanning microscopy showing the effects of Ly-294,002 treatment on cranial cartilage morphology in *Xenopus laevis* larvae. Lateral view of ZO 10 (A, B) and ZO 17 (C, D) larvae with normal *bapx1* expression (left column) and elevated *bapx1* expression (right column). In Ly-294,002-treated specimen with increased *bapx1* expression an ectopic cartilage develops within the mandibular arch lateral to the palatoquadrate. Depictions of *X. laevis* larvae in lateral view show the main differences between (E) normal and (F) perturbed development. In short, the processus muscularis is reduced in size and an ectopic cartilage arises lateral to the palatoquadrate after upregulation of *bapx1*. ch, ceratohyal; cm, Meckel´s cartilage; ec, ectopic cartilage; ir, infrarostral cartilage; pq, palatoquadrate; sp, suprarostral plate.

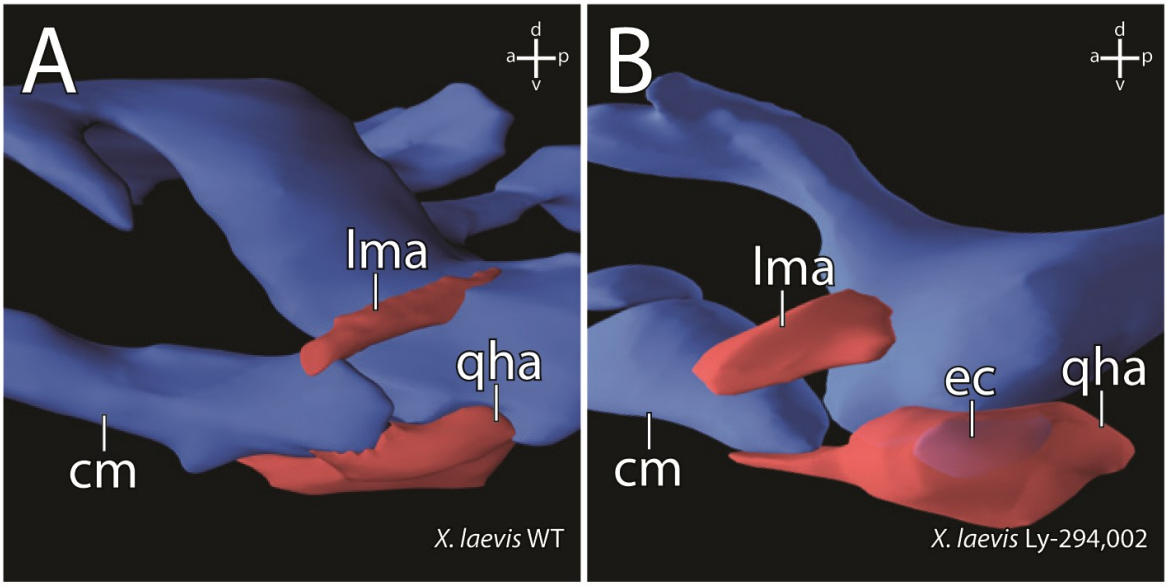

Fig. 4: 3D-reconstructions based on confocal laser scanning microscopy of specimen stained with antibodies showing the effects of *bapx1* upregulation on cranial muscle morphology in *Xenopus laevis* larvae. Lateral view of the jaw articulation and selected muscles of ZO 17 larvae. (A) Muscle morphology in a control specimen. (B) Muscle morphology in a specimen after *bapx1* upregulation. The m. levator mandibulae articularis originates more anteriorly on the dorsal surface of the processus muscularis than in control specimens. The m. quadratohyoangularis surrounds the ectopic cartilage without originating from or inserting onto this cartilage. cm, Meckel´s cartilage; ec, ectopic cartilage; lma, M. levator mandibulae articularis; qha, M. quadratohyoangularis.

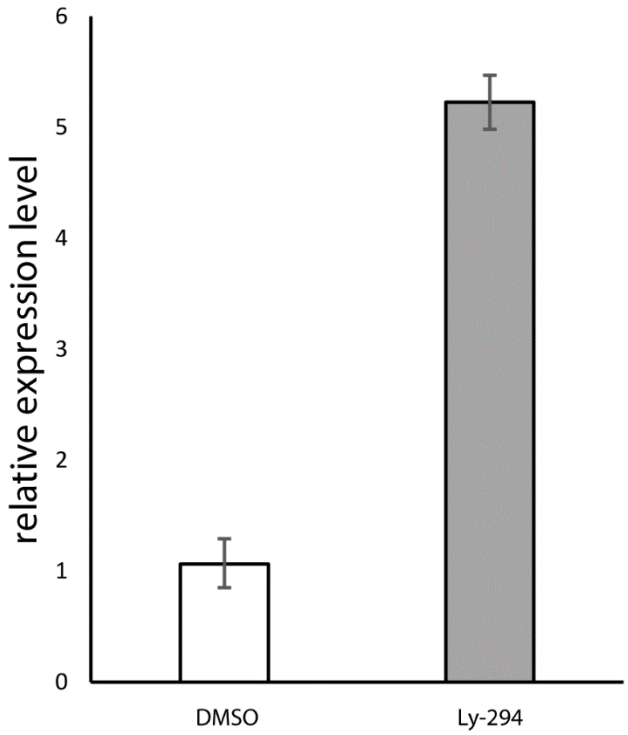

Fig. 5: Effect of Ly-294,002 treatment on *bapx1* expression in *Xenopus laevis* at NF 45. Expression levels were determined through relative quantification (Livak method). Error bars indicate standard deviation of PCR runs (n=3). DMSO reared specimens show no significant reduction in expression compared to control specimens. Ly-294,002 treated specimens show a ~5 times higher expression level of *bapx1* in comparison to controls.

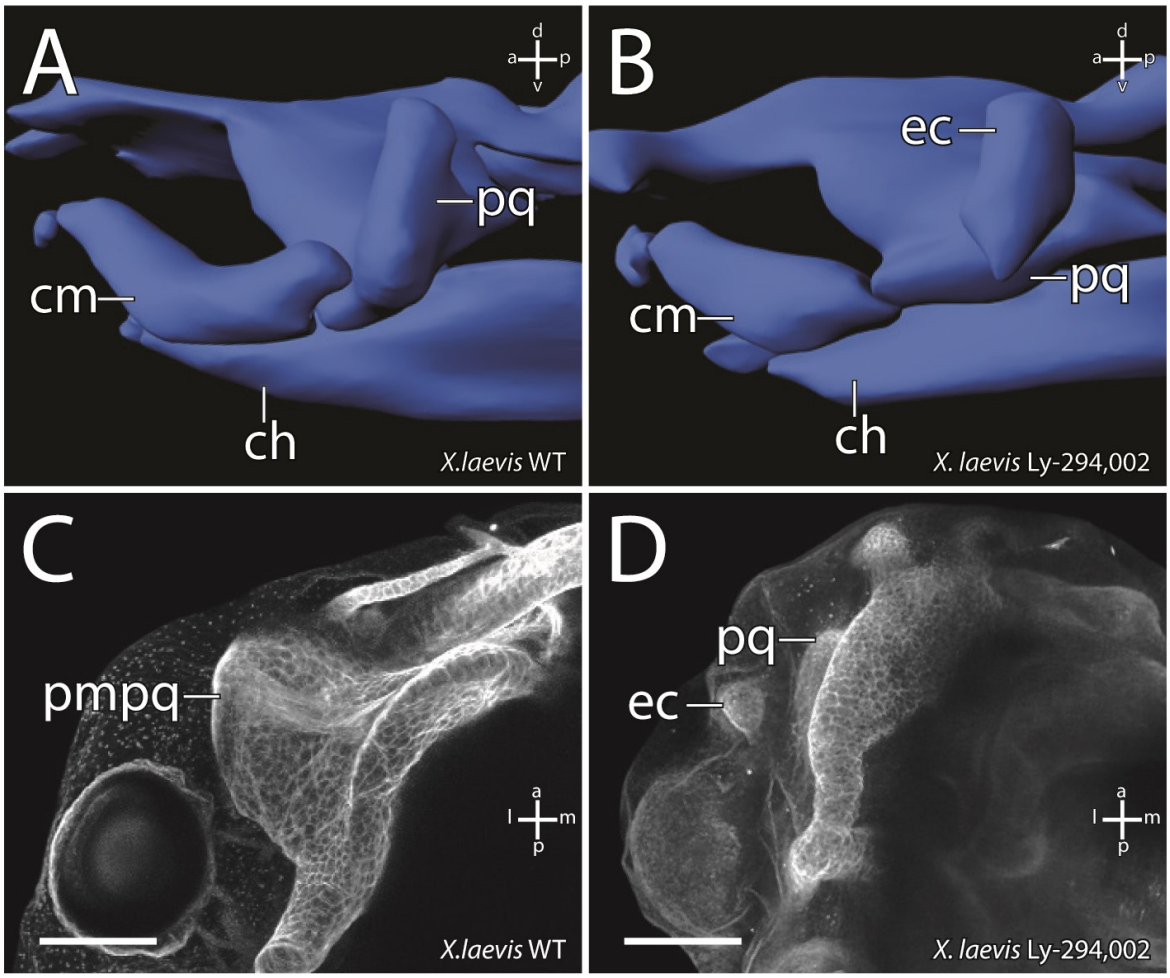

Fig. 6: Effect of Ly-294,002 injection into mandibular arch precursors on cartilaginous cranial morphology in *X. laevis* larvae. 3D-reconstructions based on confocal laser scanning microscopy of (A) control and (B) injected specimens at ZO 17 in lateral view. Maximum intensity projections of (C) control and (D) injected specimens at ZO 20 stained with monoclonal II6B3-collagen II antibody and Alexa 568 in dorsal view. The reduction of the processus muscularis and the presence of an ectopic cartilage can be observed in injected specimens. ch, ceratohyal; cm, Meckel´s cartilage; ec, ectopic cartilage; pmpq, processus muscularis of the palatoquadrate; pq, palatoquadrate. scale bar 200µm

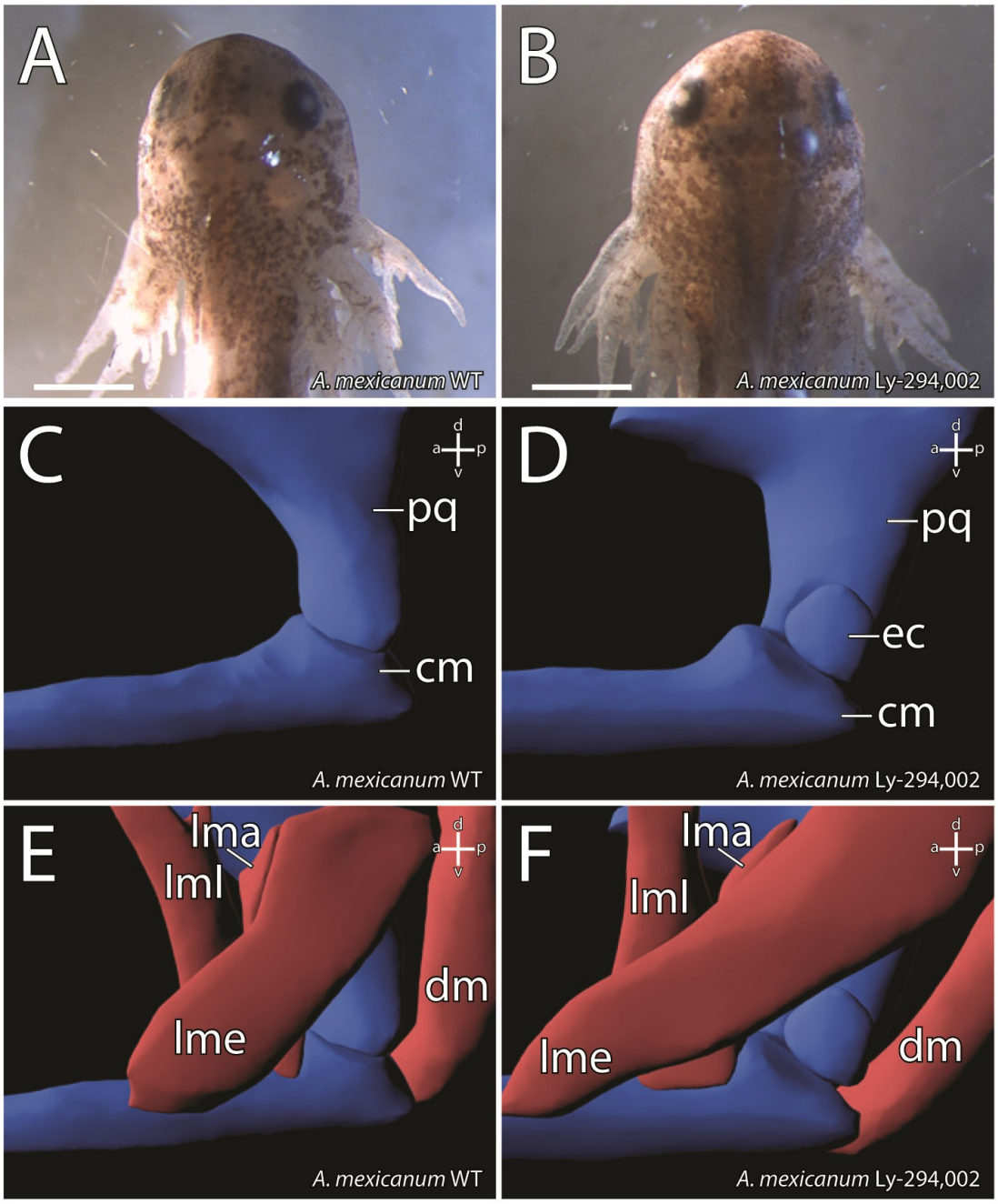

Fig. 7: Effect of Ly-294,002 treatment on the external and internal morphology of *A. mexicanum*. Dorsal view of (A) control and (B) Ly-294,002 treated specimens reveals no differences in external morphology. Lateral view of 3D-reconstructions based on confocal laser scanning microscopy of (C) control and (D) Ly-294,002 treated specimen shows the development of an ectopic cartilage lateral to the jaw articulation in treated specimens. The musculature of (E) control and (F) treated specimens are similar and no changes in origination or insertion of muscles can be observed after *bapx1* upregulation. cm, Meckel´s cartilage; dm, M. depressor mandibulae; ec, ectopic cartilage; lma, M. levator mandibulae articularis; lme, M. levator mandibulae externus; lml, M. levator mandibulae longus; pq, palatoquadrate. scale bar 500µm

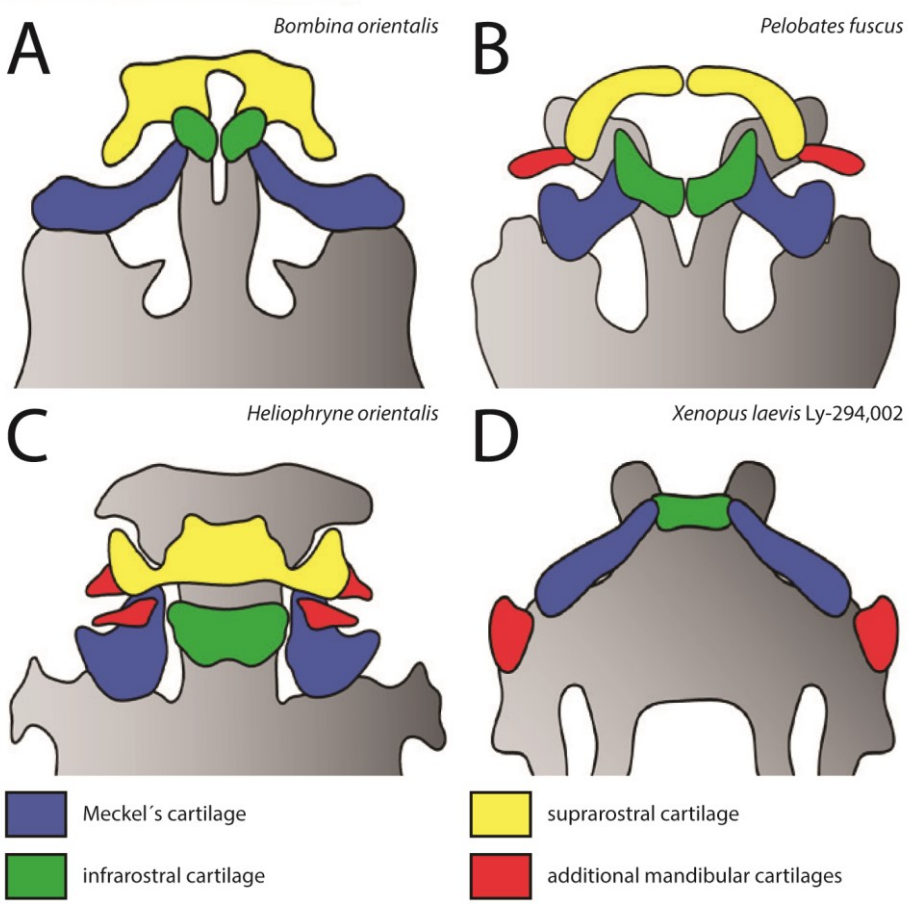

Fig. 8: Overview of the diversity of adrostral cartilages among anurans. Ventral view of the jaw region of selected anuran larvae. (A) *Bombina orientalis* shows a typical anuran condition of the jaw region consisting of paired infrarostral cartilages, a plate-like suprarostral cartilage and horizontally oriented Meckel´s cartilages. (B) In *Pelobates fuscus* (drawn after Nikitin 1986) two so-called adrostral cartilages can be observed lateral to the paired suprarostral cartilages. (C) *Heliophryne orientalis* possesses two additional cartilages in the lower jaw. The submeckelian cartilages lie beneath Meckel´s cartilages and the adrostral cartilages are situated lateral to the suprarostral cartilage. In Ly-294,002-treated *Xenopus laevis* larvae (D) the ectopic cartilages arise lateral to the palatoquadrate and are free from any muscle insertion or origination similar to *P. fuscus* and *H. orientalis*.

Discussion

The present study combines a morphological and a genetical approach to investigate the sequence of cartilaginous head development in an important model organism and how changes in the gene expression during development can alter this sequence and generate morphological abnormalities in different amphibian species.

Applied methods

The morpholino technique was used to knockdown the expression of *bapx1* in different amphibians. The sequences for the morpholinos were derived from the NK 3 homeobox 2 mRNA from *Xenopus tropicalis* provided by NCBI (XM_002940741.4). The sequence from *Xenopus tropicalis* was used because the available sequence from *Xenopus laevis* contained no information about the untranslated region upstream from the start codon, which is necessary for proper morpholino design. Two morpholinos were designed based on this sequence and initially tested in different concentrations in *Xenopus laevis* larvae. For each morpholino and each concentration thirty eggs were injected at the one-cell stage. This was performed three times for each morpholino and each concentration. Afterwards the two morpholinos were injected together in relatively lower concentrations into thirty eggs for three times at the one-cell stage. The whole procedure was repeated in the same way but instead of injecting at the one-cell stage, the morpholinos were injected into one cell at the two-cell stage. Two morpholinos were used because morpholinos often cause off-target effects. When the use of two morpholinos leads to the same morphological abnormalities, these abnormalities are based on the specific knockdown of the specific gene and not the result of off-target effects. The two morpholinos were injected together at lower concentrations to further confirm the specificity because the same abnormalities should arise after this combinatorial injection as in the respective single injection. The injections were repeated three times with thirty eggs from in each time different mating pairs to avoid observing clutch specific abnormalities. The injection of morpholinos into one cell at the two-cell stage was performed as an inner control because morpholinos can not permeate the cell membrane and therefore one half of the specimen contains the injected morpholino and one half of the specimen does not. Whether a knockdown of the *bapx1* expression was initiated by the morpholino injected was tested through in situ hybridisation. Before the morpholinos were used in *Bombina orientalis* and *Ambystoma mexicanum* PCR was performed to test if the sequence where the morpholinos bind are present in the two taxa. The same primers as for the amplification of *bapx1* in *Xenopus laevis* were used and the PCR product was tested through gel electrophoresis and sequencing. After positive results the morpholino with less mortality rate and higher phenotype occurrence was tested in the same way in *Bombina orientalis* and *Ambystoma mexicanum* as described for *Xenopus laevis*. The whole procedure confirmed the specificity of the morpholinos used. Therefore, the obtained results are based on the knockdown of *bapx1*.

LY-294,002 is a known enhancer of *bapx1* expression (Vlahos et al. 1994; Kim et al. 2015). Because it had not been used in *Xenopus laevis* before, extensive tests were needed to confirm its function in *Xenopus laevis*. In its crystallin condition LY-294,002 is not soluble in water. Initially it has to be dissolved in DMSO (dimethyl sulfoxide) before it can be dissolved in water. Groups of N=90 *Xenopus laevis* and *Ambystoma mexicanum* larvae were incubated at different concentrations of the LY-294,002 solution in different developmental stages to specify the function of *bapx1* at each of these stages. To confirm that changes in the *bapx1* expression are not based on other circumstances, additional *Xenopus laevis* and *Ambystoma mexicanum* larvae were raised in nutrient solution and in a DMSO solution. To specifically test the influence of LY-294,002 on mandibular arch development, LY-294,002 was injected in the area of the mandibular neural crest segment antero-ventral to the eye in the late tailbud stage. The changes in the expression of *bapx1* were confirmed using in situ hybridisation and quantitative PCR.

Tissues were stained with different approaches to comprehensively confirm the observation. Serial sectioning was performed transversally and frontally. The sections were stained differently. Heidenhain´s Azan technique (Heidenhain 1915) and nuclear fast red staining (Anken & Kappel 1992) were used to combine the advantages and minimize the disadvantages of the two staining methods. For additional insight into the three-dimensional shape of specific structures, whole mount antibody staining with antibodies against muscle (12/101) and cartilage (II6B3-collagen II) with subsequent confocal laser scanning microscopy and three-dimensional reconstruction using Amira 6.0.1. and Autodesk Maya® 2017 was performed. The combination of these methods enabled a comprehensive overview of the results and prevents misinterpretations of observations which were based on the individual drawback of a method.

The skeletal development of *Xenopus laevis* larvae

The first chapter describes the development of the cartilaginous head skeleton of *Xenopus laevis* tadpoles from the onset of chondrification until the formation of a premetamorphic head skeleton. Initially, this study was designed to reveal faults and inaccuracies in earlier studies of the larval head skeleton of *Xenopus laevis* and to fill the gaps within and between existing works because no investigation so far presents a continous description of the development of the larval head skeleton of *Xenopus laevis*. But as *Xenopus laevis* tadpoles are widely used in gain-of-function and loss-of-function experiments, as well as in toxicological studies which may alter the development in the larval head, a detailed reference is needed to identify morphological abnormalities or heterotopic shifts of the developmental sequence. Furthermore the overview of cartilage development was the baseline for further experimental studies.

The main result of the first chapter is a comprehensive overview on the cartilaginous development of *Xenopus laevis* tadpoles which covers the Nieuwkoop and Faber stages (NF) 37-46 and the Ziermann and Olsson (ZO) stages 6-20, respectively. This work fills an existing gap because from NF 46 and onwards the development of *Xenopus laevis* was

investigated extensively (Trueb & Hanken 1992), but earlier stages were only investigated fragmentarily. The present work revealed that the sequence in which anlagen as mesenchymal cell clusters, condensed precartilaginous cell clusters and the cartilage itself develop is not variable. Therefore, every developmental stage can be identified by its specific set of cartilages or cartilage precursors. Three incidents were identified which show variable timing. The fusion of the trabeculae cranii and the parachordal, the fusion of the commissura quadratocranialis anterior and the planum trabeculare anticum, and the fusion of the processus ascendens palatoquadrati and the subocular cartilage show variable timing. These fusion events may be altered by external factors such as differences in ingestion or behavioural differences between different tadpoles which results in different muscle activity. Muscles can build strong forces which influence skeletal development and thus influence the timing of the fusion of two skeletal elements.

Despite the compilation of a comprehensive description of the cartilaginous larval head development of *Xenopus laevis* the present study revealed a major discrepancy. For evolutionary developmental biologists a staging table is an important tool to match a set of standardized morphological traits to a specific developmental stage. If such a staging table is used by different researches they can communicate effectively about their results in certain stages. For anurans there exists a general staging table which is meant to be used for all species. The so-called Gosner staging uses traits common to most larval anurans (Gosner 1960). However, such a general and simplified staging table can not cover all the different species with its individual adaptations and different developmental modes equally. Therefore, staging tables exist which describe the development of species with a certain developmental mode (e.g. direct developing anurans), with a certain feeding mode (e.g. carnivorous anurans), which belong to a certain derived taxonomic unit or which are widely used in biological research. *Xenopus laevis* is such a widely used species which has its own staging table (Nieuwkoop & Faber 1994). The Nieuwkoop and Faber staging table for *Xenopus laevis* describes the development from the fertilized egg until the adult organism and is commonly used to define the developmental stages of *Xenopus laevis* tadpoles. The stages reach from stage 1 until stage 65. Every stage is defined through one or more external features e.g. the number of cells, appearance of the eyes, visibility of melanocytes and so on. The present study revealed, that the external features which are responsible for defining the respective stage do not correlate with the inner morphology during the stages of skeletal development. For instance, the Nieuwkoop-Faber stage 43 (NF 43) is defined as a stage where the ventral lateral line system becomes visible, the cement gland loses its pigment and the torsion of the intestine reaches 180°. Comparing the cartilaginous skeleton of several NF 43 tadpoles one can notice big differences (Figure 5). One NF 43 tadpole can have chondrified cornua trabeculae, ceratobranchial II, III and IV, otic capsule and processus retroarticularis and processus ventrolateralis whereas in another NF 43 tadpole of the same structures are in a chondroblast state and only form condensed precartilaginous cell clusters.

This observation may be the result of the lack of studies of intrastage variation in external morphology as stated by the authors of the widely used NF staging table (Nieuwkoop &

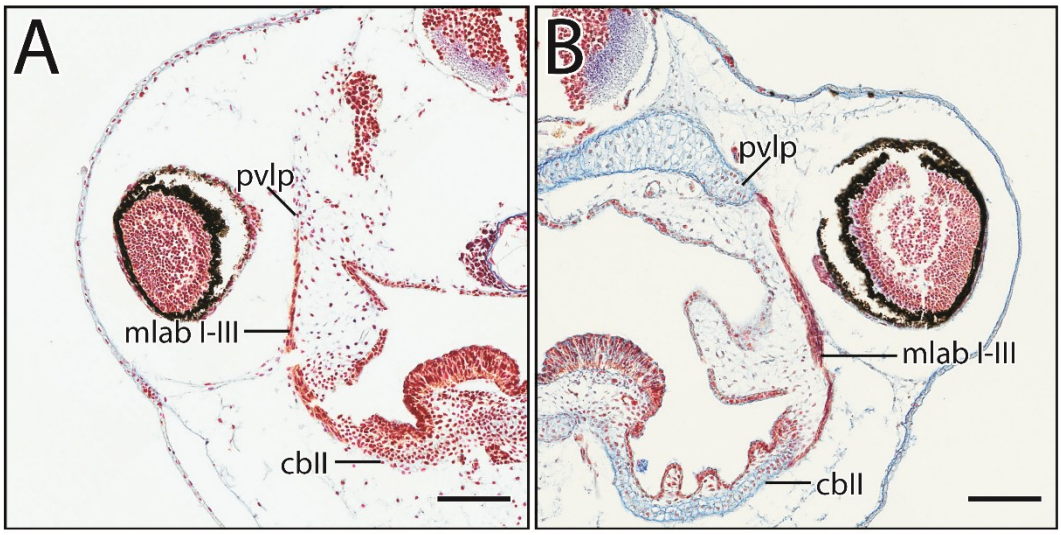

Figure 5: Skeletal differences between two NF 43 tadpoles illustrating the discrepancy between the NF staging system and cartilaginous development. **A** Processus ventrolateralis posterior and ceratobranchial II are precartilaginous and resemble the condition of a ZO 12 whereas in **B** processus ventrolateralis posterior and ceratobranchial II are chondrified as in ZO 15. Scale bar 100 µm. cbII, ceratobranchial II; mlab I – III, m. levatores arcuum branchialium I – III; pvlp, processus ventrolateralis posterior

Faber 1994). Additionally, there are only small differences between single NF stages in external morphology but large differences in internal morphology. This further shows, that the NF staging table does not sufficiently reflect changes of the cartilaginous skeleton with its respective stages. Because each NF stage represents an amount of possible variations of the state of the cartilaginous skeleton a NF stage contains no information about the specific state of the cartilaginous skeleton at a defined stage.

Therefore, the usage of an alternative staging table of *Xenopus laevis* for studies which focus on the skeletal development is recommended. The Ziermann and Olsson staging (ZO) is also based on external features to identify each stage, but it adds a specific configuaration of muscles to every stage (Ziermann & Olsson 2007). It ranges from stage 1 until stage 20 and covers the NF stages 32-46 and reduces the gaps between each stage by increasing the number of stages in this developmental range. The present study revealed, that muscle development is well correlated to skeletal development in the stages investigated. Whenever a specific set of muscles was present, the cartilaginous skeleton had a specific state. The respective state of the cartilaginous structures was added to each ZO stage and every ZO stage is now defined through a combinatorial set of muscles and cartilages. This should be helpful for further investigation which focus on the musculoskeletal system, because results will be more comparable when using this staging system. Nevertheless, NF staging remains a suitable staging system because the stage can be easily defined without harrming the organism. Therefore, it is useful for determination of the stage in the field or in the laboratory without the use of further equipment.

Investigations on the early skeletal development of *Xenopus laevis* tadpoles are present in the literature but suffer from different staging methods, inaccuracies and different anatomical ontology. The present work follows the guideline of the Xenopus Anatomy Ontology to describe the different structures (Segerdell et al. 2013; Segerdell et al. 2008).

Therefore the results are comprehensible and comparable. Unfortunately, the most reliable source for skull morphology, Gavin de Beer´s "The development of the vertebrate skull", has several mistakes in the description of the larval head skeleton of *Xenopus laevis* because he adopted the work of Kotthaus (Kotthaus 1933). Kotthaus stated that the suprarostral plate is movable against the chondrocranium, which is not the case. The suprarostral plate is unified with the posterior planum trabeculare anticum. Furthermore, the lateral projection of this plate forms the tentacular cartilage, which is supported by the processus cornu quadratus lateralis that originates from the anterior surface of the palatoquadrate. Kotthaus instead stated that the tentacular cartilage originates from the anterior surface of the palatoquadrate and has no connection to the suprarostral plate (Figure 6). Further discrepancies were discussed by Paterson, which presented the most reliable source of early skeletal development of *Xenopus laevis* so far (Paterson 1939). In the work of Weisz a configuration of cartilaginous structures is shown, which was never observed in any specimen in the present work (Weisz 1945a). Based on the presence of the basicranial fenestra, the stage shown should be stage ZO 14. At this stage Meckel´s cartilage, all four ceratobranchials, the

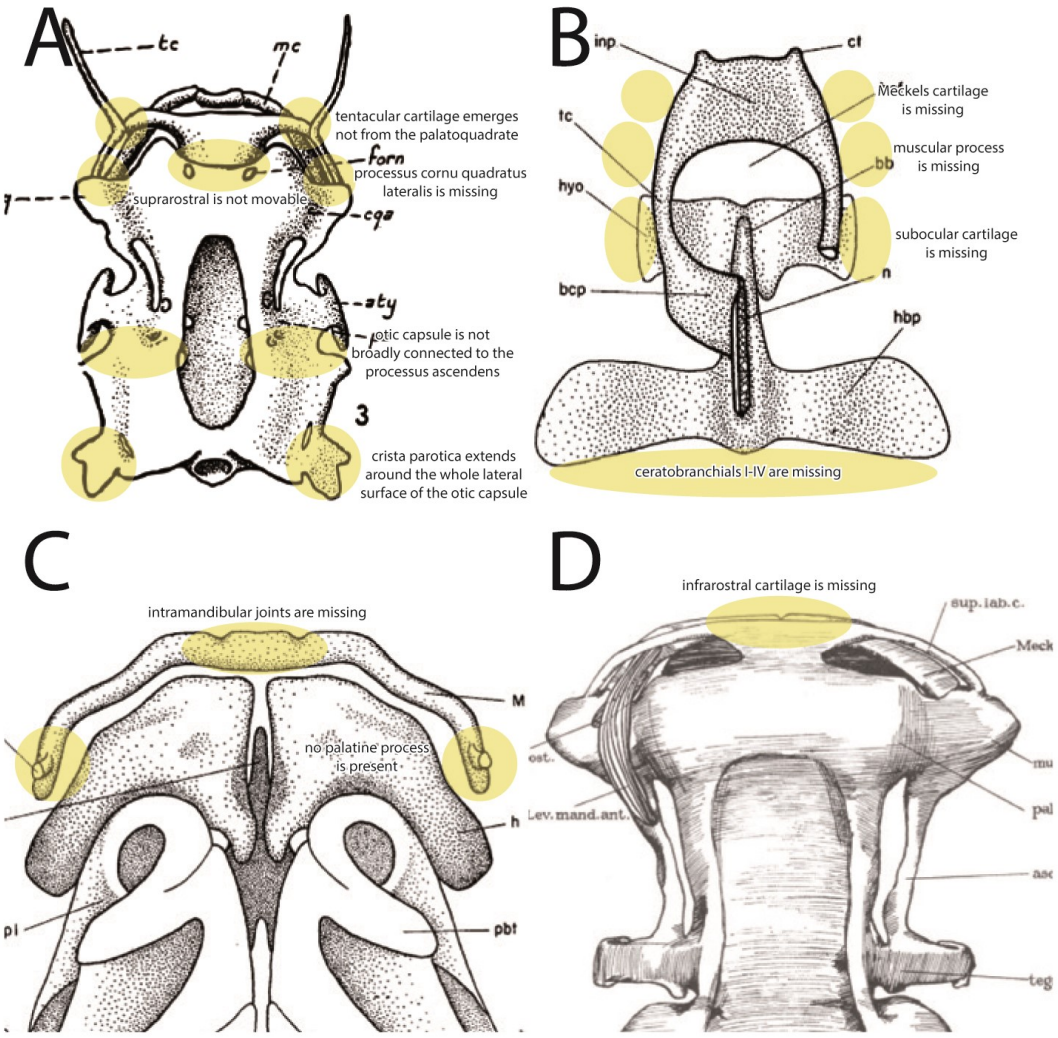

Figure 6: Selected inaccuracies in recent investigations on the larval skeleton of *Xenopus laevis*. Structures which differ from the findings in the present work are highlighted in yellow. Depictions were redrawn from **A** Kotthaus (1933), **B** and **C** Weisz (1945) and **D** Edgeworth (1930).

processus muscularis palatoquadrati and the subocular cartilage should be present, which is not the case in his depiction. Several authors oversee the presence of the infrarostral cartilage (Dreyer 1914; Edgeworth 1930; Weisz 1945a), a condition never seen in any of the investigated tadpoles in the present work. Additionally, a special emphasis was given to the presence of the commissura craniobranchialis I-III. These structures join the branchial basket to the crista parotica and is often overseen in skeletal descriptions. Most differences in earlier investigations may have been caused by the limitations of the methods available at the time. The thickness of histological slices and the use of the staining method can have a large influence on the interpretation of serial sections. Therefore different staining methods, different slice orientations and different techniques to visualise the cartilaginous skeleton were used in the present work. The results from all different approaches were then compared and unified to the present comprehensive overview of the cartilaginous development of *Xenopus laevis*.

The development of the viscerocranial and neurocranial structures in Xenopus *laevis* does not follow the strict anterior-posterior pattern observed in other vertebrate taxa. In chondrychtyans, sturgeons and teleosts the head skeleton develops in an anterior-posterior direction (Gillis et al. 2012; Langille & Hall 1987; Warth et al. 2017). The first pharyngeal arch derived cartilages Meckel´s cartilage and palatoquadrate develop first, the second arch derived ceratohyal develops second and so on. Also for anurans a strict anterior posterior pattern has been reported in earlier studies (Gaupp 1906; Stöhr 1882). *Xenopus laevis* differs from this sequence as the ceratohyal, a cartilage derived from the second pharyngeal arch, is the first cartilage which chondrifies during development (Figure 7). The ceratohyal is a paired horizontally oriented cartilage, which is situated ventrally and reaches from one side of the tadpole to the other. Dorsal to this paired cartilage lies the buccal cavity. The lateral processes of each ceratohyal are connected through the m. interhyoideus. When this muscle contracts, the ceratohyals are bent along the longitudinal axis, the capacity of the buccal cavity diminishes and water flows out due to the overpressure. When this muscle relaxes the ceratohyals return in their initial position, the capacity of the buccal cavity extends and water flows back in due to the negative pressure in the cavity (McDiarmid & Altig 1999). This mechanism is important for breathing as well as for the ingestion of *Xenopus laevis* larvae. The tadpoles are filter feeders which need to enable a constant influx of water which contains detritus. This detritus is the main resource for the tadpoles. Therefore, the precocious development of the ceratohyals may be beneficial because it enables filter feeding at an earlier stage of development. Early ingestion accelerates growth, which is important for tadpoles because more developed tadpoles of the same species retard the development of the less developed tadpoles and these retarded tadpoles barely survive until metamorphosis. This phenomenon is known as the crowding effect (Gromko et al. 1973). The early acquisition of food through filter feeding and the prevention of the crowding effect may have been selective forces which lead to the precocious formation of the ceratohyal and therefore to the alteration of the ancestral anterior-posterior pattern in *Xenopus laevis* tadpoles. Furthermore, it is possible that the development of Meckel´s cartilage is delayed. Meckel´s cartilage in *Xenopus laevis* has no primordial stage where the cartilage is horizontally oriented and stout

as it is in other anuran tadpoles. Instead, Meckel´s cartilage skips this stage in *Xenopus* and initially develops as a elongated, sigmoidal rod which is diagonally oriented. This resembles the premetamorphic condition in other anuran tadpoles. Maybe this leads to a delayed development of Meckel´s cartilage. Anuran-specific novelties such as infrarostral and suprarostral cartilages deviate from the ancestral pattern, too. If *Xenopus* tadpoles followed the ancestral pattern the infrarostral cartilage should develop simultaneous with Meckel´s cartilage at ZO 11. Instead the infrarostral cartilage develops at the transition between ZO 14 and ZO 15 when posterior elements such as the ceratobranchials and parachordals are present. The suprarostral plate is not chondrified until ZO 17 but according to the ancestral pattern it should be present at ZO 11. Additionally, the *Xenopus*-specific tentacular cartilage

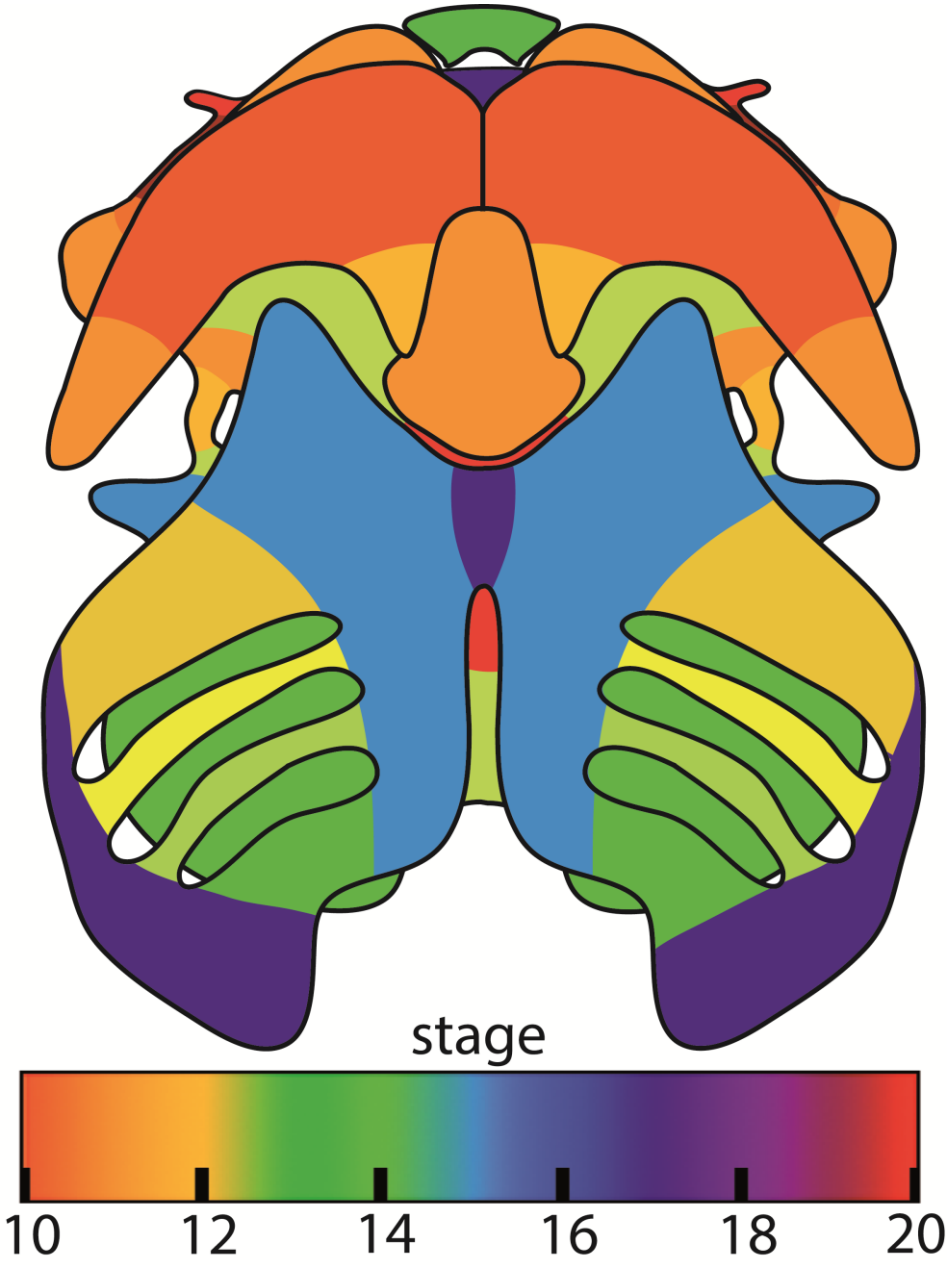

Figure 7: Development of the cartilaginous head skeleton of *Xenopus laevis* in relation to the respective Ziermann and Olsson stage. The image is colour coded and each colour represents a specific stage.

is one of the latest cartilages to develop (ZO 20). Obviously, the novelties mentioned changed the ancestral anterior-to-posterior pattern.

Nevertheless, *Xenopus laevis* tadpoles also share similarities in the skeletal development with *Rana temporaria*, another anuran whose development of the cartilaginous skeleton was investigated (Stöhr 1882; Gaupp 1906). There are three cartilaginous structures which anchor the palatoquadrate to the neurocranium. These structures chondrify in a specific order in the investigated anurans. First, the commissura quadratocranialis chondrifies, second the processus ascendens, and third the larval otic processus. The trabeculae cranii develop in a strict anterior-posterior direction until they fuse to the parachordals. The otic capsules chondrify after the parachordals and the Ceratobranchials I – IV develop separately in an antero-posterior sequence and fuse first medially and second laterally in the same order. All shared similarities are remnants of the ancestral anterior-posterior pattern.

If the delayed development of anuran- and *Xenopus*-specific cartilaginous structures is a consequence of the derived state of *Xenopus* or a general trend within anurans and which heterotopic event (accelerated ceratohyal development or delayed development of Meckel´s cartilage) caused this can not be answered with the present data. Further developmental studies of skeletal development in further anuran tadpoles are needed to specifically identify such heterochronic events.

In the second and third chapter the influence of the gene *bapx1* on the development of several amphibian species was investigated. Functional experiments on the impact of *bapx1* expression during development were missing so far in this taxonomic group despite its phylogenetically important position. Through gain- and loss-of-function experiments and the resulting morphological abnormalities it was possible to define the role of *bapx1* during amphibian development and infer its potential role during vertebrate evolution.

The role of *bapx1* in amphibian head development

The temporal and spatial expression pattern of *bapx1* in the head of *Xenopus laevis* tadpoles has been investigated before (Newman et al. 1997; Square et al. 2015). The present work can confirm the observed expression domains. Before the onset of chondrification *bapx1* is expressed in the ventral region of the first pharyngeal arch flanking the cement gland dorsolaterally and marking the precursors of the palatoquadrate and the proximal part of Meckel´s cartilage. Three stripes of expression domains which correspond to the endoderm of the pharyngeal pouches of the pharyngeal arches 3-5 are visible posterior to it. It is also expressed in the anterior gut mesoderm. During chondrification *bapx1* is also expressed around the developing jaw joint. The expression in the posterior arches is diminished and *bapx1* is further expressed in the anterior gut mesoderm. The expression in the mesoderm of the gut correlates with its ancient pregnathostome function of segmenting the developing gut. The expression of *bapx1* within the intermediate region of the first pharyngeal arch instead is conserved among gnathostomes and correlates well with the emergence of the primary jaw joint because agnathans, which are the closest recent relatives of gnathostomes lack *bapx1* expression in the first pharyngeal arch and also lack a jaw joint.

The morpholino technique was used to knock down the expression of *bapx1* in three different amphibian species. A knockdown of a certain gene often results in morphological abnormalities which can be analysed to infer the function of the specific gene which was knocked down. The knockdown of *bapx1* with 30µM bapx-morpholino lead to the loss of the jaw joint in 47% of the treated *Xenopus laevis* larvae (Fig. 8 A, B). The bapx-morpholino was also tested in the basal anuran *Bombina orientalis* and in the urodele *Ambystoma mexicanum* and the respective tadpoles displayed the same joint loss which was observed in *Xenopus laevis*. Therefore, it can be inferred that the joint loss after *bapx1* knockdown is neither the result of the derived state of *Xenopus laevis* nor an anuran-specific feature. The function of *bapx1* as an intermediate first arch patterning gene is at least conserved among amphibians. Fortunately, the observed phenotypes are similar to the results of gene expression altering experiments in non-anuran gnathostomes. In bony fish and chicken the knockdown of *bapx1* also led to the loss of the jaw joint (Wilson & Tucker 2004; Miller 2003). Overexpression of *barx1*, the antagonist of *bapx1* in the first pharyngeal arch, in zebrafish leads to similar joint loss as observed after *bapx1* knockdown in the present study. *Barx1* is able to enhance cartilage formation and repress joint development and overexpression of this gene leads to the expansion of its expression domain into the intermediate domain of the first pharyngeal arch in zebrafish (Nichols et al. 2013). It

supresses *bapx1* expression and therefore prevents joint formation. The knockdown of *bapx1* in the present study may have caused a dorsal expansion of the *barx1* domain because its repressor *bapx1* was downregulated and this may have caused the observed joint loss. The absence of the joint after *bapx1* knockdown may confirm the cartilage preventing function of *bapx1*. In mice the joint between malleus and incus, the homologous mammalian structures of Meckel´s cartilage and palatoquadrate, is not affected by the knockdown of *bapx1* (Tucker 2004). This further indicates that downstream targets of *bapx1* are responsible for proper joint induction. Through mammalian evolution *bapx1* lost its ability to regulate *gdf5* and *gdf 6* which are essential for joint formation (Tucker 2004). Thus, the role of *bapx1* in the first pharyngeal arch is gnathostome specific and conserved among all non-mammalian gnathostomes.

After the knockdown of *bapx1* expression and initial insights into its potential role during amphibian development the gene was overexpressed to further elucidate its function. *Bapx1* expression has been shown to be repressed by the activity of the Phosphatidylinositol 3-kinase (PI3K) and its subunit *Pik3ca* (Kim et al. 2015; Zhang et al. 2017). Ly-294,002 (2-(4-Morpholinyl)-8-phenyl-4H-1-benzopyran-4-one hydrochloride) is a specific inhibitor of PI3K and the suppression of PI3K causes raised *bapx1* expression levels (Vlahos et al. 1994;

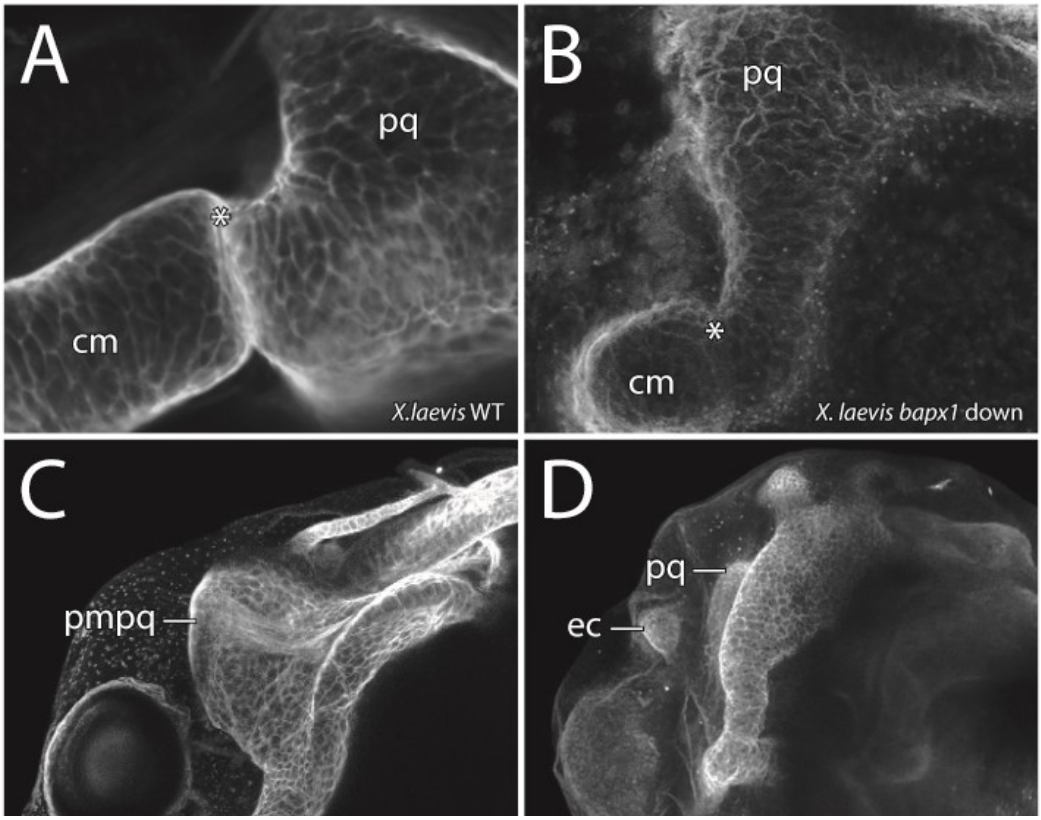

Figure 8: Results from the *bapx1* loss- and gain-of-function experiments. *Xenopus laevis* wildtype (left column) and morphants (right column) in lateral (top line) and dorsal view (bottom line). **A** The jaw joint (asterisk) is present in unperturbed tadpoles, **B** whereas it is missing in tadpoles after *bapx1* knockdown. **C** The processus muscularis is a wide u-shaped part of the palatoquadrate in unperturbed tadpoles. **D** After *bapx1* upregulation the process is clearly reduced and an ectopic cartilage is present laterally. cm, Meckel´s cartilage; ec, ectopic cartilage; pmpq, processus muscularis palatoquadrate; pq, palatoquadrate

Kim et al. 2015). Therefore, *Xenopus laevis* tadpoles were incubated from defined stages onwards in Ly-294,002 to test if *bapx1* is overexpressed after the treatment and which effects occur after successful *bapx1* overexpression. In-situ hybridisation and quantitative PCR confirm that *bapx1* expression was raised more than fivefold after Ly-294,002 treatment. 57% of the larvae treated with 20µM Ly-294,002 from the late tailbud stage onwards developed malformed first pharyngeal arch derivatives. In these larvae an ectopic cartilage occurs (Fig. 8 C, D), which has a rounded shape and is situated lateral to the palatoquadrate and the ceratohyal. This ectopic cartilage is bordered postero-dorsally by the palatoquadrate and antero-dorsally by Meckel´s cartilage and is separated from the two cartilages by a cavity-like gap. The treatment of *Ambystoma mexicanum* larvae with Ly-294,002 caused similar ectopic cartilage development and confirms the conserved role of *bapx1* among amphibians. *Bapx1* upregulation has a specific effect on the development of first pharyngeal arch derived cartilaginous elements because, similar to the knockdown experiments, no abnormalities in the posterior arch derived skeletal elements were observed. In both species tested, the ectopic cartilage appears lateral to the palatoquadrate and postero-lateral to Meckel´s cartilage. The chondrocytes which develop into this ectopic cartilage originate from the palatoquadrate and partly from Meckel´s cartilage and are covered in connective tissue. Therefore, the cartilage can not be considered as a de *novo* cartilage. The development of this ectopic cartilage may be driven by the cartilage preventing function of *bapx1*. Normally, *bapx1* keeps the region between Meckel´s cartilage and the palatoquadrate chondrocyte-free but with elevated expression levels *bapx1* function keeps additional regions chondrocyte-free. These additional chondrocyte-free regions separate developing chondrocytes from their primordial cartilage. The separated chondrocytes condense and develop into a new ectopic cartilage because chondrocytes without suitable genetic information tend to aggregate and form roundish or rod-shaped cartilages (Rose 2009). The results from the overexpression of *bapx1* further confirm its cartilage preventing function. Additionally, it has been shown that the introduction of *bapx1* into a new domain can cause the development of ectopic (“new”) cartilages.

There are doubts as to whether *bapx1* is a master regulator of joint development (Medeiros & Crump 2012). After *bapx1* inactivation in chicken and zebrafish, the jaw joint failed to develop whereas in mice, where the former jaw-forming cartilages are part of the middle ear, a normal joint develops between Meckel´s cartilage and the palatoquadrate (Tucker 2004; Wilson & Tucker 2004; Miller 2003). Especially the results in mice challenge the role of *bapx1* as master regulator of joint formation and suggest that downstream targets might be involved. The results of the present study confirm that *bapx1* does not induce joint development. In *Xenopus laevis* Meckel´s cartilage and the palatoquadrate develop from two distinct condensations (Lukas & Olsson 2018), whereas in chicken the two cartilages arise from one condensation (Wilson & Tucker 2004). If *bapx1* would be a master regulator of joint formation, the condensations of Meckel´s cartilage and the palatoquadrate should fuse during early development in *Xenopus laevis* tadpoles after *bapx1* knockdown. Instead, the two cartilages initially differentiate and chondrify separately and a proper gap which is supposed to be the joint cavity between them is established. The fusion between the two

cartilages starts at ZO 14 when the joint forming processes, the processus retroarticularis of Meckel´s cartilage and processus articularis of the palatoquadrate, are chondrified. A small band of cells migrates into the joint cavity and connects the two processes. During further development these cells chondrify and form a ventral cartilaginous fusion between Meckel´s cartilage and the palatoquadrate. Normal function of *bapx1* would prevent these cells from chondrifying which ensures the proper joint formation. This further confirms the cartilage preventing function of *bapx1*. Furthermore, this observation confirms that *bapx1* is no master regulator of joint formation but rather a maintenance gene which keeps the joint cavity, which is induced and formed by other regulators, cartilage-free and ensures its proper function.

The results from the gain- and loss of function experiments substantiate the cartilage-preventing function of *bapx1* assumed before. *Bapx1* overexpression led to additional cartilage-free regions which are capable to partitioning novel cartilages, whereas *bapx1* knockdown led to the expansion of chondrocytes into the jaw joint which results in the fusion of Meckel´s cartilage and the palatoquadrate, and therefore to the loss of the jaw joint. Furthermore, the data presented convincingly shows that *bapx1* function does not initiate joint formation. Instead proper *bapx1* function is essential to prevent cells within the joint cavity from differentiate into chondrocytes and therefore ensures proper joint function. Despite expression in more posterior arches and in the developing anterior gut changes in the expression levels of *bapx1* only affect first pharyngeal arch derived skeletal elements. The first pharyngeal arch is defined by the absence of *Hox*-transcripts. In the more pharyngeal arches the expression of *Hox*-transcripts may supress the abilities of *bapx1* displayed in the first pharyngeal arch.

The potential role of b*apx1* in the evolution of novelties

The present work offers new pieces of evidence to understand vertebrate evolution because through the induced ontogenetic malformations it is possible to explain phylogenetic changes of several structures. The loss of *bapx1* function in bony fish (Miller 2003), chicken (Wilson & Tucker 2004) and amphibians (present study) all led to the loss of the jaw joint through the fusion of Meckel´s cartilage and the palatoquadrate during early cartilaginous development. Agnathans, the closest relatives to gnathostomes, have an unjointed first pharyngeal arch which lacks any *bapx1* expression (Cerny et al. 2010). The experimental reduction of *bapx1* expression in zebrafish, chicken and at least in *Xenopus* caused the development of an unjointed first pharyngeal arch which is comparable to the agnathan condition. Therefore, the anomalies caused by the loss of *bapx1* function can be interpreted as a first pharyngeal arch "primitivization" and the observed morphants all mirror the ancient condition of an unjointed first arch which must have been present in the last common ancestor of gnathostomes and agnathans (Fig. 9). In this ancestor a primordial patterning system must have been present which patterned the pharyngeal arches in anterior-posterior and dorsoventral direction. The rise of the gnathostomes might have begun when *bapx1* expression was heterotopically shifted into the first pharyngeal arch dorsoventral patterning

system. There the expression of *bapx1* alters the ancestral first pharyngeal arch specific *barx1* expression, which normally prevents joint formation. This co-option of *bapx1* expression refined the ventral first pharyngeal arch patterning system (Cerny et al. 2010) and led to a spatial prevention of chondrification within this arch. Combinatorial evolution of *bapx1* regulators and effectors might have ensured that the cartilage free domain developed into a proper joint and therefore contributed to the evolution of the jaw joint.

The configuration of the musculature after *bapx1* knockdown provides further insight into what a jawless stem line gnathostome may have looked like. The muscles which open and close the jaw were not significantly perturbed by the *bapx1* knockdown and retained their proper function. Morphants which lacked a jaw joint behaved normally and were able to open and close the jaw to breathe and ingest. Derivatives of the larval musculature responsible for proper jaw movement persist during metamorphosis and are part of the adult jaw musculature as well. The morphants which lack *bapx1* expression in the first pharyngeal arch and therefore possess no jaw joint may be mirror images from extinct unknown stem line gnathostomes. Possibly, the feeding apparatus of such a hypothetical stem line gnathostome consisted of a continuous, cartilaginous first pharyngeal arch and a set of muscles which insert onto the jaw cartilages similar to the condition found in the *bapx1* downregulation morphants. Through the resilient and elastic traits of cartilaginous tissue the proper opening and closing of the jaw may have been ensured. At least filter feeding would have been possible with this jaw configuration and filter feeding is the predominant way of ingestion in tunicates and cephalochordates, the closest relatives of vertebrates. Therefore, the hypothesized stem line gnathostome would fill a gap between chordates and basal vertebrates. Furthermore, in this scenario the musculature could be refined over thousands of years to fit the requirements for proper jaw movement before a distinct joint appeared. Therefore, the evolution of the jaw would appear less saltatory and more continuous.

The potential of *bapx1* to prevent cartilage formation and subdivide existing cartilages during development was observed after *bapx1* upregulation in *Xenopus laevis* and *Ambystoma mexicanum*. *Bapx1* is able to divide a single cartilage into two cartilages where one keeps its former function whereas the other appears as novelty. Instead, the cartilage-free domain which separates the two cartilage is the actual novelty (comparable to the third hypothesis from Svensson and Haas in Figure 1 C). This function may also have driven the evolution of additional cartilages in anurans. There exist several anurans which develop additional mandibular arch derived cartilages. For instance, *Alytes obstetricans* and *Pelobates fusucs* have an admandibular cartilage (named adrostral cartilage in *Pelobates*) which is a dorsoventral processing rod lateral to the intramandibular joint between Meckel´s cartilage and infrarostral cartilage (Haas 2003; Heatwole 2003). *Heliophryne purcelli* has even two additional cartilages in the lower jaw (van der Westhuizen 1961). One is the rod-like adrostral cartilage lateral to the suprarostral cartilage and the other is a cuneiform cartilage ventral to Meckel´s cartilage which is named submeckelian cartilage. The location of these naturally developing additional cartilages and the fact that all of them are free from any muscle origination and insertion are two points which are similar to the morphants observed after *bapx1* upregulation. The morphants developed laterally situated, muscle-free

and rod-like ectopic cartilages. These experimental similarities together with the ability of *bapx1* to subdivide existing cartilages leads to the hypothesis that changes in the *bapx1* expression during anuran evolution may have driven the evolution of novel cartilages within the mandibular arch (Fig. 9). Another anuran-specific feature, the intramandibular joint which separates the infrarostral cartilage from Meckel´s cartilage, remains unperturbed after *bapx1* knockdown and upregulation. Therefore, the present work provides no support that the evolution of this cartilage was caused by *bapx1*. It is rather considered that the gene *zax* which is a paralogue of *bapx1* is involved in the development and evolution of the intramandibular joint (Svensson & Haas 2005).

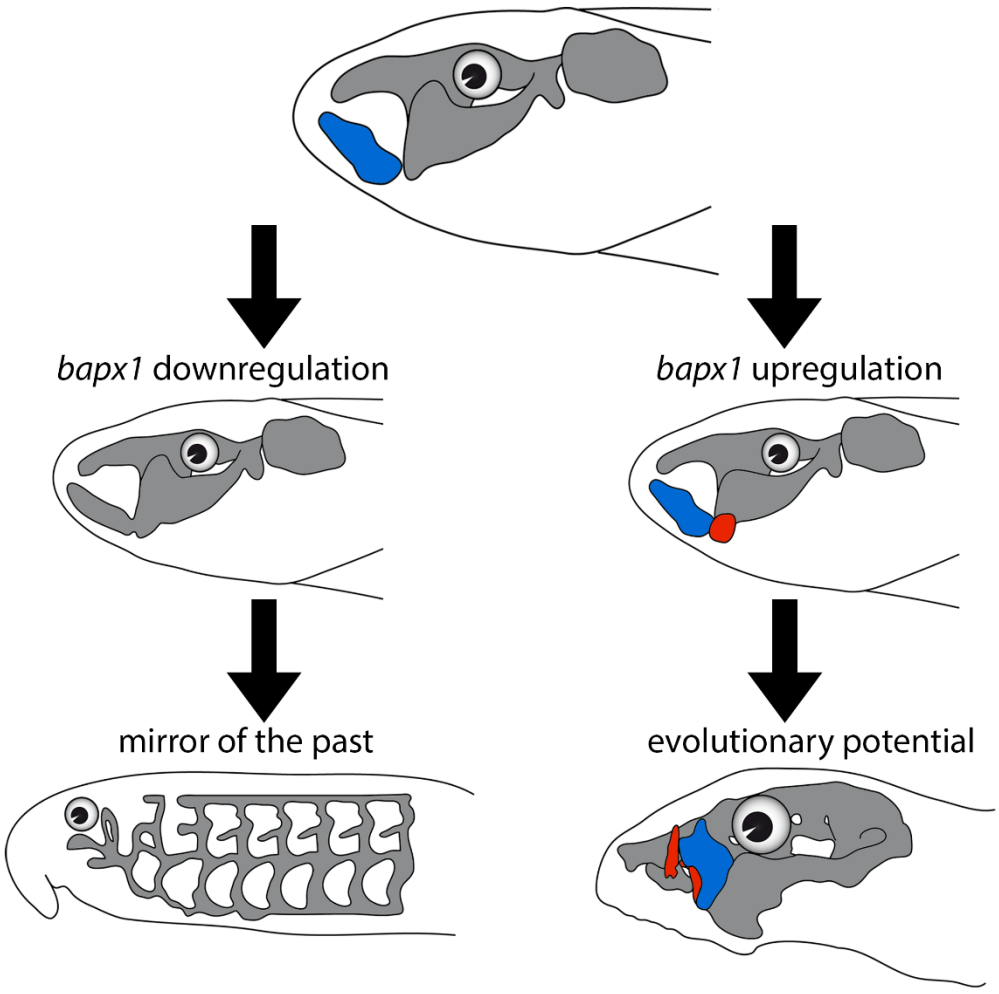

Figure 9: Summary of the results from the *bapx1* expression experiments and their implications for the explanation of evolutionary events. In the top row a normal developed *Xenopus laevis* tadpole is depicted in lateral view (Meckel´s cartilage is coloured in blue). The middle row depicts the results from the *bapx1* expression experiments in *Xenopus*. A continuous first pharyngeal arch without jaw joint after *bapx1* knockdown resembles the ancient condition found in recent jawless vertebrates and may mirror the condition of a gnathostome ancestor (left column, bottom row). After bapx1 upregulation an ectopic cartilage develops in *Xenopus laevis* (coloured in red). This is similar to a condition found in several anuran tadpoles and clearly shows the evolutionary potential of *bapx1* (right column, bottom row). Through further evolution it seems possible that additional cartilages arise in more anuran species because of raised *bapx1* expression caused by mutation or extrinsic factors.

Conclusion

The present work provides a comprehensive overview on the timing and sequence of the condensation and chondrogenesis of the larval head skeleton in *Xenopus laevis* from initial cartilaginous anlagen until a fully differentiated premetamorphic head skeleton. Obviously, anuran and pipoid-specific structures develop later and therefore deviate from the ancestral anterior-to-posterior sequence. Additionally, results from successful upregulation of *bapx1* in two amphibian species and from successful downregulation of *bapx1* in three amphibian species were presented. The downregulation of *bapx1* caused specific loss of the primary jaw joint, whereas upregulation of this gene led to the development of mandibular arch-derived ectopic cartilages. These results revealed, that partitioning of existing cartilages can lead to the development of novel structures. Furthermore, the cartilage preventing function of *bapx1* was confirmed through the observed morphological abnormalities after alteration of *bapx1* expression. Additionally, it was shown that *bapx1* is not able to induce joint development but is responsible for keeping the joint cavity cartilage-free. The unjointed mandibular arch after *bapx1* knockdown mirrors features of a possible jawless gnathosthome ancestor and thus gives insight into how the integration of a new gene into a pre-existing gene regulatory network can lead to major morphological changes. This further substantiates the role of *bapx1* in the evolution of the gnathostome jaw joint. The development of an ectopic cartilage after *bapx1* upregulation may give a hint about the possible evolutionary origin of the anuran sub-meckelian and adrostral cartilages. Overexpression or heterotopic shifts of the *bapx1* expression domain might have caused the evolution of these unique cartilages.

Summary

The presence of novel traits and how they originate during evolution is a key question in biology. To address this question, the present study combines a morphological and a genetical approach to investigate the sequence of cartilaginous head development in an important model organism and how changes in the gene expression during development can alter this sequence and generate morphological abnormalities in different amphibian species. The present work wants to reveal how evolutionary novelties may have arose during evolution by taking the example of the primary jaw joint, the defining feature of gnathostomes. The obtained results provide new pieces of evidence to understand gnathostome evolution by interpreting ontogenetic malformations which are exemplary for phylogenetic changes of several structures

The present dissertation is partitioned into five chapters. The first chapter provides a general introduction into the framework of the present work. It is followed by three chapters which cover different aspects of the introduced issues presented before. These three chapters are meant to be published in peer-reviewed journals and are in each case independent pieces of work. The last chapter discusses the results gained from the experiments and analyses done in the present work in the context of evolutionary novelties and the evolutionary origin of the primary jaw joint.

Xenopus laevis is a widely used model organism in biological research. In chapter two a detailed description of the pattern and timing of early cartilage differentiation and development of the larval head of *Xenopus laevis* is provided. This description offers a powerful tool for developmental biologist which alter the skeletal development or which investigate the skeletal development in different taxa and it also fills a gap in the literature. It is meant to be an encouragement for researchers to investigate the skeletal development of further species to identify heterochronic effects and homologies between distant related taxa. The development of the cartilaginous structures in the larval head of *Xenopus laevis* does not follow the strict antero-posterior pattern observed in other vertebrate taxa. The ceratohyal develops before Meckel´s cartilage. The feeding through filtration may be the reason for this precocious development. The development of the anuran-specific infrarostral cartilage and of the *Xenopus*-specific tentacular cartilage is delayed. Whether the development of these specific cartilages is a consequence of the derived state of *Xenopus laevis* or a general trend within anurans remains unclear. To address these questions further developmental studies in further anuran species are needed.

The general overview of the development of *Xenopus laevis* was the starting point for this work to interpret the following experimental results. In the second and third chapter the influence of the gene *bapx1* on the development of several amphibian species was investigated. Functional experiments on the impact of *bapx1* expression during development were missing so far in this taxonomic group despite its phylogenetically important position.

Through gain- and loss-of-function experiments and the resulting morphological abnormalities it was possible to define the role of *bapx1* during amphibian development and infer its potential role during vertebrate evolution.

Results from successful downregulation of *bapx1* in three amphibian species were presented in chapter two. The downregulation of *bapx1* caused specific loss of the primary jaw joint in *Xenopus laevis*, *Bombina orientalis* and *Ambystoma mexicanum*. Normal *bapx1* expression prevents existing cells in the joint cavity from differentiating into chondrocytes. Reduced expression of *bapx1* instead promotes chondrification of these cells, which leads to the fusion of Meckel´s cartilage and the palatoquadrate. This unjointed mandibular arch mirrors features of a possible jawless gnathostome ancestor and thus gives insight into how the integration of a new gene into a pre-existing gene regulatory network can lead to major morphological changes. *Bapx1* is not able to induce joint development in amphibians, but it is responsible for keeping the joint cavity free of chondrocytes and thus for maintaining the primary jaw joint.

In chapter three the results from successful upregulation of *bapx1* in *Xenopus laevis* and *Ambystoma mexicanum* were shown. The upregulation of *bapx1* is correlated to the development of mandibular arch-derived ectopic cartilages. These results revealed, that partitioning of existing cartilages can lead to the development of novel structures. Furthermore, the joint inducing and cartilage preventing function of *bapx1* was confirmed through the observed morphological abnormalities after alteration of *bapx1* expression. This further substantiates the role of *bapx1* in the evolution of the gnathostome primary jaw joint. Additionally, the development of an ectopic cartilage simultaneous to *bapx1* upregulation may give a hint about the possible evolutionary origin of the anuran sub-meckelian and adrostral cartilages. Overexpression or heterotopic shifts of the *bapx1* expression domain might have caused the evolution of these unique cartilages.

It has been shown that the cartilaginous development of *Xenopus laevis* larvae does not follow the strict ancestral anterior-posterior pattern because the anuran-specific and *Xenopus*-specific features develop relatively late. *Bapx1* was suggested to play an important role in both the development and the evolution of the primary jaw joint in earlier studies. The present thesis extends this concept. *Bapx1* is not able to induce joint development because in the absence of *bapx1* a proper joint develops initially. Without *bapx1* expression the joint cavity is invaded by chondroblast which differentiates into chondrocytes and connects Meckel´s cartilage and the palatoquadrate. This cartilaginous connection of these two cartilages causes the joint loss. The unjointed mandibular arch possibly mirrors the ancient condition of a possible unknown gnathostome ancestor. The development of an ectopic cartilage after Ly-294,002 treatment may be linked to the evolution of additional larval anuran cartilages. *Bapx1* is able to prevent cartilage formation and therefore its functioning can lead to the development of novel cartilages through separation of pre-existing cartilages.

Zusammenfassung

Wie evolutionäre Neuheiten im Verlauf der Evolution entstehen ist eine bedeutende Frage, die schon Generationen von Biologen beschäftigt hat. Um diese Frage näher zu beleuchten kombiniert die vorliegende Arbeit morphologische und genetische Ansätze. Einerseits wird die Sequenz der Knorpelentwicklung im larvalen Kopf von *Xenopus laevis*, einem wichtigen Modelorganismus, untersucht und andererseits wie Veränderungen der Genexpression während der Entwicklung diese Sequenz verändern und morphologische Anomalien in verschiedenen Amphibienarten entstehen können. Am Beispiel des primären Kiefergelenks der Gnathostomata wird dabei eingehend erläutert, wie evolutionäre Neuerungen entstanden sein könnten. Die Ergebnisse der Arbeit liefern neue Beweise für das Verständnis der Evolution der Gnathostomata Die Interpretation ontogenetischer Fehlbildungen gibt dabei Aufschluss über die phylogenetischen Veränderungen einzelner Strukturen.

Die vorliegende Dissertationsschrift besteht aus fünf Kapiteln. Im ersten Kapitel wird die Arbeit im gesamtwissenschaftlichen Kontext vorgestellt und eingeleitet. In den drei folgenden Kapiteln werden die in der Einleitung aufgeworfenen Fragen durch verschiedene experimentelle Ansätze untersucht. Diese drei Kapitel werden oder wurden in Fachzeitschriften veröffentlicht und sind jeweils eigenständige Arbeiten. Im letzten Kapitel werden die Ergebnisse der vorliegenden Arbeiten im Kontext der evolutionären Neuheiten und des evolutionären Ursprungs des primären Kiefergelenks diskutiert und ausgewertet.

Xenopus laevis ist seit Langem ein beliebter Modellorganismus in der biologischen Forschung. In Kapitel zwei wird die Differenzierung und Entwicklung der Knorpel im Kopf von *Xenopus laevis* Kaulquappen übersichtlich beschrieben. Diese Beschreibung stellt eine grundlegende Übersicht für Entwicklungsbiologen dar, die die Skelettentwicklung experimentell verändern oder die Skelettentwicklung in verschiedenen Taxa untersuchen. Für den Vergleich ihrer Ergebnisse sind sie auf eine standardisierte Übersicht angewiesen. Außerdem wird durch diese Übersicht der Knorpelentwicklung eine bestehende Lücke in der Fachliteratur geschlossen. Die Entwicklung der knorpeligen Strukturen im Larvenkopf von *Xenopus laevis* folgt nicht dem strengen anterior-posterior Muster, das bei anderen Vertebraten beobachtet wurde. Die Ceratohyale z.B. entwickelt sich zeitlich vor dem Meckelschen Knorpel. Die filtrierende Lebensweise der Kaulquappen könnte der Grund für diese vorgezogene Entwicklung sein. Außerdem ist die Entwicklung des anuraspezifischen Infrarostralknorpels und des Xenopus-spezifischen Tentakelknorpels verzögert. Ob die Entwicklung dieser spezifischen Knorpel eine Folge des abgeleiteten Zustandes von *Xenopus laevis* oder ein allgemeiner Trend innerhalb der Froschlurche ist, kann mit den vorhandenen Daten nicht abschließend geklärt werden. Um diese und weitere Fragen zu beantworten, sind zusätzliche Entwicklungsstudien an anderen Froschlurchen notwendig.

Der allgemeine Überblick über die Entwicklung von *Xenopus laevis* stellt die Grundlage für die Interpretation der folgenden experimentellen Ergebnisse dar. Im zweiten und dritten Kapitel wurde der Einfluss des Gens *bapx1* auf die Entwicklung mehrerer Amphibienarten näher untersucht. Trotz der phylogenetisch wichtigen Position der Amphibien fehlten bisher Untersuchungen zur Wirkung von bapx1 in dieser Tiergruppe. Infolge des Herauf- bzw. Herabsetzens der *bapx1* Expression kam es während der Ontogenese zu morphologischen Abnormalitäten. Die Interpretation dieser Abnormalitäten gab Aufschluss über die mögliche Funktion von bapx1 während der Entwicklung von Amphibien.

Im zweiten Kapitel werden die Ergebnisse des erfolgreichen Herabsetzens der *bapx1* expression in drei Amphibienarten (*Xenopus laevis*, *Bombina orientalis* und *Ambystoma mexicanum*) vorgestellt. In allen drei Arten führte das Herabsetzen der Expression zum Verlust des primären Kiefergelenks. Normalerweise verhindert die Expression von *bapx1,* dass die sich im Gelenkspalt befindliche Zellen zu Knorpelzellen differenzieren. In Abwesenheit von *bapx1* differenzieren sich diese Zellen zu Knorpelvorläuferzellen und schließlich zu Knorpelzellen, wodurch der Meckelsche Knorpel und das Palatoquadratum miteinander verschmelzen und das primäre Kiefergelenk somit verschwindet. Dieser durchgehende Kiefer ohne Gelenk spiegelt womöglich die Eigenschaften eines bisher unbekannten Gnathostomata-Vorfahren wieder. Außerdem geben die Ergebnisse Aufschluss darüber, wie die Integration eines neuen Gens in ein bereits bestehendes genregulatorisches Netzwerk zu großen morphologischen Veränderungen führen kann. Es konnte außerdem gezeigt werden, dass b*apx1* nicht in der Lage ist die Gelenkentwicklung bei Amphibien zu induzieren. Allerdings ist es dafür verantwortlich, den Gelenkspalt knorpelfrei zu halten und somit das Bestehen des primären Kiefergelenks zu sichern.

Im dritten Kapitel wird das erfolgreiche Heraufsetzen der *bapx1* Expression in *Xenopus laevis* und *Ambystoma mexicanum* und die Auswirkung auf die Morphologie beschrieben. Die Überexpression von *bapx1* führte zur Entwicklung von ektopischen Knorpeln. Diese Ergebnisse legen nahe, dass die Unterteilung von bestehenden Knorpel durch die Expressionsveränderung von bestimmten Regulatoren zur Entwicklung neuer Strukturen führen kann. Darüber hinaus konnte bestätigt werden, dass *bapx1* die Entwicklung von Knorpeln regional unterdrücken kann. Dies bestätigt die in Kapitel zwei gemachte Aussage, dass *bapx1* an der Entwicklung und Evolution des primären Kiefergelenks beteiligt gewesen sein könnte. Außerdem weist das Vorhandensein der ektopischen Knorpel darauf hin, dass eine Expressionsveränderung von *bapx1* während der Evolution der Froschlurche zur Entstehung zusätzlicher Knorpel im Bereich des larvalen Kiefers beigetragen haben könnte. Eine Überexpression oder eine räumliche Verschiebung der *bapx1*-Expressionsdomäne könnten der Evolution dieser einzigartigen Knorpel zugrunde liegen.

Die vorliegende Dissertationsschrift konnte darlegen, dass die Entwicklung der Knorpel der Kaulquappen von *Xenopus laevis* nicht dem strengen und ursprünglichen anterior-posterior Muster folgt. Die spezifischen Merkmale der Froschlurche und von *Xenopus laevis* entwickeln sich erst relativ spät und durchbrechen damit das ursprüngliche Muster. In früheren Studien wurde bereits angenommen, dass *bapx1* sowohl bei der Evolution als auch

bei der Entwicklung des primären Kiefergelenks eine wichtige Rolle spielt. Die vorliegende Arbeit kann diese Annahme entscheidend erweitern. Die Expression von *bapx1* ist nicht in der Lage die Gelenkentwicklung zu induzieren, da sich in Abwesenheit von *bapx1* zunächst ein Gelenk entwickelt. Ohne die Expression von *bapx1* jedoch wird der Gelenkspalt durch Knorpelvorläuferzellen, die sich im weiteren Verlauf der Entwicklung zu Knorpelzellen differenzieren und dann den Meckelschen-Knorpel mit dem Palatoquadratum miteinander verbinden, verschlossen. Diese knorpelige Verbindung der beiden Knorpel verursacht schlussendlich den Verlust des Gelenks. Diese durchgehende Verbindung zwischen Unter- und Oberkiefer könnte ein Hinweis darauf sein, wie die Vorfahren der Gnathostomata ausgesehen haben könnten. Die Entwicklung der ektopischen Knorpel nach der Überexpression von *bapx1* kann mit der Entwicklung zusätzlicher larvaler Knorpel bei einigen Froschlurchen in Verbindung gebracht werden. Die Fähigkeit von *bapx1* Knorpelbildung zu verhindern unterstütz die Annahme, dass evolutiv neue Knorpel durch die Unterteilung bereits bestehender Knorpel entstehen können.

Literature cited

Allin, E.F. & Hopson, J.A., 1992. Evolution of the Auditory System in Synapsida ("Mammal-Like Reptiles" and Primitive Mammals) as Seen in the Fossil Record. In *The Evolutionary Biology of Hearing*. New York, NY: Springer New York, pp. 587–614.

Anken, R.H. & Kappel, T., 1992. Die Kernechtrot-Kombinationsfärbung in der Neuroanatomie. *Winke fürs Labor*, 81(2), pp.62–63.

Azpiazu, N. & Frasch, M., 1993. tinman and bagpipe: two homeo box genes that determine cell fates in the dorsal mesoderm of Drosophila. *Genes & development*, 7(7B), pp.1325–40.

Baltzinger, M. et al., 2005. Hoxa2 knockdown in Xenopus results in hyoid to mandibular homeosis. *Developmental Dynamics*, 234(4), pp.858–867.

Beverdam, A. et al., 2002. Jaw transformation with gain of symmetry after Dlx5/Dlx6 inactivation: Mirror of the past? *Genesis*, 34(4), pp.221–227.

Bles, E.J., 1906. XXXI.—The Life-History of Xenopus lævis, Daud. *Transactions of the Royal Society of Edinburgh*, 41(3), pp.789–821.

Bronner, M.E. & LeDouarin, N.M., 2012. Development and evolution of the neural crest: an overview. *Developmental biology*, 366(1), pp.2–9.

Cannatella, D.C. & Sá, R.O. De, 1993. Xenopus laevis as a Model Organism. *Systematic Biology*, 42(4), p.476.

Cantley, L.C., 2002. The phosphoinositide 3-kinase pathway. *Science*, 296(5573), pp.1655–1657.

Cerny, R. et al., 2010. Evidence for the prepattern/cooption model of vertebrate jaw evolution. *Proc Natl Acad Sci U S A*, 107(40), pp.17262–17267.

Compagnucci, C. et al., 2013. Pattern and polarity in the development and evolution of the gnathostome jaw: Both conservation and heterotopy in the branchial arches of the shark, Scyliorhinus canicula. *Developmental Biology*, 377(2), pp.428–448.

Couly, G. et al., 1998. Determination of the identity of the derivatives of the cephalic neural crest: incompatibility between Hox gene expression and lower jaw development. *Development (Cambridge, England)*, 125(17), pp.3445–59.

Couly, G.F., Coltey, P.M. & Le Douarin, N.M., 1992. *The developmental fate of the cephalic mesoderm in quail-chick chimeras*,

Depew, M.J., 2002. Specification of Jaw Subdivisions by Dlx Genes. *Science*, 298(5592), pp.381–385. Available at: http://www.sciencemag.org/cgi/doi/10.1126/science.1075703.

Depew, M.J., Lufkin, T. & Rubenstein, J.L.R., 2002. Specification of jaw subdivisions by Dlx genes. *Science*, 298(5592), pp.381–385.

Dreyer, T.F., 1914. The Morphology of the tadpole of Xenopus laevis. *Transactions of the Royal Society of South Africa*, 4(1), pp.241–258.

Edgeworth, F.H., 1930. On the Masticatory and Hyoid Muscles of Larvae of Xenopus Laevis. *Journal of Anatomy*, 64(Pt 2), pp.184–188.

Engelman, J.A., Luo, J. & Cantley, L.C., 2006. The evolution of phosphatidylinositol 3-kinases as regulators of growth and metabolism. *Nature Reviews Genetics*, 7(8), pp.606–619.

Fischer, S. et al., 2006. Histone acetylation dependent allelic expression imbalance of BAPX1 in patients with the oculo-auriculo-vertebral spectrum. *Human Molecular Genetics*, 15(4), pp.581–587.

Fleischer, G., 1978. Evolutionary principles of the mammalian middle ear. *Advances in anatomy, embryology, and cell biology*, 55(5), pp.3–70.

Fox, M.A., 1986. *The case for animal experimentation : an evolutionary and ethical perspective*, University of California Press.

Gaupp, E., 1906. Die Entwickelung des Kopfskelettes. In *Handbuch der vergleichenden und experimentellen Entwickelungslehre der Wirbeltiere 3 (2)*. pp. 718–756.

Gillis, J.A., Dann, R.D. & Shubin, N.H., 2009. Chondrogenesis and homology of the visceral skeleton in the little skate, leucoraja erinacea (Chondrichthyes: Batoidea). *Journal of Morphology*, 270(5), pp.628–643.

Gillis, J.A., Modrell, M.S. & Baker, C.V.H., 2012. A timeline of pharyngeal endoskeletal condensation and differentiation in the shark, Scyliorhinus canicula, and the paddlefish, Polyodon spathula. *Journal of Applied Ichthyology*, 28(3), pp.341–345.

Gosner, K.L., 1960. A Simplified Table for Staging Anuran Embryos Larvae with Notes on Identification. *Herpetologists' League*, 16(3), pp.183–190.

Gromko, M.H., Mason, F.S. & Smith-Gill, S.J., 1973. Analysis of the crowding effect in Rana pipiens tadpoles. *Journal of Experimental Zoology*, 186(1), pp.63–71.

Gross, J.B. & Hanken, J., 2008. Segmentation of the vertebrate skull: Neural-crest derivation of adult cartilages in the clawed frog, Xenopus laevis. *Integrative and Comparative Biology*, 48(5), pp.681–696.

Gurdon, J.B. & Hopwood, N., 2000. The introduction of Xenopus laevis into developmental biology: of empire, pregnancy testing and ribosomal genes. *The International journal of developmental biology*, 44(1), pp.43–50.

Haas, A., 2003. Phylogeny of frogs as inferred from primarily larval characters (Amphibia: Anura). *Cladistics*, 19(1), pp.23–89.

Hanken, J. & Thorogood, P., 1993. Evolution and development of the vertebrate skull: The role of pattern formation. *Trends in Ecology & Evolution*, 8(1), pp.9–15.

Harland, R.M. & Grainger, R.M., 2011. Xenopus research: metamorphosed by genetics and genomics. *Trends in genetics : TIG*, 27(12), pp.507–15.

Heatwole, H., 2003. *Amphibian biology*, Surrey Beatty & Sons.

Heidenhain, M., 1915. Über die mallorysche bindegewebsfärbung mit karmin und azokarmin als vorfarben. *Z wiss Mikrosk*, 33, pp.361–372.

Hellemans, J. et al., 2009. Homozygous Inactivating Mutations in the NKX3-2 Gene Result in Spondylo-Megaepiphyseal-Metaphyseal Dysplasia. *American Journal of Human Genetics*, 85(6), pp.916–922.

Jiang, X. et al., 2002. *Tissue origins and interactions in the mammalian skull vault*,

Kim, J.A. et al., 2015. Suppression of Nkx3.2 by phosphatidylinositol-3-kinase signaling regulates cartilage development by modulating chondrocyte hypertrophy. *Cellular Signalling*, 27(12), pp.2389–2400.

Kim, Y. & Nirenberg, M., 1989. Drosophila NK-homeobox genes. *Proceedings of the National Academy of Sciences of the United States of America*, 86(20), pp.7716–7720.

Kotthaus, A., 1933. Die Entwicklung des Primordial-Craniums von Xenopus laevis vor der Metamorphose. *Zeit. Wiss. Zool.*

Kuratani, S., 2012. Evolution of the vertebrate jaw from developmental perspectives. *Evolution and Development*, 14(1), pp.76–92.

Langille, R.M. & Hall, B.K., 1987. Development of the head skeleton of the Japanese medaka,Oryzias latipes (Teleostei). *Journal of Morphology*, 193(2), pp.135–158.

Larroux, C. et al., 2007. The NK Homeobox Gene Cluster Predates the Origin of Hox Genes. *Current Biology*, 17(8), pp.706–710.

Livak, K.J. & Schmittgen, T.D., 2001. Analysis of Relative Gene Expression Data Using Real-Time Quantitative PCR and the 2−ΔΔCT Method. *Methods*, 25(4), pp.402–408.

Lukas, P. & Olsson, L., 2018. Sequence and timing of early cranial skeletal development in Xenopus laevis. *Journal of Morphology*, 279(1), pp.62–74.

McDiarmid, R.W. & Altig, R., 1999. *Tadpoles : the biology of anuran larvae*, University of Chicago Press.

Medeiros, D.M. & Crump, J.G., 2012. New perspectives on pharyngeal dorsoventral patterning in development and evolution of the vertebrate jaw. *Developmental Biology*, 371(2), pp.121–135.

Meulemans, D. & Bronner-Fraser, M., 2007. Insights from Amphioxus into the Evolution of Vertebrate Cartilage J.-N. Volff, ed. *PLoS ONE*, 2(8), p.e787.

Miller, C.T., 2003. Two endothelin 1 effectors, hand2 and bapx1, pattern ventral pharyngeal cartilage and the jaw joint. *Development*, 130(7), pp.1353–1365.

Minoux, M. et al., 2010. Molecular mechanisms of cranial neural crest cell migration and patterning in craniofacial development. *Development (Cambridge, England)*, 137(16), pp.2605–21.

Newman, C.S. et al., 1997. Xbap, a vertebrate gene related to bagpipe, is expressed in developing craniofacial structures and in anterior gut muscle. *Developmental biology*, 181(2), pp.223–33.

Nichols, J.T. et al., 2013. Barx1 Represses Joints and Promotes Cartilage in the Craniofacial Skeleton. *Development*, 140(13), pp.2765–2775.

Nicolas, S. et al., 1999. Two Nkx-3-related genes are expressed in the adult and

regenerating central nervous system of the urodele Pleurodeles waltl. *Developmental genetics*, 24(3–4), pp.319–28.

Nieuwkoop, P. & Faber, J., 1994. Normal Table of Xenopus laevis (Daudin). *New York: Garland Publishing*.

Olsson, L. & Hanken, J., 1996. Cranial neural-crest migration and chondrogenic fate in the oriental fire-bellied toadBombina orientalis: Defining the ancestral pattern of head development in anuran amphibians. *Journal of Morphology*, 229(1), pp.105–120.

Parker, W.K., 1876. On the Structure and Development of the Skull in the Batrachia. Part II. *Philosophical Transactions of the Royal Society of London*, 166(0), pp.601–669.

Parker, W.K., 1879. On the Structure and Development of the Skull in the Batrachia. Part III. *Proceedings of the Royal Society of London*, 30.

Pasqualetti, M. et al., 2000. Ectopic Hoxa2 induction after neural crest migration results in homeosis of jaw elements in Xenopus. *Development*, 127, pp.5367–5378.

Paterson, N.F., 1939. The Head of Xenopus laevis. *The Quarterly journal of microscopical science*, 81(322), pp.161–234.

Peter, K., 1931. The Development of the External Features of Xenopus laevis, based on Material collected by the late E. J. Bles. *Journal of the Linnean Society of London, Zoology*, 37(254), pp.515–523.

Ramaswami, L.S., 1941. Some aspects of the head of Xenopus laevis. *Proceedings of the Indian Science Congress.*, 28, pp.183–184.

Reichert, C., 1837. Über die Visceralbogen der Wirbeltiere im Allgemeinen und deren Metamorphosen bei den Vögeln und Säugetierene. *Archiv für Anatomie, Physiologie, und Wissenschaftliche Medizin, Leipzig*, 1837, pp.120–222.

Ridewood, W.G., 1897. On the Structure and Development of the Hyobranchial Skeleton and Larynx in Xenopus and Pipa; with Remarks on the Affinities of the Aglossa. *Journal of the Linnean Society of London, Zoology*, 26(166), pp.53–128.

Rijli, F.M. et al., 1993. A homeotic transformation is generated in the rostral branchial region of the head by disruption of Hoxa-2, which acts as a selector gene. *Cell*, 75(7), pp.1333–1349.

Rose, C., 2009. Generating, growing and transforming skeletal shape: insights from amphibian pharyngeal arch cartilages. *BioEssays*, 31(3), pp.287–299.

Rose, C.S., 2014. The importance of cartilage to amphibian development and evolution. *International Journal of Developmental Biology*, 58(10–12), pp.917–927.

De Sá, R.O. & Swart, C.C., 1999. Development of the suprarostral plate of pipoid frogs. *Journal of Morphology*, 240(2), pp.143–153.

Sadaghiani, B. & Thiébaud, C.H., 1987. Neural crest development in the Xenopus laevis embryo, studied by interspecific transplantation and scanning electron microscopy. *Developmental biology*, 124(1), pp.91–110.

Schneider, A. et al., 1999. The homeobox gene NKX3.2 is a target of left-right signalling and is expressed on opposite sides in chick and mouse embryos. *Current Biology*,

9(16), pp.911–914.

Schreckenberg, G.M. & Jacobson, A.G., 1975. Normal stages of development of the axolotl, Ambystoma mexicanum. *Developmental Biology*, 42(2), pp.391–399.

Segerdell, E. et al., 2008. An ontology for Xenopus anatomy and development. *BMC Developmental Biology*, 8(1), p.92.

Segerdell, E. et al., 2013. Enhanced XAO: the ontology of Xenopus anatomy and development underpins more accurate annotation of gene expression and queries on Xenbase. *Journal of Biomedical Semantics*, 4(1), p.31.

Shigetani, Y., Sugahara, F. & Kuratani, S., 2005. A new evolutionary scenario for the vertebrate jaw. *BioEssays*, 27(3), pp.331–338.

Shubin, N., Tabin, C. & Carroll, S., 2009. Deep homology and the origins of evolutionary novelty. *Nature*, 457, p.818.

Sokol, O.M., 1977. The free swimmingPipa larvae, with a review of pipid larvae and pipid phylogeny (Anura: Pipidae). *Journal of Morphology*, 154(3), pp.357–425.

Sokol, O.M., 1981. The larval chondrocranium ofPelodytes punctatus, with a review of tadpole chondrocrania. *Journal of Morphology*, 169(2), pp.161–183.

Square, T. et al., 2015. A gene expression map of the larval Xenopus laevis head reveals developmental changes underlying the evolution of new skeletal elements. *Developmental Biology*, 397(2), pp.293–304.

Square, T. et al., 2016. The origin and diversification of the developmental mechanisms that pattern the vertebrate head skeleton. *Developmental Biology*.

Stathopoulos, A. et al., 2004. pyramus and thisbe: FGF genes that pattern the mesoderm of Drosophila embryos. *Genes & development*, 18(6), pp.687–99.

Stöhr, P., 1882. Zur Entwickelungsgeschichte des Anurenschädels. *Z. wiss. Zool.*, 36, pp.68–103.

Svensson, M.E. & Haas, A., 2005. Evolutionary innovation in the vertebrate jaw: A derived morphology in anuran tadpoles and its possible developmental origin. *BioEssays*, 27(5), pp.526–532.

Takio, Y. et al., 2004. Evolutionary biology: lamprey Hox genes and the evolution of jaws. *Nature*, 429(6989), p.1 p following 262.

Takio, Y. et al., 2007. Hox gene expression patterns in Lethenteron japonicum embryos—Insights into the evolution of the vertebrate Hox code. *Developmental Biology*, 308(2), pp.606–620.

Talbot, J.C., Johnson, S.L. & Kimmel, C.B., 2010. hand2 and Dlx genes specify dorsal, intermediate and ventral domains within zebrafish pharyngeal arches. *Development*, 137(15), pp.2507–2517.

Tinsley, R., 2010. Amphibians, with Special Reference to Xenopus. In *The UFAW Handbook on the Care and Management of Laboratory and Other Research Animals*. Wiley-Blackwell, pp. 741–760.

Tribioli, C., Frasch, M. & Lufkin, T., 1997. Bapx1: an evolutionary conserved homologue of the Drosophila bagpipe homeobox gene is expressed in splanchnic mesoderm and the embryonic skeleton. *Mechanisms of development*, 65(1–2), pp.145–62.

Trueb, L.L. & Hanken, J.J., 1992. Skeletal development in Xenopus laevis (Anura: Pipidae). *Journal of Morphology*, 214(1), pp.1–41.

Tucker, A.S., 2004. Bapx1 regulates patterning in the middle ear: altered regulatory role in the transition from the proximal jaw during vertebrate evolution. *Development*, 131(6), pp.1235–1245.

Vlahos, C.J. et al., 1994. A specific inhibitor of phosphatidylinositol 3-kinase, 2-(4-morpholinyl)-8-phenyl-4H-1-benzopyran-4-one (LY294002). *Journal of Biological Chemistry*, 269(7), pp.5241–5248.

Wagner, G.P., 2014. *Homology, Genes, and Evolutionary Innovation*, Princeton University Press.

Wagner, G.P. & Lynch, V.J., 2010. Evolutionary novelties. *Current Biology*, 20(2), pp.R48–R52.

Warth, P. et al., 2017. Development of the skull and pectoral girdle in Siberian sturgeon, Acipenser baerii , and Russian sturgeon, Acipenser gueldenstaedtii (Acipenseriformes: Acipenseridae). *Journal of Morphology*, 278(3), pp.418–442.

Weisz, 1945a. The development and morphology of the larva of the south african clawed toad, Xenopus laevis. *Journal of Morphology*, 77(2), pp.193–217.

Weisz, 1945b. The development and morphology of the larva of the South African clawed toad, Xenopus laevis. I. The third-form tadpole. *Journal of Morphology*, 77(2), pp.163–192. Available at: http://doi.wiley.com/10.1002/jmor.1050770204 [Accessed March 6, 2017].

van der Westhuizen, C.M., 1961. The development of the chondrocranium of Heleophryne purcelli Sclater with special reference to the palatoquadrate and the sound-conducting apparatus. *Acta Zoologica (Stockholm)*, 42(1–2), pp.1–72. Available at: http://doi.wiley.com/10.1111/j.1463-6395.1961.tb00059.x [Accessed February 1, 2018].

Wilson, J. & Tucker, A.S., 2004. Fgf and Bmp signals repress the expression of Bapx1 in the mandibular mesenchyme and control the position of the developing jaw joint. *Developmental Biology*, 266(1), pp.138–150.

Yoshiura, K.I. & Murray, J.C., 1997. Sequence and chromosomal assignment of human BAPX1, a bagpipe-related gene, to 4p16.1: a candidate gene for skeletal dysplasia. *Genomics*, 45(2), pp.425–8.

Zhang, Z. et al., 2017. Similarity in gene-regulatory networks suggests that cancer cells share characteristics of embryonic neural cells. *Journal of Biological Chemistry*, 292(31), pp.12842–12859.

Ziermann, J.M. & Olsson, L., 2007. A new staging table for stages relevant to cranial muscle development in the African Clawed Frog, Xenopus laevis (Anura: Pipidae). *Journal of Morphology*, 268.

Ehrenwörtliche Erklärung

Ich versichere hiermit, dass ich die vorliegende Dissertation mit dem Titel „The influence of *bapx1* on amphibian head development and its role for the development of evolutionary novelties.“ selbständig angefertigt und keine anderen als die angegebenen Hilfsmittel, persönlichen Mitteilungen und Quellen benutzt habe. Die Stellen, die anderen Werken dem Wortlaut oder dem Sinn nach entnommen wurden, habe ich in jedem einzelnen Fall durch die Angabe der Quelle, auch der benutzten Sekundärliteratur, als Entlehnung kenntlich gemacht. Ich erkläre weiterhin, dass mir die Promotionsordnung der Fakultät für Biowissenschaften bekannt ist. Alle Personen die bei der Auswahl und Analyse des Materials, sowie bei der Erstellung des Manuskriptes geholfen haben sind in der jeweiligen Publikation als Autor aufgeführt und deren Anteil in Bezug auf Inhalt und Umfang ist entsprechend ausgewiesen.

Die Hilfe eines Promotionsberaters wurde nicht in Anspruch genommen und es wurden keine Dritten weder mittelbar noch unmittelbar durch geldwerte Leistungen, die im Zusammenhang mit dem Inhalt dieser Dissertation stehen, entlohnt. Die Dissertation wurde nicht bereits zuvor als Prüfungsarbeit für eine staatliche oder andere wissenschaftliche Prüfung eingereicht.

Paul Lukas